A STUDY OF BANKLINE SHIFTING OF THE SELECTED REACH OF JAMUNA RIVER LEFT BANK USING NUMERICAL MODELS

A THESIS SUBMITTED TO THE

DEPARTMENT OF WATER RESOURCES ENGINEERING

In partial fulfillment of the requirement for the degree of

MASTER OF SCIENCE IN WATER RESOURCES ENGINEERING

BY

AKRAMUL HAQUE

Student ID: 0419162002

DEPARTMENT OF WATER RESOURCES ENGINEERING

BANGLADESH UNIVERSITY OF ENGINEERING AND TECHNOLOGY

DHAKA 1000, BANGLADESH

CERTIFICATION OF APPROVAL

We hereby recommended that the M.Sc. Engg. Research work presented by Akramul Haque, Roll No. 0419162002, session April 2019, entitled " **A study of bankline shifting of the selected reach of Jamuna river left bank using numerical models**" has been accepted as satisfactory in partial fulfillment of the requirements for the degree Master of Science in Water Resources Engineering on 9th January 2023.

Dr. Md. Abdul Matin
Professor
Department of Water Resources Engineering, BUET
Dhaka-1000, Bangladesh.

Chairman of the Committee
(Supervisor)

Dr. A.T.M Hasan Zobeyer
Professor and Head
Department of Water Resources Engineering, BUET
Dhaka-1000, Bangladesh.

Member(Ex officio)

Dr. Md. Mostafa Ali
Professor
Department of Water Resources Engineering, BUET
Dhaka-1000, Bangladesh.

Member

Dr. A.K.M. Saiful Islam
Professor,
Institute of Water and Flood Management, BUET
Dhaka-1000, Bangladesh

Member (External)

DECLARATION

This to certify that this project entitled "**A study of bankline shifting of the selected reach of Jamuna river left bank using numerical models**" has been done by me under the supervisor of Dr. Md. Abdul Matin, Professor, Department of Water Resources Engineering, Bangladesh University of Engineering and Technology, Dhaka. I do hereby declare that this project or any part of it has not been accepted elsewhere for the award of any degree or diploma from any other institution.

Signature of the candidate

Akramul Haque

Akramul Haque

ACKNOWLEDGEMENT

First of all, the author would like to pay his gratitude to the Almighty Allah (SWT) for providing the opportunity and giving the ability to complete this thesis work.

The author acknowledges his profound gratitude, sincerest appreciation and indebtedness to his supervisor Dr. Md. Abdul Matin, Professor, Department of Water Resources Engineering, BUET for providing an interesting idea for the research work and giving the unique opportunity to work on such an important topic, and also encouraging working with it. His cordial supervision, valuable advice, affectionate encouragement, generous help, constructive comments, enormous expertise, critical analysis of observation, detecting flaws & amending made the study a success.

The author expresses his gratitude to the respected members of the Board of Examiners Dr. A T M Hasan Zobeyer, Professor and Head, Department of WRE, BUET, Dr.Mostafa Ali, Professor, Department of WRE, BUET and Dr. A.K.M. Saiful Islam, Professor and Director, IWFM, BUET for their valuable comments and constructive suggestions regarding this thesis work.

The author is grateful to the BWDB for their help and cooperation in collecting the required data and information.

In this regard, the author remains ever grateful to his beloved parents and siblings, who always exist as sources of inspiration behind every success.

Finally, the author would like to express his sincere gratitude to all other teachers and members of the Water Resources Engineering Department, BUET, for their cooperation and help in the successful completion of the work.

Akramul Haque

9th January. 2023.

ABSTRACT

The present study deals with the development of a computational procedure to predict the morphological behavior of the Jamuna river such as bed level changes and bankline shifting. A reach of 80 kms long left bank of the Jamuna river from Bahadurabad to Sirajganj was selected for this study . Numerical models named RIVERFLOW 2D, HEC-RAS 1D and multi-variate regression modeling tools have been used. This study also proposes a machine learning technique for the prediction of bank line shifting of river Jamuna based on the results of numerical models. Accordingly, models have been set for the hydro-morphological computation. RIVERFLOW 2D hydro-morphological model has been used for the assessment of erosion-deposition and bed level changes. This model was calibrated utilizing the water level data collected from BWDB for the year 2018 and then validated for the year 2019 . For calibration and validation, the R^2 was found to be about 0.86 and 0.93 respectively. In addition, the HEC-RAS 1D hydrodynamic model has been setup, calibrated and validated using the same data.

In broad category, two Scenarios have been carried out in the present computational procedure. These are Scenario i) use of the output of HEC-RAS 1D and regression tools and Scenario ii) use of results of HEC-RAS 2D and regression tools. In Scenario-i , five variables such as maximum velocity, maximum water level, maximum left over bank discharge, maximum slope and minimum water level were taken from the validated 1D hydro-dynamic model. Performance of the prediction of bankline shifting obtained from the computation have been evaluated using statistical parameters, such as RMSE, R^2, MSE, and MAE. These performance evaluation have also been carried out for various types of regression models such as linear regression, tree type regression, boosted, Gaussian, and SVM type regression models. Performance evaluation showed that that the Boosted regression model outperforms the others. For the boosted regression model, the values of RMSE, R^2, MSE, and MAE were 25, 0.80, 700, and 10 respectively. On the other hand, in the Scenario- ii, use of results of HEC-RAS 2D and regression tools, three variables such as the minimum water depth, maximum water depth and maximum velocity have been extracted for the purpose of various regression models run. It is found that the prediction of bankline shifting obtained from calibrated and validated boosted regression model performed satisfactorily in which for the calibration, the RMSE, R^2, MSE, and MAE values were found 38, 0.60, 1444, and 13 respectively. Computational performance of all the models used in the study has also been assessed in terms of discrepancy ratio.

Assessment of bed level changes in terms of net erosion and deposition has been analyzed using RIVER FLOW 2D. Model results showed that maximum erosion was 17.7 m/year and maximum depositions have been found 7.3 m/year near Bhuapur hard point area. In order to verify the efficacy of prediction of bank line erosion, Jamuna river left bank data from Google satellite images for the year 2018-2021 were also compared. It is found that boosted regression model performed better when compared with others regression models. Based on the statistical parameters (RMSE, MSE, R^2, MAE) and discrepancy ratio, Scenario one (HECRAS 1D and regression model) performed comparatively better (RMSE=56, MSE=3200, R^2 =0.60, MAE=23). On the other hand, Scenario two (HECRAS 2D and regression model) performed relatively better (RMSE=50, MSE=2500, R^2 =0.65, MAE=20) than that of Scenario one. It is hoped that computational procedure suggested in this study based on river models and multi-variate regression tools can be helpful for the analysis of river bank shifting of alluvial rivers.

Table of contents

LIST OF FIGURES

LIST OF TABLES

LIST OF ABBREVIATION

ACRONYM	ELABORATION
BWDB	Bangladesh Water Development Board
CEGIS	Center for Environment and Geographic Information Services
PWD	Public works department
MARS	Multivariate Adaptive Regression Splines
NARX	Non-linear Auto Regressive eXogenous
RFD-2D	Riverflow 2d
BSTEM	Bank Stability and Toe Erosion Model
WSE	Water surface elevation
LOB	Left Over bank
GBM	Ganges-Brahmaputra-Meghna
JNA	Joint Needs Assessment
D.R.	Discrepancy ratio

LIST OF NOTATIONS

r_c	Critical shear stress (N/m^2)
r_a	Hydraulic shear stress (N/m^2)
ε	Erosion rate (mm/hr)
k_d	Erodibility co-efficient ($Cm^3/N\text{-}s$)
c	Cohesion (Kn/m^2)
γ	Unit weight (KN/m3)
φ	Angle of internal friction (°)
d_{50}	Median soil diameter (mm)
Q	Discharge (m^3/s)
V	Velocity (m/s)
σ	Effective stress (KN/m^2)
r	Frictional shearing resistance (KN/m^2)
k	Hydraulic conductivity (m/s)
γ_{dry}	Dry unit weight (KN/m3)
τ_b	Bed shear stress

CHAPTER ONE
INTRODUCTION

1.1 General

Riverbank erosion is a common phenomenon particularly for major rivers of Bangladesh. It is assessed by many researchers that about 6 per cent of Bangladesh's total floodplain is affected by erosion. According to Joint Needs Assessment , about 28 districts are affected by the severe river bank erosion and floods, the most severely affected districts are: Jamalpur, Sirajgonj, Tangail, Bogura, Kurigram, Gaibandha (JNA,2017). In those districts, millons of people have been dislocated from their home due to intense river bank shifting due to bank erosion. lateral erosion and bed lowering are two causes of river erosion. Hydraulic parameters directly affect riverbank erosion. Near bank velocity, discharge condition, bed slope, bank slope, water level, seepage and piping, shear stress, wave action, soil parameters such as bank material size, gradation and cohesion inherently affects riverbank erosion.The rivers of Bangladesh are alluvial rivers. The major rivers of Bangladesh carry vast amount of sediment every year. The river erosion process is therefore very complex because of the interaction of water dynamics and geotechnical parameters.

1.2 Present state of the problem

Hydraulic and geotechnical parameters are vital for the analysis of bankline shifting, erosion and deposition of the river bed and bank. In addition, tension crack in the riverbank, pore water pressure, bank erosion at the toe, seepage, weathering and weakening, and mass failure are also becoming the determining factor of bankline shifting. Many researchers proposed different approach to determine river erosion. Among different approach, coupled hydrodynamic and bank stability model are prefer according to many researchers. In previous times, various probabilistic approaches and use of satellite images were used to determine riverbank erosion of alluvial rivers. Now-a days, different numerical models, machine learning and artificial intelligence are used to predict the bank erosion. In this study, an attempt will be made for the analysis of bank line shifting and bed level changes. bank line shifting will be predicted using numerical models and compared with the multivariate regression model.

1.3 Objectives of the study

Bank erosion and bed level changes have been ongoing processes for the Jamuna river. The goal of the current study is to use a 2D numerical model to analyze the morphological behavior of the Jamuna river, including changes in bed level. This work also suggests a machine learning method to predict bankline shifting of the chosen reach of the Jamuna river using HEC-RAS and the MATLAB regression tool.

Specific objectives of this study can be set as follows:

i) To set up a two-dimensional hydro-morphological and one-dimensional model for the selected reach of Jamuna River.

ii) To assess the bed level changes in terms of net erosion deposition of the selected reach of Jamuna using the RIVERFLOW2D model

iii) To compute the bank line changes of the selected reach of Jamuna river(left bank) using HEC-RAS 1D in conjunction with MATLAB .

1.4 Study area

The Jamuna River is one of Bangladesh's three major rivers. One of the most well-known braided rivers is the Brahmaputra-Jamuna. It is prone to channel migration and avulsion. It is located in northeast and north central region of Bangladesh. It is the Brahmaputra River's lower stream. It rises in Tibet as the Yarlung Tsangpo before flowing into India and then southwest into Bangladesh. Before meeting the Meghna River close to Chandpur, the Jamuna flows south and merges with the Padma River . the total length of the Jamuna river is 240 kms. The soil formation is composed of sandy types and small amount of clayey soil. The average width of the river varies from 6 km to 12 kms. The study area has started from Bahadurabad station and ended at Sirajgonj station(Fig1.1).

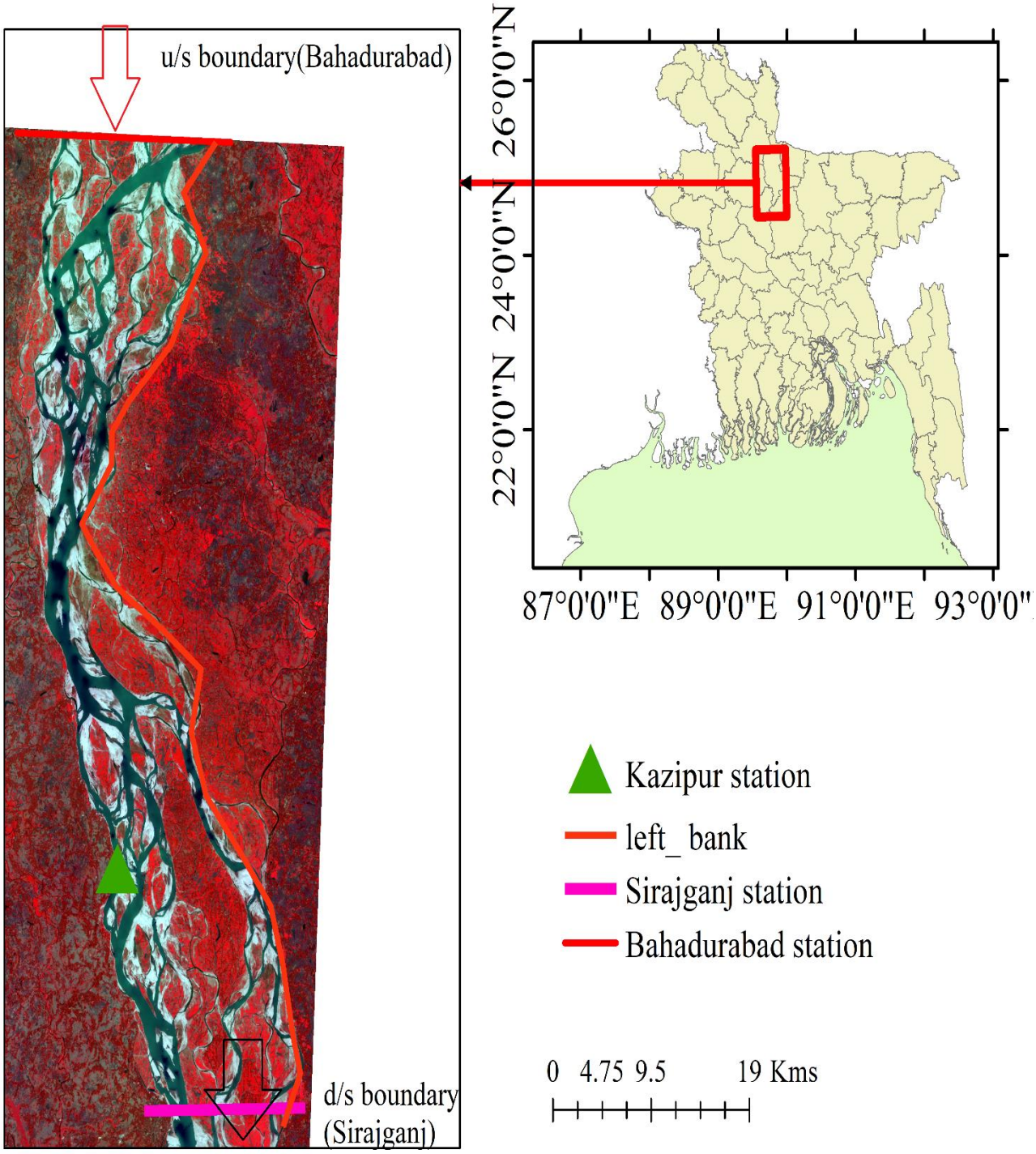

Figure 1.1: Study area

1.5 Organization of the Thesis

This thesis consists of five chapters. Chapter one describes the background, present state and objectives of the study. In chapter two, previous works and general terminology have been discussed related to this study. In chapter three, theory of the bank erosion and model has been described. Chapter four shows the development of a 2D morphological model using RIVERFLOW 2D and development of multivariate regression model in conjunction with HECRAS. Chapter five contains results and discussion. Chapter six shows conclusions drawn from this study and recommendation for further research.

CHAPTER TWO
LITERATURE REVIEW

2.1 General

Riverbank erosion is a natural hydro-geological process. Salient aspects such as river flow,size, shape, slope and other morphological properties, undergoes mutual interactions. Consequently, morphological changes like river bed erosion and bank line shifting occurs. Most of the available numerical models only count bed erosion but do not take into account of bank erosion explicitly. The purpose of this section is to give a general description of the related theories about bank erosion processes. To predict bank erosion, especially for composite river banks, is very complex. the composite river banks are connected with many controlling variables. Again there are many uncertainty associated with these controlling variables. Therefore it is very difficult to predict bank erosion for large rivers (Karmaker & Dutta, 2011). However, few notable works performed by previous researchers have been discussed in this chapter.

2.2 Review of existing literature related to the riverbank shifting

CEGIS (2020) reported that about 93000 ha land were eroded along the bank from the Jamuna river. It was recognized that bank failure contributes about 80% of sediment to the total sediment load of rivers ((Bull & Kirkby, 1997; Evans et al., 2006; Sekely et al., 2002; Simon & Collinsion, 2002). The nature of the erosion in a composite riverbank is dependent on hydraulic parameters and soil characteristics. The nature of erosion in cohesionless soilis the removal of individual particles. By contrast, the erosion occurs after the elimination of aggregates from the soil in a cohesive soil as the soil particles are attracted by electrochemical forces (Buffington & Montgomery, 1997; Lawler et al., 1997; Shields, 1936).

Riverbank erosion is a result of complex combinations of several processes. These processes are well studied (Abidin et al., 2017; Darby et al., 2010; Davis & Harden, 2014; Julian & Torres, 2006; Lawler, 1992; Lawler et al., 1999; Lawler, 1993; R. Grove et al., 2013; Semmad & Chalermyanont, 2018; Thorne, 1982; Yu et al., 2019) and are described below.

Subaerial processes are climate-related phenomena. It reduces soil strength. It makes the bank more susceptible to fluvial erosion by desiccation, cracking, slaking, piping, sapping etc.(Thorne, 1982). Such fluvial erosion occurs in the surface of riverbank in contact with air. Therefore, exclude

processes during periods of inundation. Land use, meandering, shear stress, soil characteristics, hydraulic variables control the erosion rate of the river bank (Atkinson et al., 2003). It has found that the rate of erosion for alluvium river largely depend on maximum discharge and slightly with rainfall intensity, duration. It was concluded in a research work that soil moisture can accelerate rate of soil erosion if the bank material consists of sandy, silty materials. But it can suggest that to find the correlation between variables and bank erosion, it is necessary analyze for the period of 5-10 years (Hooke, 1979)

wetting and drying of the riverbank are commonly thought as 'preparatory' for erosive processes (Duijsings, 1987; Green et al., 1999; Lawler et al., 1997; Throne, 1990; Wolman, 1959). Mainly wetting and drying process is very dangerous for the river bank that consists of stratified soil layers (Thorne & Tovey, 1981). The lower the height difference between water level and bank top surface and if wetting and drying process continues that bank surface is vulnerable to river bank erosion.

Subaerial 'weakening and weathering' of the soil can occur for number of variables, for this number of variables bank erosion is a complex phenomenon (Dietrich & Gallinatti, 1991; Osman & Thorne, 1988; Thorne, 1992) They found that the highest rates of bank erosion does not depend on the largest storms or floods, it depends as a result of high flows during prolonged wet period. So it can say that weakening and weathering of bank materials occur due to soil composition and dynamics of soil moisture.

Based on past researches, wind and water are two major components for erosion. Wind direction and speed is the main variable for coastal erosion (Musa etal., 2010). In river, Water has been identified as a major cause of soil erosion problems, comparedto the wind. Water transported sediment from one location to another and sediment is deposited in lower land and eroded in steep slope (Singer & Munns, 2006).

Jana,2021 applied the digital shoreline analysis system supported statistical models to determine the riverbank erosion. Bankline prediction was done considering the six different multi-temporal bank lines. They found that this approach is easy for rapid and precise estimation of the riverbank shifting. High rates of shifting were found in the meandering bend and the model accuracy is also very good.

Moddy, 2022 found that the variables that are responsible for underwater erosion vary from year to

year. He estimated underwater bank erosion rate based on dominant annual peak discharge. He tried to found out the effect of discharge and orientation of bank on annual riverbank erosion along powder river in Montana, USA. He found that the correlation of the underwater bank erosion rate with bank variables and channel geometry was small ($R2 < 0.31$) but the correlation was higher for peak discharge having $R2 > 0.50$. he concluded that the underwater bank erosion rate is a function of different combinations of variables at different sites in same river reach.

Islam and Matin, 2022 did research work on bank erosion of the selected reach of Jamuna river. The selected river reach bank was classified as vulnerable to very vulnerable based on shear stress. SRH-2D hydrodynamic model was run and based on simulated shear stress, the average bank erosion rate was predicted. It was found that the maximum bank erosion rate varies from 55 m/yr to 70 m/yr.

Ojile & Ogwara, 2020, Developed 2D morphological model. The prediction of bank erosion was done based on numerical simulation. It was found that the sand bars are important feature to predict bank erosion on short time scale. Based on the high flow rates , the evolution of channel pattern and geometry are also important variable to locate area that is vulnerable to bank erosion.
Rahman et al.,2022 estimated the annual deposition and erosion area of the left and right bank of the Jamuna river. It was found that the accretion rate is higher in right bank and erosion rate was higher in left bank. It was also found that anthropogenic factor such that the launches velocity accelerate the bank erosion.

Haque & Matin, 2022 studied bank erosion of a selected reach of the Jamuna River. Hydrodynamic model and multivariate regression model was used to predict bank erosion. Five variables were extracted from the calibrated and validated hydrodynamic model. Then five variables and bank erosion rate were processed in MATLAB regression Tool. The results of calibration was found very good. The prediction results was also good. But it can suggest that prediction of bank erosion of such large rivers need the parameters that from 2D hydrodynamic model.

Saha et al.,2022 estimated soil erosion of the Jamuna floodplain using GIS based RUSLE model. Average 600000 tons of soil was lost from the study area in one year. Five parameters were

introduced to estimate soil erosion. But it can suggest that for that kind of flat floodplain human induced variables should also need to be incorporated to estimate accurate soil erosion rate.

Ghosh & Dwivedi, 2022 predicted soil erosion and deposition around island of a natural stream. The relationship between planform change with soil erosion and deposition was assessed in the research work.

Baruh at el., 2022 used 2d hydraulic model near the eroded river bank of the Jamuna river. It was found that dredging of the river bed helps to flow more water during high floods thus reduce bank erosion. A numerical Scenario was done by introducing dredging and series of permeable spurs and it was found that these setup reduce the bank erosion.

Yusoff at el., 2022 did a research work on river erosion and the study area was located on the downstream part of Sg Kelantan river. They determined the potential risk of bank erosion of the study area with no vegetative cover. According to final grain size distribution, the study area was classified against the RON index to obtain the potential risk of either “critical”, “moderate”, “very high”, “high” or “low” erosion.

Sultana, 2022 did spatial and temporal analysis of riverbank erosion and sediment deposition of Teesta river along five districts using multi-temporal Landsat images of MSS, TM, and OLI-TIRS. The collected images have been classified through ERDAS Imagine software. The study analyzed the decadal variation of erosion-deposition for last 42 years and concluded that dredging and bank protection measures should be implemented on most erosive districts.

Khan at el.,2022 studied on the river bar dynamics and bankline shifting in both short- and long-term time scale. The study area was Dharala river. ArcGIS and Google Earth pro satellite images were used for the analysis. The average deposition of the right bank has been found to be less than the average deposition in the left bank. The right bank faces severe bank erosion during monsoon period because of the meandering nature of the river.

Majumder & Mandal, 2022 assessed geotechnical properties of Ganges riverbank in the Malda

district, West Bengal, India. They determined the stability of riverbank by determining the value of uniformity Coefficient, Coefficient of Gradation and Sorting Coefficient. Developing particle size distribution curves of the bank of the study area, it has been found that the riverbank composed of fine to very fine sand. the soil formation of the bank helps to develop tension cracks. Percolation and sub-surface flow can easily occur due to this kind of soil formation which introduces riverbank erosion.

Saadon et al. (2020) used the Nonlinear AutoRegressive model with eXogenous inputs and QR factorization parameter (NARX-QR Factorization model). This model can estimate bank erosion rate of Sg. Bernam,Selangor, Malaysia. Near bank velocity, water depth and soil characteristics were given as the input variables. A straight least-squares procedure was followed to measure riverbank erosion rates. Number of models were run under the NARX-QR Factorization model. From 14 models, it has found that Models 1 and 9 has the most significant and the highest R2 at about 76% and 89%, respectively.

Saadon at el., 2021 developed multiple linear, non-linear and logarithmic functions to predict bank erosion for river Bernam in Selangor, Malaysia. To evaluate the model performance different statistical parameters were used such as degree of determination, discrepancy ratio were estimated. This research concluded that the logarithmic-transformation empirical equation is the best predictor.

Saadon at el.,2021 developed various empirical equations to predict bank erosion for the river Bernam, Malaysia. The length of the study area was about only 50 meters.Multiple linear and non-linear equations has been derived and the best predictor model was selected based on R2 and RMSE. Then the accuracy of the developed model was evaluated using graphical analysis and discrepancy ratio. If the D.R. lied between the range 0.5-2, it remarks as ‘yes’. The number of yes was the accuracy of the predicted values. Then percentage of yes is the accuracy of the predicted model.

Ali, M. and Zobeyer, H., (2021) studied recently research on river bank erosion using numerical modeling and deep learning techniques. The erosion deposition characteristics of the selected bank were determined using 32 years of satellite images. Hydrological characteristics of the selected

reach was determined by maximum, mean and median of historical discharge and water level data. In this research, 2D morphological numerical model was developed for the prediction of morphological changes and then compared with observed data. The developed model predicted bankline shifting for the year 2017,2018,2019 and 2020. It has found that out of 24 erosion locations, the developed model predicted erosion in 80% of the locations.

Khan, M. (2015) worked on bank erosion using MIKE21C and introduced revetment in the bank during setup of 2D morphodynamic model. He found that revetment helps to reduce near bank velocity. A correlation between hydraulic erosion and shear stress was established. He used hydrodynamic model but did not predict bank erosion .

Hasan, M.(2018) used the DELFT3D model to assess the hydro-morphological response of the Jamuna river by introducing gyrones in the river bank and concluded that the shear stress and velocity gradually decrease with the increasing number of gryones which will prevent bank erosion.

Hossain (1992) made an investigation of the total amount of sediment load in the lower Ganges and Jamuna river.According to the study, the average annual sediment flow through Bangladesh's main rivers was around 1.2 billion tons, with a high of 1.5 billion tons. Additionally, a correlation between water flow and sediment flow was constructed for use in real-world design issues. Moreover, the predicted total sediment flow was compared to the findings of earlier studies.

Laz, U. (2012) did research work on the hydro-morphological assessment of the Jamuna river by DELFT-3D. Her study area was some of the vulnerable areas such as Subaghacha, Sirajganj, Jamuna Bridge and also in the upstream near Kazipur and downstream near Chauhali. She found that the observed bed level was in good agreement with the model simulated bed level. Results reveal that erosion takes place in the channel bed and the deposition mainly takes place to the adjacent char areas and increased its width and area. It was also evident that the channel has been shifted westwards of the reach due to the shifting of the bank line of the river.

Surface Water Modeling Center, SWMC (2001), under the project titled "Morphological Assessment of the Rivers of Bangladesh," studied the morphological behavior of the river

Brahmaputra and some other rivers in Bangladesh, with a special emphasis on the river Brahmaputra.The study discovered that the river experienced overall aggradations from 1988-1989 to 1997-1998.

Pal, P. K et al. (2017) inspected the hydro-morpho dynamic changes of Jamuna River using the HEC-RAS 1D model and historical data analysis. Results revealed that between 1980 to 2014 during monsoon period discharge, water level, sediment transport rate and velocity significantly increased than pre-monsoon and post-monsoon period.

According to Akhand (2008), the Ganges flows through a morphologically active corridor with a highly mobile channel. The rate of erosion varies dramatically from year to year. During the study period, the rate of widening, rate of bank migration, and annual rate of erosion, were extremely high. The nature of the Ganges upstream is meandering, with bends migrating within an active corridor.During the last three decades (1980-2008), the Padma river's planform shifted from braided to straight and back again.

Paudel at al. (2022) did research on the effect of initial boundary conditions and sediment input for the changes of bed level composed of gravels. It has found that there is effect of initial boundary conditions in bed level changes. But there is a significant effect of sediment input for bed level changes for gravel river bed and also there is little impact of discharge on bed level changes.

Haque at el. (2020) applied 1d hydro-morphological modeling for Kobadak river. It has found that in the bifurcation the bed level rises abruptly up to 3meters in one year. The model was calibrated for the water level with Manning’s n. The width of the channel is small and this model gave satisfactory results in calibration and validation. Invert changes of bed level was simulated by 1D hydro-morphological model.

The Brahmaputra and Jamuna rivers' morphological behavior was investigated by Mukherjee (1995). The data source for this study was cross-sectional data for a number of chosen stations. According to this study, the left and right banks are vulnerable to river bank erosion. The variation in effective width and total width was also studied. It was found that the variation in effective width

changed more quickly than the variation in total width changed . It was found that the roughness co-efficient varied from 0.019 to 0.037 in the wet season and from 0.0103 to 0.0337 in the dry season.

Dey at el. (1998) has made some assumptions to derive the exponent "b" analytically for various total and bed load predictors. In this analysis, eight prediction formulas for five-load and three-bed loads were considered. In addition, the relationship between the exponent "b" and the Shields parameter (Θ) was examined.

Haque at el.(2020) applied GIS tools to analyze morphological conditions of Kobadak river. It has found that significant bed deposition was occurred during last 15 years. It has also found that the bank remains stable. It was analyzed by GIS and superimposing cross-sections of different years.

CEGIS, (2021) has developed an innovative device. It can predict the riverbank erosion one year in front of the Jamuna, the Ganges and the Padma Rivers. It is predicted based on time-series dry season satellite pictures.

Zhang et al. (2020) applied soft computing techniques in the braced excavations. The aim of this research work is to determine the maximum lateral displacement of wall. Four Deep learning technique were introduced. The performance of these model were evaluated based on four statistical parameters such as RMSE, R2, bias factor and MAPE. Ensemble method showed very accurate result from these four methods.

Zhang et al. (2021) also applied some methods of soft computing techniques in the prediction of the settlement of surfaces due to the construction of the tunnel. Then he found that XGBoost Extreme Gradient Boosting method response better than other soft computing methods that he used in the study.

Zhang & Goh (2016) modeled pile drivability using neural network models(BPNN) and Multivariate adaptive regression splines (MARS). They compared two models based on models predictions result and found that MARS can be effectively used to predict different parameters during pile driving .

Zhang et al. (2020) applied two ensemble learning methods for the prediction of undrained shear strength of clays. They found that Extreme gradient Boosting method respond with observed data very accurately than other models they used. This machine learning model can be very effective for geotechnical Engineers to estimate different important parameters of clay soils .

Zhang at el. (2021) wrote a review paper in the field of geotechnical Engineering about the application of deep learning. He specifically described four major algorithms of the Deep learning in Geotechnical field . Zhang et al. (2020) applied an Extreme gradient Boosting and random forest regression model to estimate the factor of safety(FS) in clayey soil in braced excavation

CHAPTER THREE
THEORETICAL BACKGORUND ON BANK EROSION AND NUMERICAL MODELS

3.1 General

Many research relevant to river bed and bank erosion were conducted by many scientists. Many literatures review has been done related to river bank and bed erosion. This chapter describes the theoretical backgrounds of riverbank erosion and stability. different concept such as hydrodynamic fluvial process, riverbank erosion mechanism, bank erosion rate, factors affecting bank erosion, hydrodynamic analysis etc. Besides, various mathematical equations and formula of RIVERFOW 2D, HECRAS, Regression model are also explained in this chapter. Terminologies, theories and mechanism of riverbank erosion have also been briefly described.

3.2 Bank failure Mechanisms

Bank erosion, mass failure , land use, seepage, surface erosion of banks, bank augmentation etc. are the main reasons of riverbank movement.

When water flows it exerts drag and lift forces on the boundaries. The generated forces tends to separate and entrain surface particles. Boundary of the river need to provide a force capable of resisting erosive forces to maintain in place the soil particles by the flow. This resisting force depends on median grain size, size distribution curve and particles chemical,electro-magnatic bonding. Bank erodibility can differ distance to distance along the reach due to different composition of bank materials.

Failures of bank material to resist erosion

Weakening and weathering of bank materials can increase bank erosion. Soil moisture condition and soil stratification beneath the bank surface are responsible for weakening and separation of soil grains. Moisture conditions of soil significantly influence the erosion rate of the riverbank. Rapid wetting and drying can cause swelling and shrinkage of soil. Thus wetting and drying contribute to tension cracks in the soil and induce to increase erosion rate of the soil.

Mass failure causing bank instability

Mass failure occurs due to imbalance between soil mass and gravitational forces. It occurs when river bed is eroded near the bank and thus there is increased in bank height. Hence it creates bank instability. To equal the imbalance force, forces tend to move soil down the slope, and mass failure occurs.

Surface erosion of banks

- The main reasons for surface erosion of river banks are:
- Surface runoff.
- current or waves which is generated by wind.
- sub-surface flow which is known as seepage
- shear stress.
- Mechanical action (desiccation, ship impact, activities of humans and animals).

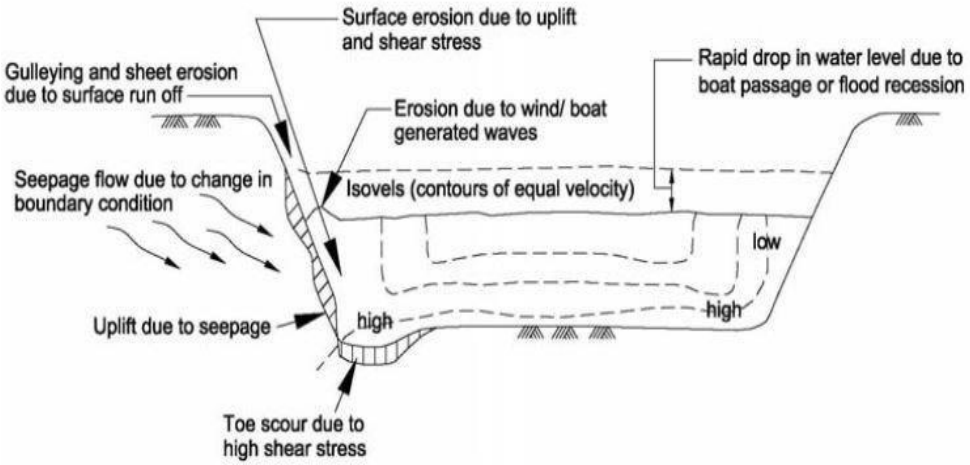

Figure 3.1: Processes of surface erosion (Hemphill & Bramley, 1989).

When water flows, it pulls a force in the direction of flow in the channel bed which is known as shear force. The shear which is generated by current flow is the main factor of bank erosion. Typical shear stress- induced distribution in a trapezoidal cross-section of a straight channel is shown in the following Figure 3.2:

primary and secondary flow

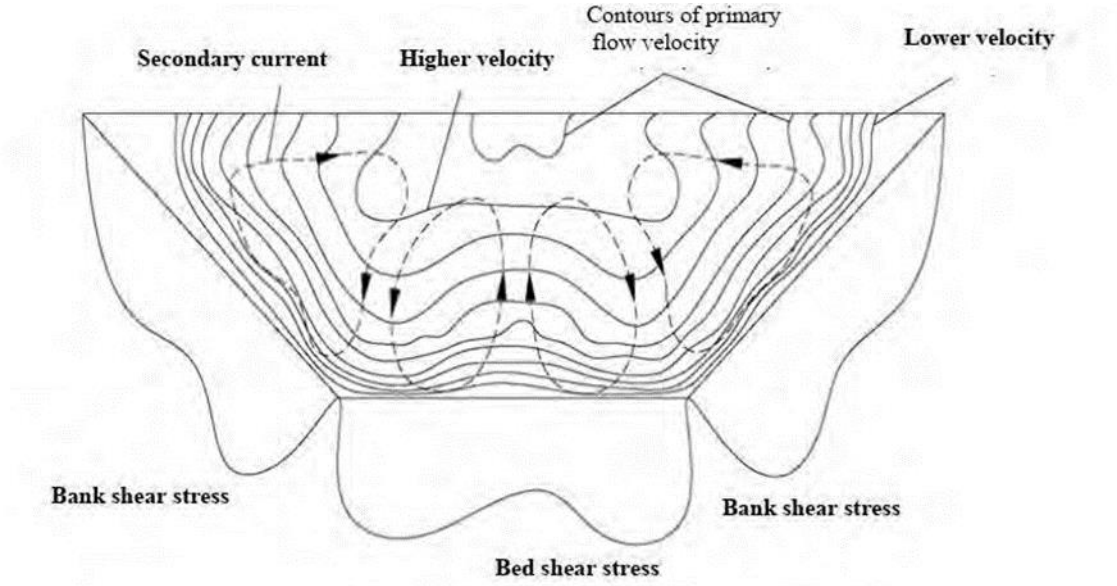

Figure 3.2: Contours of primary and secondary flows as well as the shear stress

Hydraulic fluvial process

Occurrence of hydraulic fluvial erosion is due to imbalance between bank material shear strength and water induced shear stress. Generally fluvial erosion process initiates if the hydraulic shear stress surpasses shear strength of bank material. As the shear stress is proportional to the square of friction velocity, shear stress will increase with the increase of velocity of flow. bank strength reduces as the bank becomes saturated due to increase in flow. Hydraulically induced failure may be of three types: bed degradation(vertical), basal cleanout, and undercutting.

Bed degradation

Bed degradation means erosion of river bed. It occurs when the shear stress of flowing water increases to the point that it initiates movement of channel bed soil particles. Generally, it occurs in the vertical direction. This it increases bank height. It also steepens bank slope and makes the bank vulnerable to undercutting.

Toe erosion

The process of removing supportive or protective materials at the bank toe is toe erosion. This usually occurs when discharge is high. The protective material may cause mass failure. The repeated cycle of the basal cleanout, undercutting, mass failure, and bank toe accumulation plays an important role in controlling the erosion rate of the riverbank.

Undercutting

The direct removal of bank materials laterally by running water is undercutting. Local effects suchas vegetation, presence of debris, bank soil characteristics such as poor drainage, and/or presence of a layer of non-cohesive materials. It often occurs on the outside bend of a meandering river. Undercutting is a fundamental process for the initiation of mass failure with the cohesive bank materials.

Mass failure process

Gravitation is one of the main reasons for mass failure.

Shallow slide

In this process, a soil layer moves along a plane parallel to the bank surface. Shallow slide failure generally occurs after a rotational and/ or slab failure (Thorne, 1998).This type of failure occurs when cohesion of bank material is low, and angles are steep, and whenbank angle, due to hydraulic fluvial erosion, exceeds the angle of internal friction of the bank material.

Rotational failure

Rotational failure is a deep-seated movement of a soil layer along a curved surface both downward and outward. After failure, the upper slope of the slipped block is typically tilted inward the bank. The failure causes the formation of the tensile crack along the vertical direction and/ or high pore water pressure in the bank material . It often occurs during water level drawdown after high flow events on banks. Rotational failure generally occurs on the Cohesive bank with a tall bank and shallow profile. It generates more significant sediment discharge than planer failure (Dapporto et al., 2003).

Wet Earthflow

In this process, the soil of a bank flows down the bank to form lobes of material at the toe and flows as a highly resistive liquid. This type of material is very weak . It can be easily removed by the flow of water (Thorne, 1998). Increase in flow causes increase in saturation which cause wet earthflow and

results in loss of strength on a section of a bank. Wet earth flow generally occurs on a low bank angle. As a result, bank is subjected to intense seepage and poor drainage.

Piping failure

Piping failure is the another failure mood but it slightly different form other failure.

Sand particles of river bank are removed in a particular way due to high groundwater seepage pressures and seepage flows. It results in the collapse of part of the bank. The failure is the result of groundwater flow along with layers of saturated river banks, with sand and coarser material sandwiched between layers of finer coarser material .

3.3 Equation of bank erosion rate

Normally, the excess shear stress is applied to determine erosion rate of the river bank. Widely accepted formula to estimate riverbank erosion is(Arulanandan et al., 1980; Partheniades, 1965)

$$\varepsilon = K_d(r - r_c)^a \quad ..(3.1)$$

where $\varepsilon(m/s)$ is the fluvial bank-erosion rate per unit time and unit bank area. (Pa) is the boundary shear stress applied by the flow, K_d (m^2s/kg) and (Pa) are erodibility parameters, and a (dimensionless) is an empirically derived exponent commonly assumed to be unity (Hanson, 1990a, 1990b; Hanson & Cook, 2004). If the river boundary shear stresses are below the critical shear stress (shear stress at which erosion begins), it is assumed that no erosion rate will be occured (Hanson,Osman & Thorne, 1988). Erosion occurs when the boundary shear stress exceeds the critical shear stress(Semmad et al., 2019).

Factors affecting the bank erosion

Knighton (1998) provided detailed information on factors influencing bank erosion processes. Some important factors are discussed below:

Properties of flow

Water induced shear stress initiate the bank erosion process. Near bank velocity is the important

factor that controls hydraulic erosion. High flows lower the river bed and it also removes bank material. Seepage depends of the properties of flow. Continuous drying and wetting also depends on the properties of flow.

Geometry of channel

Channel geometry means size, shape of the channel, longitudinal slope of the channel, straight or meandering appearance . Distribution of shear stress depends of channel geometry. Bank erosion largely depends on shear stress. Erosion rates are very high in the curve portion of the river bank because higher velocity is observed in the curved portion which results in higher shear stress. The locations which are very potential to riverbank instable can be determined from the geometry of the cross-sections.

Geometry of bank

The parameters of the bank geometry are height, slope length, profile and shape of the bank. For cohesive bank material, bank height and slope are critical parameters for assessing river bank erosion. When toe erosion occurs, the bank's height and steepness gradually increase and failures occur. There are types of failure mechanism of river bank and it depends on the geometry of the bank, flow properties and characteristics of soil at the point of collapse.

Characteristics of Bank material

The erosion rates largely depend on the characteristics of bank material. It is characterized by size, gradation, cohesiveness and stratification of bank materials. A river bank is generally composed of cohesive and non-cohesive material. It can be stratified or non-stratified. Pore water pressure is an important parameter for initiation of the river bank erosion. Pore water pressure is a significant problem for cohesive bank materials (Thorne & Tovey, 1981).When the water level gradually decreases in recession period of flood, positive pore water pressure is developed in the cohesive bank which lead to the mass movement of bank materials (Thorne & Tovey, 1981). Tension crack causes weakening of the river bank thus it creates bank instability(Morgan et al., 1999). The stratified bank consists of alternate cohesive and non-cohesive soil layers of different grain size distribution and permeability (Group, 1998; Simons & Li, 1982). Piping is very familiar in this type of stratified alluvial banks.

Soil-moisture condition of bank

Bank soil-moisture conditions depend on many factors such as soil moisture content, seepage, pore

water pressure and piping. Weakening and weathering is another factor which reduces the strength of bank material. It also decreases stability. Tension cracks in the river bank are developed due to continuous wetting and drying process which lead to failure of riverbank. Seepage forces developed soil pipes in the riverbank. It can reduce the cohesion of bank material (Knighton, 1998).

During recession period , the water level gradually decreases and at this time the bank is very suspicious to failure. The bank failure occurs if the bank material is near saturation and the confining pressure of the water approaches zero (Casagli et al., 1999; Simon & Collison, 2001). In stratified banks with lenses of sand and coarser material sandwiched between layers by river stage changes (Simons & Li, 1982). If the flow through the permeable layers is capable of dislodging and transporting particles, the material is slowly removed. This can lead to the undermining of properties of the cohesive upper bank leading to gravitation induced block failures.

3.5 Descriptions of the Mathematical Model used

3.5.1 Hydraulic Model in HEC-RAS

The open-source software HEC-RAS has been applied for assessing the flow of the northeast region of Bangladesh. HEC-RAS, which is dependent on finite difference solutions of the Saint-Venant equations (Peters et al., 2006) will be used to simulate the flood.

$$\frac{\partial \mathrm{A}}{\partial \mathrm{t}} + \frac{\partial \mathrm{Q}}{\partial \mathrm{x}} = 0 \qquad \ldots.4.1$$

$$\frac{\partial Q}{\partial t} + \frac{\partial (Q^2/A)}{\partial x} + gA\frac{\partial H}{\partial x} + gA\left(S_0 - S_f\right) = 0 \qquad \ldots.4.2$$

Here A = cross-sectional area normal to the flow; Q =discharge; g = acceleration due to gravity; H = elevation of the water surface above a specified datum, also called stage; S_0 = bed slope; Sf = energy slope; t = temporal coordinate and x = longitudinal coordinate. Equations 4.17 and 4.18 are solved using the well-known four-point implicit box finite difference scheme.

Hydro-morphological Model RIVERFLOW 2D

- It is a combined hydrologic-hydraulic model
- Finite volume numerical engine.
- Flexible non-structure mesh.
- It can ensure model stability during subcritical and supercritical flow regimes.
- Robust dry-wet bed algorithm.

- This model was validated for real world projects.
- It is not only hydrodynamic model. Different modules such as sediment transport,pollutant transport can be added with hydrodynamic model.

RIVERFLOW 2D uses the Navier-stokes equation and the model does not consider turbulence terms. The assumption about bed shear stress is that it follows the depth average velocity directions. Depth averaged mass and momentum conservation equations are used to describe shallow water flows. Partial differential equations of the shallow water flows will be expressed here. The conservative form of these equations are is as follows:

$$\frac{\partial U}{\partial t} + \frac{\partial F(U)}{\partial x} + \frac{\partial G(U)}{\partial y} = S(U, x, y) \quad \ldots.4.2$$

where U = (h, q_x , q_y)T is the vector of preserved variables and h is representing the water depth, q_x= uh and q_y = vh the unit discharges, (u, v) represents the depth averaged depth-averaged components of the velocity of vector u along with the x and y coordinates respectively. The flux vectors are given by:

$$\text{F} = (qx, \frac{q2y}{h} + \frac{gh\text{^}2}{2}, \frac{qxqy}{h})T, G = qy, \frac{qxqy}{h}, (\frac{q2}{yh} + \frac{gh\text{^}2}{2})T \quad \ldots.4.3$$

where g is the acceleration due to gravity. After assuming a hydrostatic pressure distribution, the term 0.5gh^2 in the fluxes have has been found in every water column. The source term vector (S) combines the effect of pressure force over the bed and the tangential forces generated by the bed stress

$$S = (0, gh(S0x - Sfx), gh(S0y - Sfy))T \quad \ldots.4.4$$

where the bed slopes of the bottom level z_b are

$$S0x = -\frac{\partial zb}{\partial x}, S0y = -\frac{\partial zb}{\partial y} \quad \ldots.4.5$$

and the bed stress contribution is modeled using the Manning friction law so that:

$$\text{Sfx=n\^2u}\frac{\sqrt{(\text{u\^2+v\^2})}}{\text{h\^4/3}}, Sfy = n\text{^}2v\frac{\sqrt{(u\text{^}2 + v\text{^}2)}}{h\text{^}4/3} \quad \ldots.4.6$$

with n the roughness coefficient.

The relevant formulation of the model derives from the depth averaged equations expressing water volume conservation, solid volume conservation and water momentum conservation.

3.6 Model Sediment Equations

system of partial differential equations can be expressed in coupled form as follows

$$\frac{\partial U}{\partial t} + \frac{\partial F(U)}{\partial x} + \frac{\partial G(U)}{\partial y} = S(U) + R(U) \quad \ldots.4.7$$

Where U =(h, q_x , q_y , h φ1 , . . . , hφN , zb)T 4.8

are the conserved variables. Here h is representing the water depth, q_x = hu and q_y = hv are the unit discharges, with (u, v) are the depth averaged components of the velocity vector u along the x and y coordinates respectively. φp, with p = 1, ..., N is the scalar depth-averaged concentration of the N different sediments transported. The total bed elevation z_b is defined as $z_b = \sum 1N\ z_p$ allowing the possibility of a heterogeneous soil composition. It means different fractions of material may coexist.

Bedload model

Wn bedload is the dominant sediment transport mechanism. At that condition the influence of the suspended load is negligible, system (4.6) reduces to Mass conservation

$$\frac{\partial h}{\partial t} + \frac{\partial (hu)}{\partial x} + \frac{\partial hv}{\partial y} = 0 \quad \ldots.4.9$$

Momentum conservation in x direction

$$\frac{\partial (hu)}{\partial t} + \frac{\partial [hu\text{^}2 + (\frac{1}{2})gh\text{^}2}{\partial x} + \frac{\partial (huY)}{\partial y} = \frac{\rho bX}{\rho W} - \tau bX/\rho W \quad \ldots.4.10$$

Momentum conservation in y direction

$$\frac{\partial (\mathrm{hu})}{\partial \mathrm{t}} + \frac{\partial (\mathrm{huY})}{\partial \mathrm{x}} + \frac{\partial [\mathrm{hv\text{^}2}+(\frac{1}{2})\mathrm{gh\text{^}2}]}{\partial \mathrm{y}} = \frac{\rho \mathrm{bY}}{\rho \mathrm{b}} - \frac{\tau \mathrm{by}}{\rho \mathrm{W}} \quad \ldots.4.11$$

Bed elevation changes for the bed sediment

$$\frac{\partial zP}{\partial t} + \frac{\partial}{\partial x}(\frac{1}{1-\rho P})qb\rho x + \frac{\partial \{(1-pP)qbpy\}}{\partial y} = 0 \quad \ldots.4.12$$

where pP is representing the porosity of each sediment fractions present in the bed layer. Here qbp,x and qbp,y are the corresponding volumetric sediment fluxes per unit time and width. It can be determined through several deterministic laws or sediment transport formulas.

Engelund-Hansen Transport equation

The total load transport equation by Engelund-Hansen (1967) was created using flume data and relatively uniform sand sizes between 0.18 mm and 0.95 mm. England Hansen is the simplest transport equation which explicitly depends on the stream power (V2τ3/2) and the material's d_{50} . It

frequently can compute low transports for large grain classes. Typically, Engelund-Hansen should only be used in sand systems. The equation is :

$$g_s = V\left(\frac{\tau}{(\gamma s-\gamma)}\right)^{\frac{3}{2}} * \sqrt{\left(\frac{d50}{g\left(\frac{\gamma s}{\gamma}-1\right)}\right)} = V^2(\tau *)^{\frac{3}{2}}\sqrt{(\frac{d50}{g(\frac{\gamma s}{\gamma}-1)})} \quad \ldots 4.13$$

Where:

g_s = Sediment transport by unit width

γ = Unit weight of water

τ_b = Bed shear stress

V = velocity of flow

γ_s= Unit weight of sediment

τ^*= Dimensionless Shields Number ($\tau b/\gamma s$-$\gamma d50$))

d50 = Median particle size

Meyer-Peter Muller transport equation

One of the first equations created and still one of the most popular is the Meyer-Peter and Müller (MPM) equation from 1948. This relationship is just an excess shear one. In its most basic, dimensionless, volumetric form, Parker (2006) describes MPM as.

$$q_{*b} = 8(\tau_* - \tau_{*c})3/2\ ,\ \tau_{*c} = 0.047 \quad \ldots 4.14$$

Where q_{*b} and τ_* are dimensionless transport and mobility parameters respectively, where:

$$\tau_* = \frac{\pi}{(\gamma_s-\gamma)d_m}, q_{*b} = \frac{q_b}{\sqrt{Rgd_m d_m}} \quad \ldots 4.15$$

The MPM equation was developed from sand and gravel flume Scenarios with plane bed conditions. Since uniform gravel was the focus of the majority of the MPM Scenarios, gravel systems are where the transport function MPM is most useful. MPM frequently underestimates the transport of finer materials.

Suspended Load Model

When the suspension load is dominant, the term of bed load can be neglected. The system (4.6) is written as Mass conservation

$$\frac{\partial(h)}{\partial t} + \frac{\partial(hu)}{\partial x} + \frac{\partial(hv)}{\partial y} = \frac{\sum Rp}{1-\ pp} \quad \ldots . 4.16$$

Momentum conservation in x direction

$$\frac{\partial(hu)}{\partial t} + \frac{\partial[hu\text{^}2 + (\frac{1}{2})gh\text{^}2]}{\partial x} + \frac{\partial(huy)}{\partial y} = \frac{pbx}{\rho w} - \frac{\tau bx}{\rho w} \quad \ldots 4.17$$

Momentum conservation in y direction

$$\frac{\partial(hu)}{\partial t} + \frac{\partial(huy)}{\partial x} + \frac{\partial[hv2 + (1/2)gh2]}{\partial y} = \frac{pby}{\rho w} - \frac{\tau by}{\rho w} \quad \ldots 4.18$$

Sediment mass of the fluid layer for the suspended sediment p

$$\frac{\partial(h\varphi p)}{\partial t} + \frac{\partial(hu\varphi p)}{\partial x} + \frac{\partial(hv\varphi p)}{\partial x} = Rp \quad \ldots 4.19$$

Bed level evolution

$$\frac{\partial(zb)}{\partial t} = -N\sum P = 1\,(\frac{Rp}{1 - pp}) \quad \ldots 4.20$$

where Rp = αpωs,p(φP – φP) accounting for the volumetric solid exchange flux between the bed and the flow for the sediment p. The term φ∗p is the equilibrium volume concentration. It is obtained through a solid transport discharge law. The term φp represents about the information about the suspension sediment quantity that is transported. The presence of the settling velocity ωS,p is considered by both concentrations. The empirical factor αP representing the difference between the near-bed sediment concentration and the depth-averaged suspended concentration. The settling velocity ωS,p can be estimated through several laws. It is a function of the sediment density and the grain diameter.

3.7 Regression Modeling using Machine Learning

Regression models are the relationship between a response (output) variable, and one or more predictor (input) variables. Statistics and Machine Learning Toolbox™ allows to fit linear, generalized linear, and nonlinear regression models. Once a model is fitted, it can be used to predict or simulate responses.

Statistics and Machine Learning Toolbox also provides nonparametric regression methods to accommodate more complex regression curves without specifying the relationship between the response and the predictors with a predetermined regression function. The trained model can be predicted for new data. Gaussian process regression models can be applied to compute prediction intervals.

Regression Tree Ensembles

Random forests, boosted and bagged regression trees

A predictive model is a group of regression trees. A weighted combination of multiple regression trees make up its structure. In general, combining multiple regression trees can improve predictive performance.

Ensemble methods can enhance the predictive performance of a given statistical learning or model fitting technique. The main principle of ensemble methods is straightforward. Instead of using a single fit of the method, it is a linear combination of a few model fitting techniques.

For calculating a real-valued function and considering the framework of the function estimation is very simple.

$$g : IRd \rightarrow IR \quad \ldots 4.18$$

based on data (X1, Y1), . . . , (Xn, Yn) where X is a dimensional predictor variable and Y is a univariate response. Generalizations to other functions g(·) and other data-types are possible. Assuming a function gˆ(·) and given data as input (as above) and this can be called as base procedure. If d is small, the base procedure could be a nonparametric estimation. On the other hand, if dis greater than 2, the base procedure could be nonparametric statistical method with some structural restrictions such as a regression tree. Running a base procedure many times with the changing the input data, the original idea of ensemble methods is to use reweighted original data to obtain different estimates gˆ1(·), gˆ2(·), gˆ3(·), . . . based on different reweighted input data. An ensemble-based function can be constructed to estimate gens(·) by taking linear combinations of the individual function estimates gˆk(·):

$$\hat{g}ens(\cdot) = \sum_{K=1}^{M} ck\hat{g}k(\cdot) \quad \ldots 4.19$$

where the gˆk(·) are obtained from the base procedure based on the kth reweighted data-set. For some ensemble methods, e.g. for bagging, the linear combination coefficients ck ≡ 1/M are averaging weights;for other methods ΣMck increases as M gets larger.The relatively easy-to-use ensemble method gained popularity for its ability to boost a base procedure's predictive performance. The bagging procedure turns out to be a variance reduction scheme, at least for some base procedures, which is one of several causes for this. However, the (model) bias of the base procedure is primarily being reduced by boosting methods. This alone suggests that ensemble

methods like bagging and boosting are very different.

3.8 Statistical parameters performance evaluation

Four statistical parameters such as RMSE,MAE, MSE and R^2 were used to evaluate the performance of the multi-variate regression models.

The root-mean-square error (RMSE) is a commonly used metric for determining the discrepancies between values (sample or population values) predicted by a model or estimator and the values actually observed.

$$RMSE = \sqrt{\frac{\sum_i^N (y_i - y_{pi})\text{^}2}{N}} \quad \ldots 4.20$$

Mean absolute error (MAE) is a statistical measure of mistakes between paired observations describing the same phenomena.

$$MAE = \frac{|y_i - y_p|}{N} \quad \ldots 4.21$$

Mean squared error (MSE), a measure of statistical model error.It evaluates the average squared difference between the values that were anticipated and those that were observed.

$$MSE = \frac{\sum_i^N (y_i - y_{pi})\text{^}2}{N} \quad \ldots 4.22$$

Correlation coefficient(R^2) is a statistical indicator of how strongly two variables are linearly related.

$$R\text{^}2 = 1 - \frac{RSS}{TSS} \quad \ldots 4.23$$

Where, Y_{pi} = The predicted value for the i^{th} observation,

y_i = The observed(actual) value for the i^{th} observation,

N = Total number of observations.

RSS=sum of squares of residuals,

TSS=total sum of squares.

CHAPTER FOUR
METHODOLOGY

4.1 General

Various types of data such as sediment data, bathymetry and hydraulic data, need to be collected to perform numerical model. Data collection is the most important step for conducting any research work to represent the field condition in a realistic model. For this analysis, two types of data are collected for hydrodynamic, morphological and regression modelling. This chapter describes briefly the collection of data and methodology of performing the work.

4. 2 Methodology of the study

All data required for the study have been collected from relevant sources. After collecting of data, first 2D hydro-morphological model was setup using RIVERFLOW 2D. The hydro-morphological model was calibrated and validated for the water level with Manning's 'n'. This model was run for different options and bed level changes were analyzed. Then hydro-dynamic model HEC-RAS 1D and HEC-RAS 2D was setup. After the calibration and validation the hydro-dynamic models, the model was simulated. After simulation of hydraulic model, five variables were extracted such as maximum water level, maximum velocity, maximum left over bank discharge, minimum water level and maximum bed slope. Bank erosion of the selected reach was estimated from Google satellite images.Five variables and one output variables were processed in MATLAB to calibrate the model. The multi-variate regression models were evaluated based on four statistical parameters such as RMSE, MSE, MAE and R^2 .Then the multivariate regression model was applied to predict the model for the year 2019,2020 and 2021 . The output bank erosion rate was compared with observed bank erosion rate and the performance of the models were evaluated based on statistical parameters and discrepancy ratio.

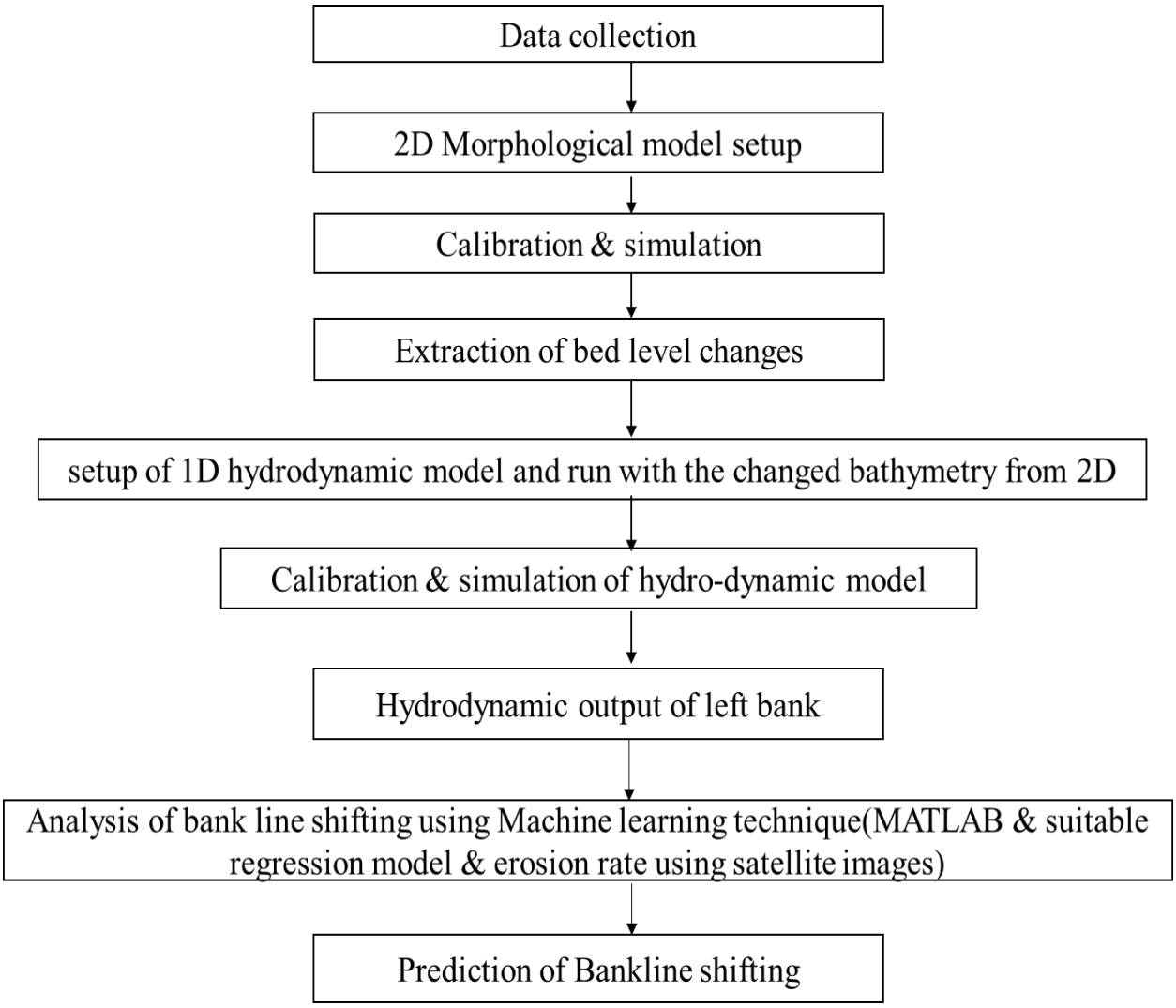

Figure 4.1: Flow chart showing the methodology of study

4.2.1 Data collection

Quality data are a prerequisite for reliable model setup, model results, and understanding to understand the existing physical process. To determine bed level changes of the Jamuna river and bankline shifting of the selected reach of Jamuna river various data have been collected. With proper care, data are gathered to make the result more realistic. A brief description of data collection are as follows:

4.2.1.1 Satellite image

satellite image of the study area for the year 2014-2021 was analyzed in Google earth pro and

erosion rate was estimated.

4.2.1.2 Water level data

Water level data at different locations were collected from Bangladesh Water Development Board (BWDB). Water level data of three stations that are Bahadurabad (SW46.9L), Kazipur (SW49A) and Sirajganj (SW49) were collected for the year 2011-2020.

4.2.1.3 Discharge Data

Discharge data was collected for the station Bahadurabad for the year 2011-2020(Table 4.1) to investigate hydro-morphological conditions of the Jamuna River.

4.2.1.4 Bathymetry data

The bathymetry data of the Jamuna river have been collected from IWM and BWDB. These surveyed bathymetry data covers the entire 77 Km reach of Jamuna river from Bahadurabad to Sirajganj station. The spacing between transect line is about 200 m interval.
The summary of the data collection has shown in Table 4.1.

Table 4.1 : Summery of data Collection

Data type	**Source**	**Data location**	**Period**
Discharge	BWDB	Bahadurabad	2011-2020
Water level	BWDB	SW49A,SW49, SW46.9	2010-2020
Cross-section	BWDB & IWM	Bahadurabad-Sirajganj	2011, 2018,2019,2014
Sediment data	BWDB	Bahadurabad	2010-2019
Satellite images	Google earth pro	Bahadurabad-Siarjganj	2014-2021

4.3 Two dimensional hydro-morphological Model setup

The steps that are followed to setup 2D hydro-morphological model are given below:

- Setup WGS projection file;

- Processing of cross-sections.
- Generation of domain outline,
- Generation of trimesh,
- boundary condition shapefile;
- Set up model parameters and simulation;
- Run the model simulation;
- Analyze the simulation results.

4.3.1 Setup WGS projection file

The DEM is originally in Geographic co-ordinate (Lat-Long) system. For the transformation of the coordinate system, ARC-GIS 'Define Projection' Tool needs to use and set to WGS 1984 UTM 46N projection. Then Riverflow 2d_Qgis was opened and projection was set to WGS 1984 UTM 46N.

4.3.2 Processing of cross-sections data

The cross-sections of the study area was inserted in Q-GIS. This includes the geometric extents, geometric feature definition such as channels or banks. After creation of raster file from cross-sections data, several cross-sections were extracted which are represented in Fig.4.2,4.3, 4.4 and 4.5. Cross-section Map was shown in Fig.4.6.

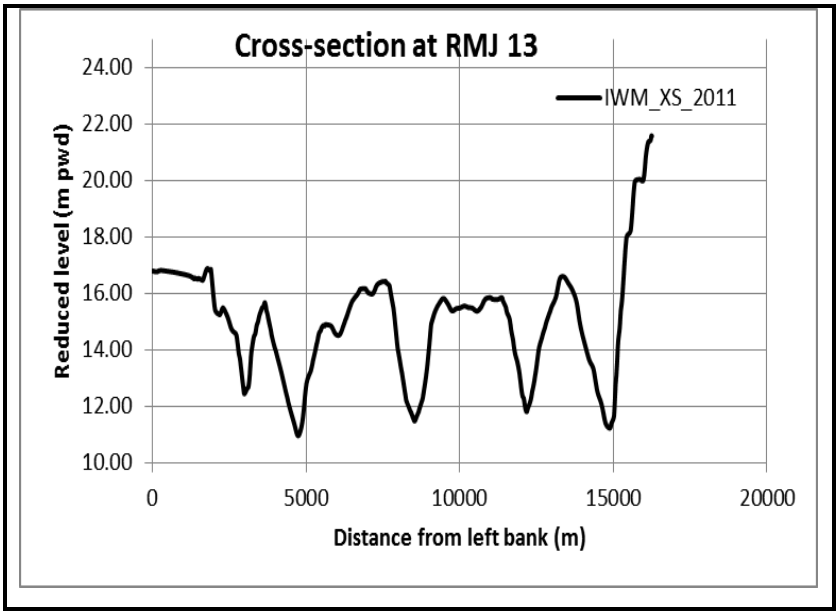

Figure 4.2 :Cross-section at RMJ 13

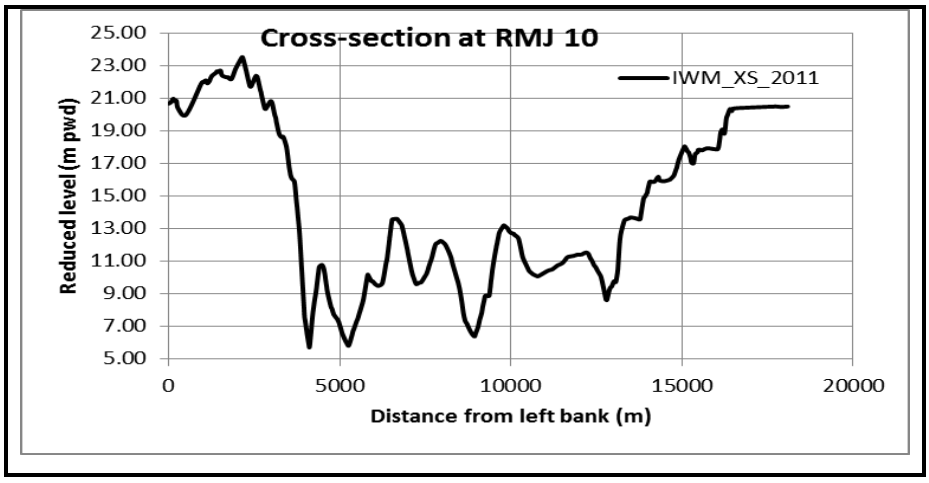

Figure 4.3 : Cross-section at RMJ 10

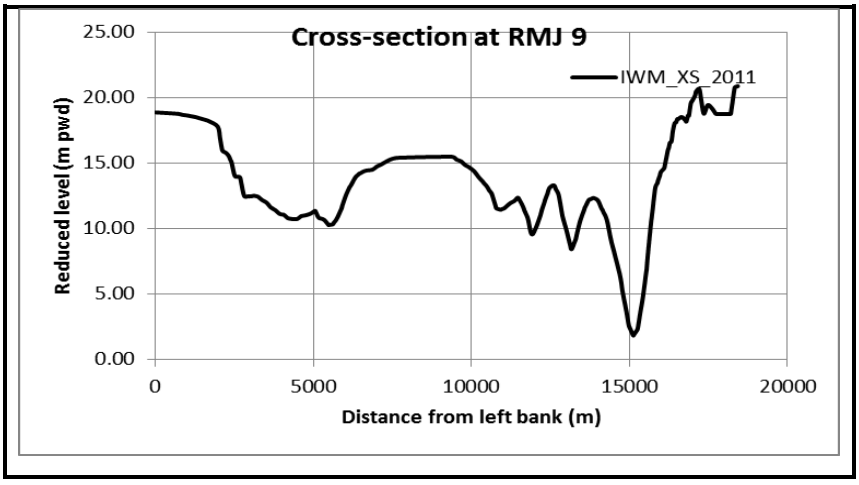

Figure 4.4 : Cross-section at RMJ 9

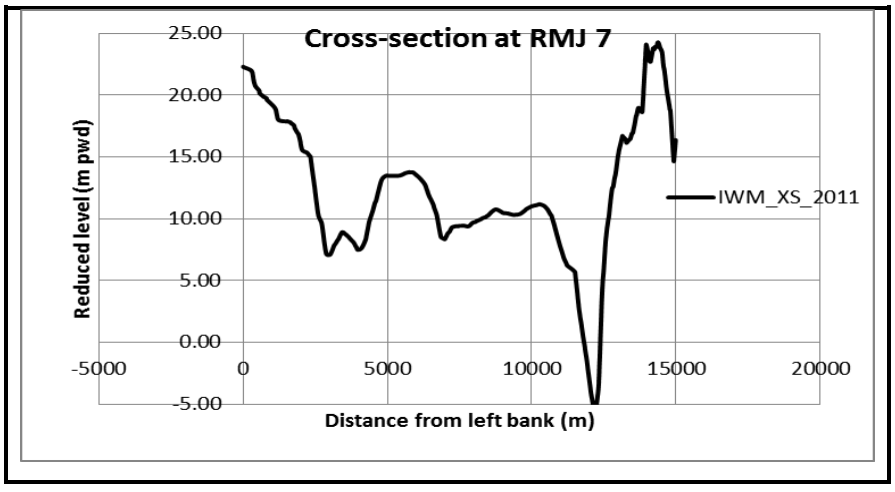

Figure 4.5 : Cross-section at RMJ 7

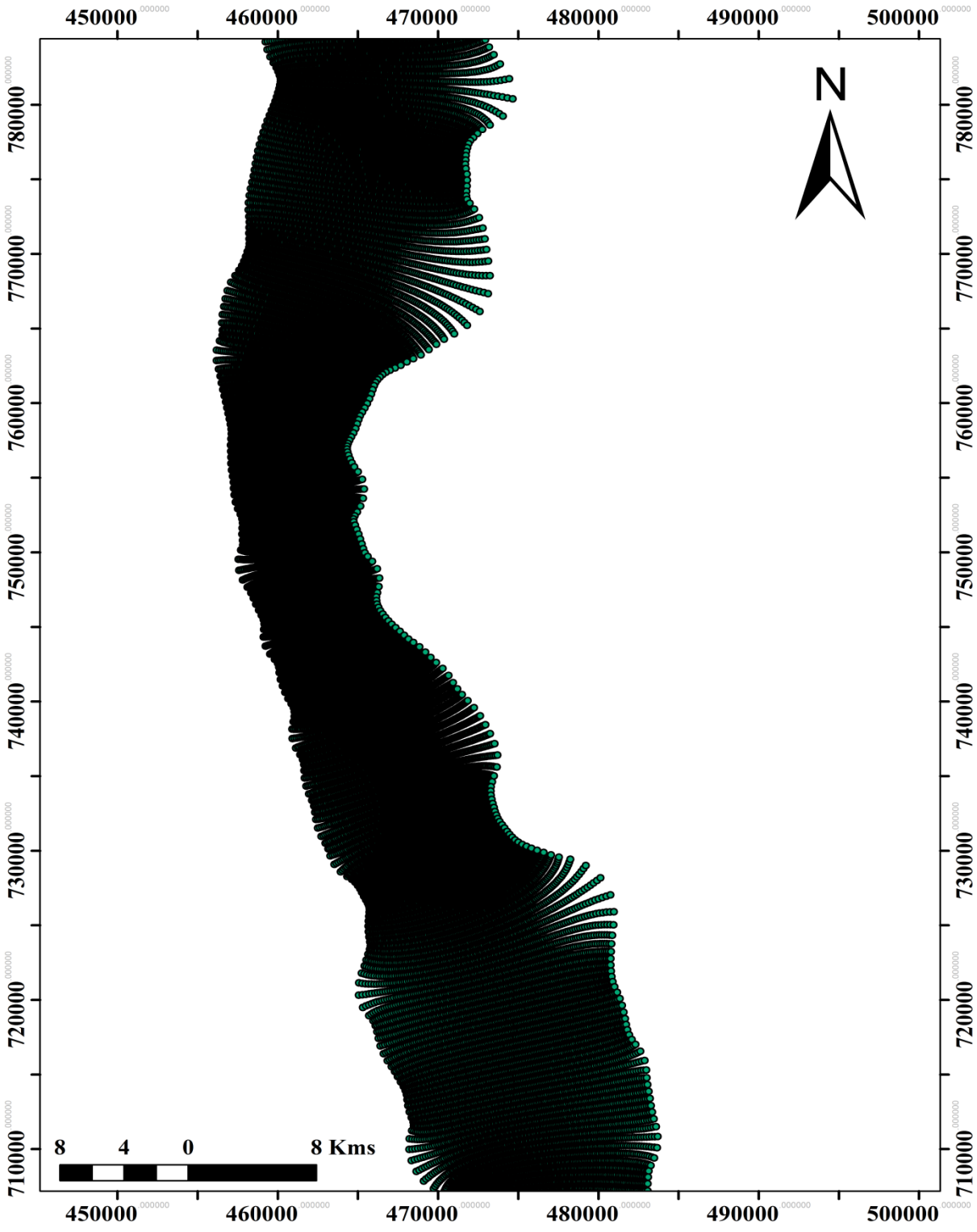

Figure 4.6 : Cross-section Map of the study area

4.3.3 Creation of Domain outline

The domain outline was created which represent the study area which is shown in Figure 4.6. Cell size is very important because due to cell size the model can become instable and it can also take a lot of time to complete the simulation.The cell size was given 500 meter.

Figure 4.7 : Creation of domain outline

4.3.4 Creation of Tri-mesh

After creation of domain outline, trimesh was generated (Fig.4.8). The shape of trimesh is triangle. It is created according to the cell size.

4.3.5 Boundary condition

upstream boundary condition was given as .QVT file at Bhadurabadh staion for the year 2011-2020.The downstream boundary condition in stage hydrograph for the year 2011-2020 at the Kazipur station .

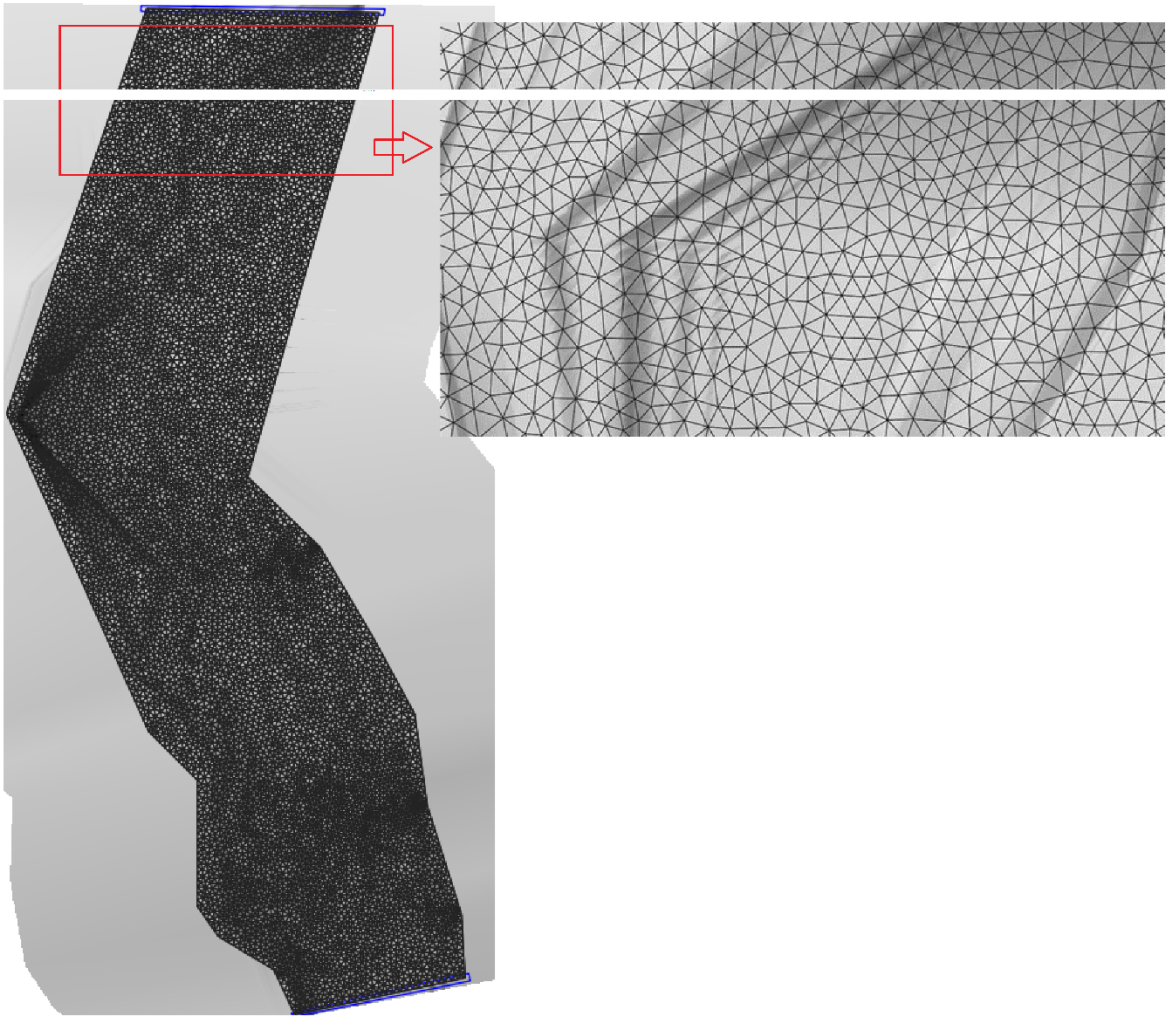

Figure 4.8 : Tri-mesh for RIVERFLOW 2D model setup

4.3.6 Boundary data

It is necessary to use hydrological and morphological data at the model boundaries to simulate the hydro-morphological model. For this model, time-series data of discharge and sediment data has been used as an upstream boundary condition, and the stage hydrograph has been used as the downstream boundary condition.

4.3.7 River flow 2D model control

The model is simulated for Engelund-Hansen transport function . To determine bed level changes of the some specific cross-section and profile of the study area, a period of time of 39696 hours was considered. The hydro-morphological timestep has been set to 1 hour for the simulations. The 2D hydro-morphological model was run under Engelund-Hanseen formula. Reduction factor was also introduced.Different parameters used in the model domain shown in following Table 4.2 .

Table 4.2: Riverflow 2D model control parameter

Simulation Description	Start time (hr)	Time step (hr)	End time (hours)	Transport function	Reduction factor
Mobile bed	0	1	39696	Engelund-Hansen	1

4.4 One dimensional model setup

4.4.1 HEC-RAS 1D model setup

4.4.1.1 Creation of new project and projection setup

First, new project was created and WGS 1984 UTM 46 N projection file was assigned in Ras-Mapper.

4.4.1.2 Cross-section generation in RAS-Mapper

Raster file was inserted (Fig. 4.9) and cross-section was drawn at 300 meters interval. Automatic extraction of these elevation values by RAS Mapper results in the creation of a geometry file in the HEC-RAS geometry window.Then the geometry data was saved.The created bathymetry is opened in the geometry editor window of HEC-RAS after being pre-processed in RAS Mapper. The river's roughness values were provided in a table.

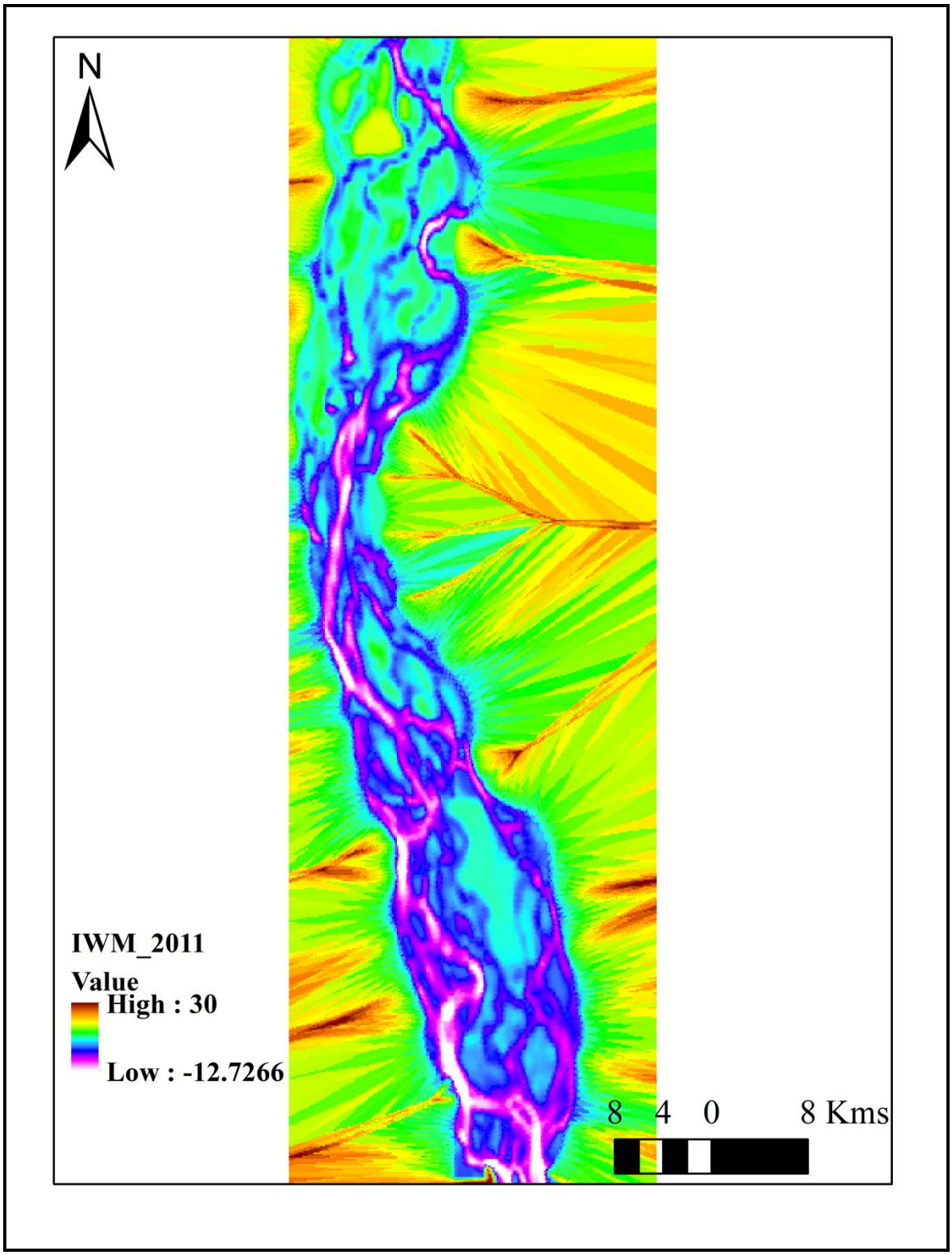

Figure 4.9: Terrain used in RAS Mapper

4.4.1.3 Flow Data and Boundary Condition

For hydro-dynamic modeling, unsteady flow model was developed for which boundary conditions are as following(Fig.4.10):

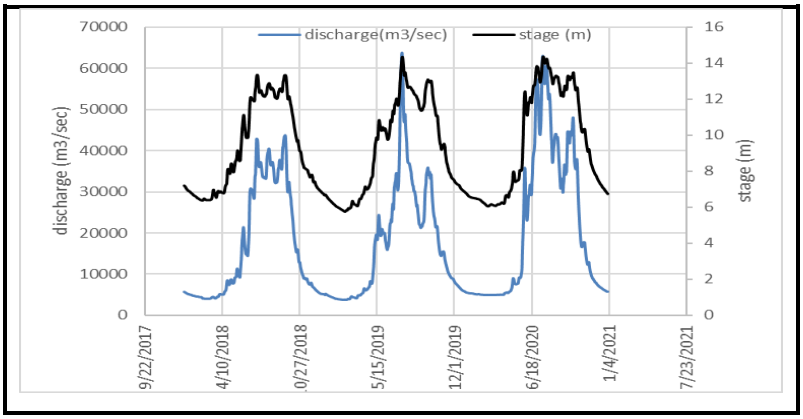

Figure 4.10: Flow and stage hydrograph as boundary data

4.4.1.4 Performing Hydraulic Computations:

Most often, a hydrodynamic-numerical model such as HEC-RAS is used for the assessment of floods in rivers and channels. These types of numerical models give simulation based on mathematical expressions. The "numerical" discretization of the continuum is typically the only method that can be used to solve the difficult mathematical equations that describe the flow process of surface water (space and time).

HEC-RAS can perform three types of hydraulic computations. Such as-

•Steady flow analysis

When the flow parameters such as discharge,velocity, water depth, viscosity, temperature remain constant with time at a specific location is called steady flow.

•Unsteady flow analysis

When the flow parameters such as discharge,velocity, water depth, viscosity, temperature changes with time at a specific location is called unsteady flow.

•Hydraulic design function

The primary objective of hydraulic design is to make sure structures are strong enough to prevent worsening of natural flooding. It is also need to ensure that the structure can withstand the design

flood and still be accessible. This is necessary to safeguard both the people and property upstream and downstream of a highway structure.

Scour is a hydraulic design parameter. The term "scour" describes washing away of streambed.

4.4.2 Two dimensional hydrodynamic model setup

To setup a hydro-dynamic model first, new project was created. Then WGS 1984 UTM 46 N projection file was set. Projection is very important to correctly locate the study area. After projection file setup, Cross-sections were processed to create raster file and then it was added in RAS-Map. 2D flow area was selected which describes the boundary of the study area. Rectangular mesh was generated where length and width of the each rectangular mesh was 300 meter (Fig. 4.12). Upstream and downstream boundary condition was assigned in the model. In Bahadurabad station, discharge was given as upstream boundary condition for the year 2018,2019 and 2020. In Sirajganj station,stage hydrograph was given as downstream boundary condition for the same year(Fig.4.10).

4.5 Regression model setup in MATLAB

4.5.1 Regression learner

First, Mat lab software was opened. Then, Regression learner was selected. Data set for calibrating the regression model was saved in a excel file in definite folder. Then this excel file was selected manually. After that, this selected data set was run for calibration to predict Bankline shifting. Suitable regression model was developed.

4.5.1.1 Scenario one (HECRAS 1D and regression model)

Five hydrodynamic variables were extracted from 1D hydrodynamic modeling for the year 2018 (Figure 4.11). Erosion rate was estimated for the year 2018 from Bahadurabad station to Sirajganj station at 300 meters interval. Then five input variables and one output variable were proccessed in MATLAB regression tool. Different parameters such as leaf size, learning rate was adjusted to calibrate the regression model. Data set has been given in appendices in Table 4.3.

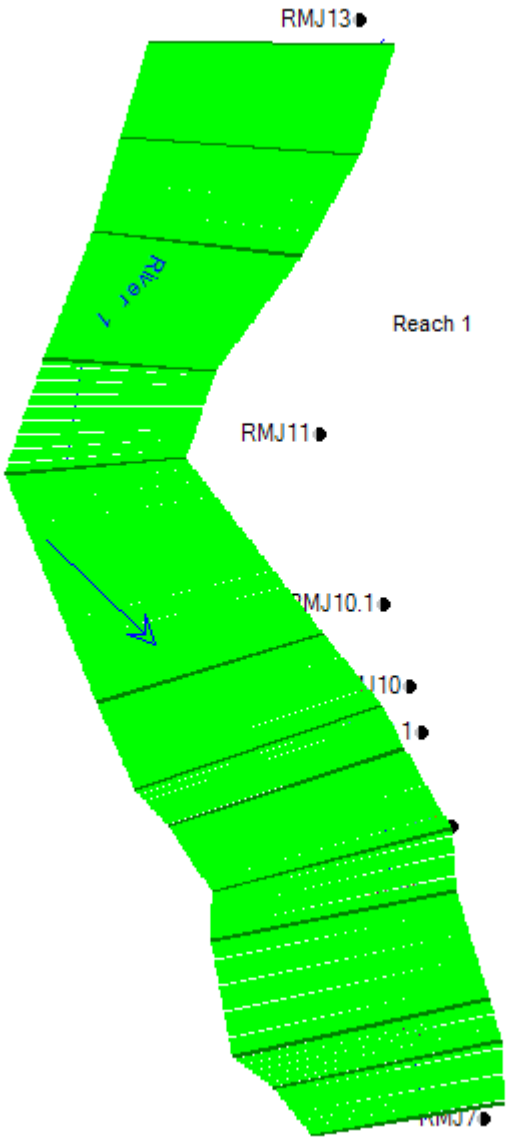

Figure 4.11: cross-sections that were used to extract hydraulic parameters (scenario 1)

4.5.1.2 Scenario two (HECRAS 2D and regression model)

Here in this Scenario, 3 variables such as minimum, maximum water level and maximum velocity along the length of channel were extracted from 2D hydrodynamic modeling (Figure 4.12). Then three input variables and one output variable has been processed in MATLAB regression tool. Different parameters such as leaf size, learning rate was adjusted to calibrate the regression model. Data set has been given in appendices in Table 4.4.

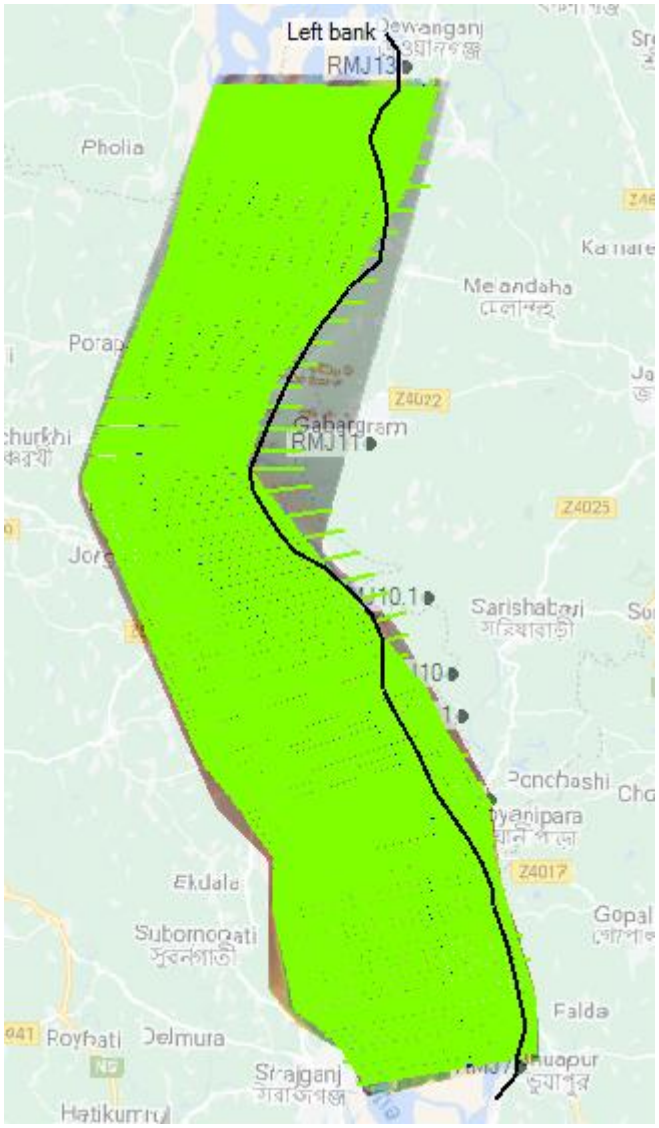

Figure 4.12: cross-sections that were used to extract hydraulic parameters (scenario 2)

CHAPTER FIVE
ANALYSIS, RESULTS AND DISCUSSION

5.1 General

The results of the hydro-morphological conditions and bankline shifting in the chosen reach of the Jamuna River are presented in this chapter. Using numerical modeling rfd2d qgis, the first section will display the bed level changes of the selected reach and net area changes of some selected cross-sections. The bed level changes at various points along the longitudinal profile and cross-section will be discussed in this chapter. The second section will focus on the prediction of river bank shifting as a result of five variables, including discharge, velocity, minimum, maximum, and channel slope. Utilizing MATLAB, regression models were set up. After the calibration of the regression model, the output results of the multi-variate regression model will be discussed and compared with the output results of the CEGIS prediction model.

5.2 Hydro-morphological model results

5.2.1 Model calibration

Model calibration means the adjustment of model parameters. It helps to obtain real field representation. Therefore, it is mandatory to calibrate the model before the simulation of model. In this study, model has been calibrated for the month May, June and July for the year 2018 and validated for the same month for the year 2019 as shown in Figure 5.1 and 5.2. The R^2 was found 0.86 for calibration and 0.93 for validation. It means that there is very good agreement between observed and simulated water level. The morphological model was also calibrated using some cross-sections such as RMJ 13, 12, 10, 9, 8, 7. The simulated and measured cross-sections are shown in Figure-

Figure 5.1 : Water level calibration at Kazipur station

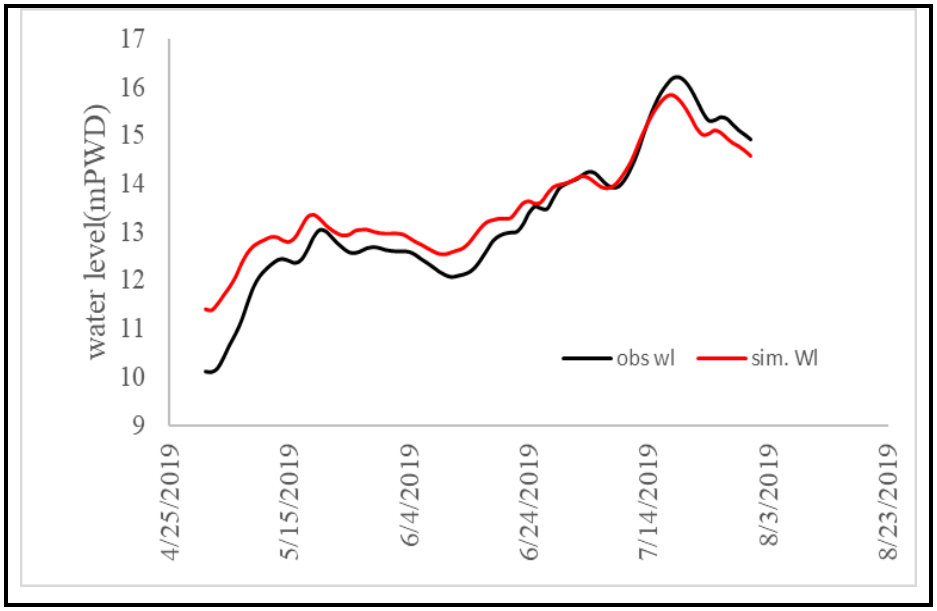

Figure 5.2: Water level validation at Kazipur station

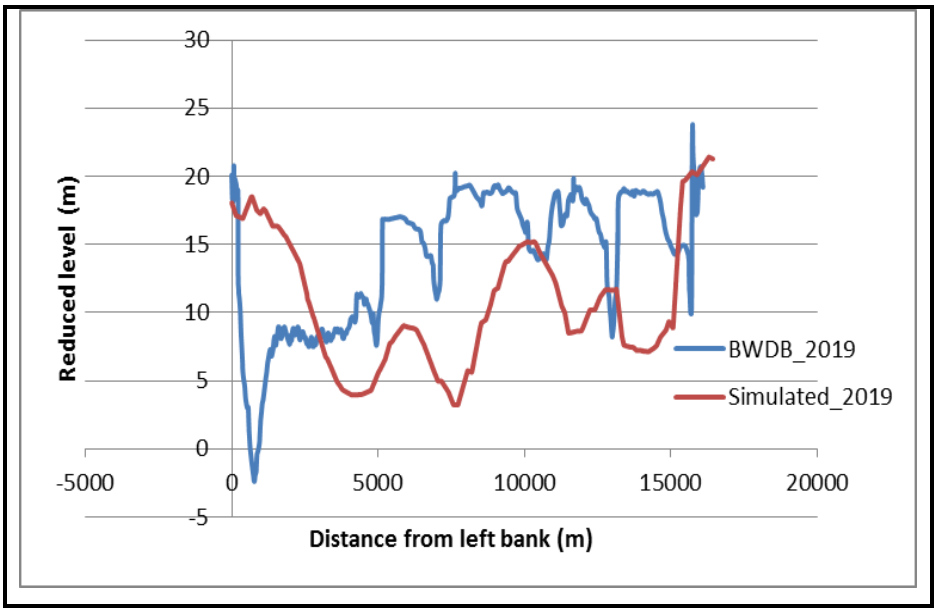

Figure 5.3: simulated and measured cross-section at RMJ 13

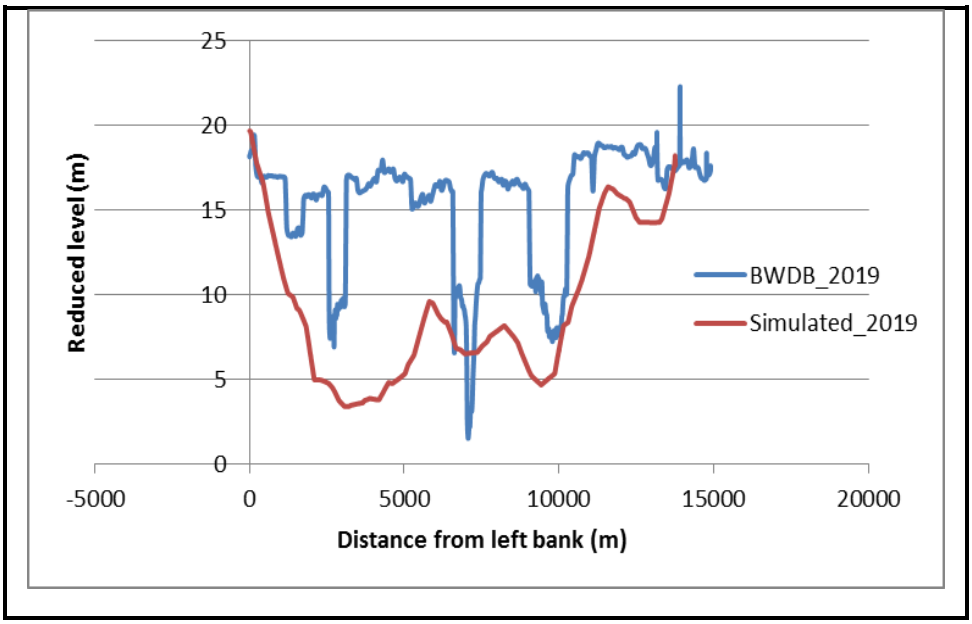

Figure 5.4: simulated and measured cross-section at RMJ 12

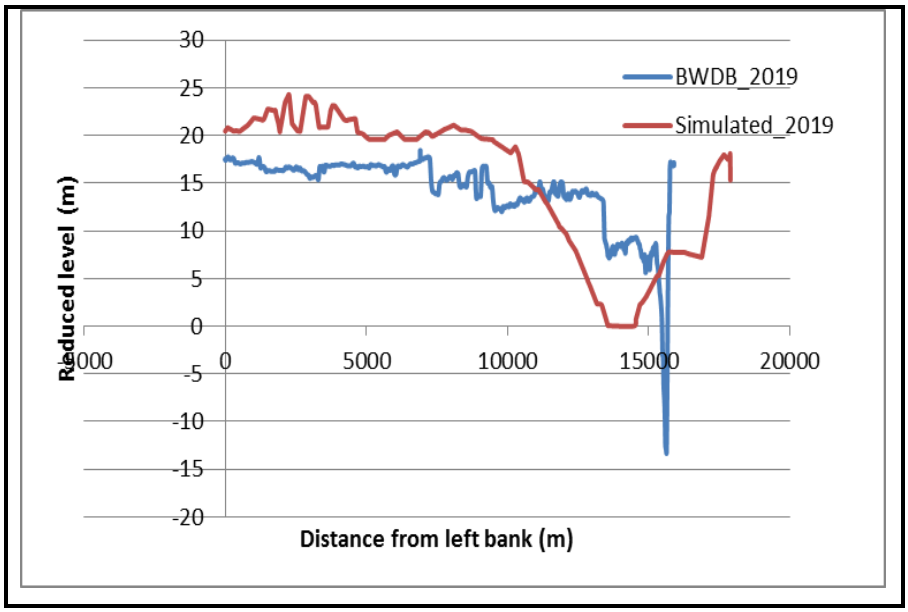

Figure 5.5: simulated and measured cross-section at RMJ 10

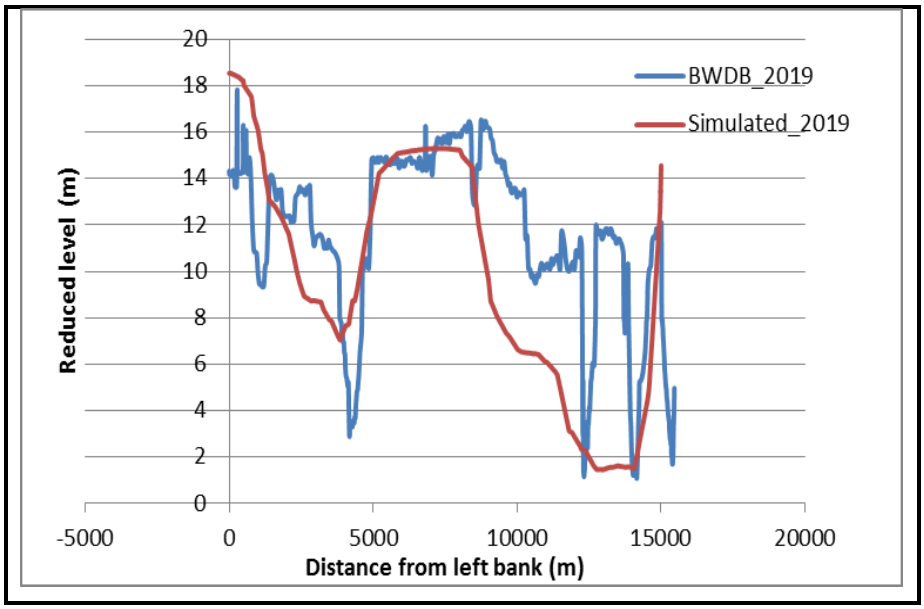

Figure 5.6: simulated and measured cross-section at RMJ 12

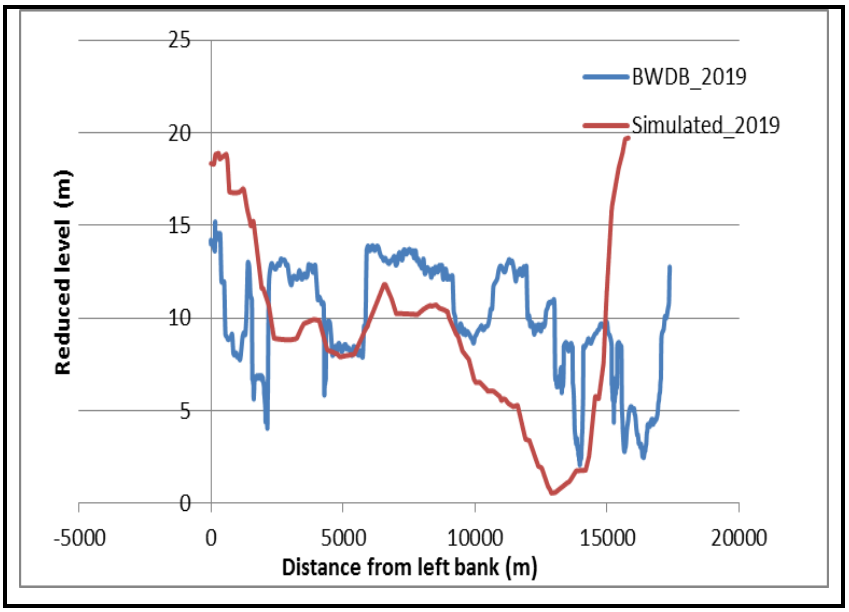

Figure 5.7: simulated and measured cross-section at RMJ 12

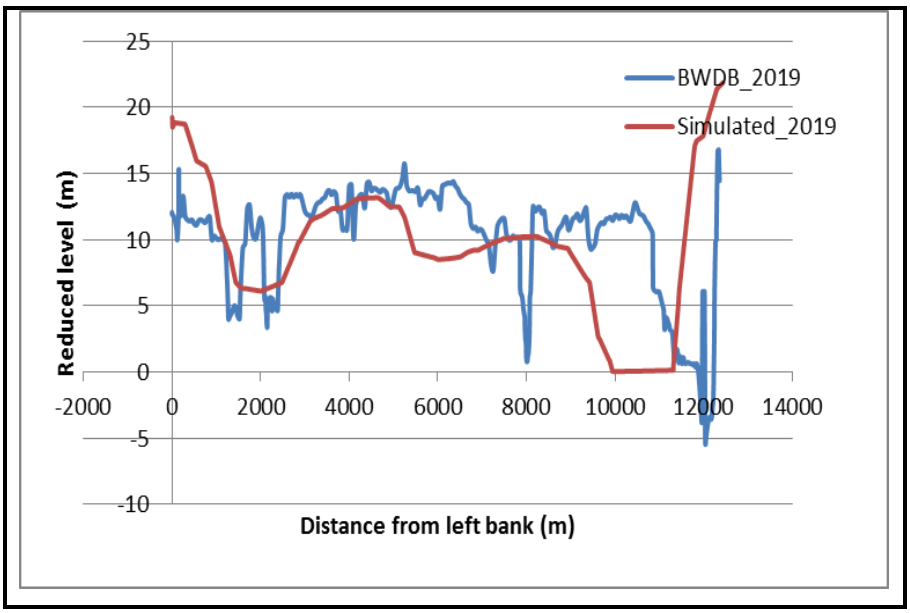

Figure 5.8: simulated and measured cross-section at RMJ 12

5.2.2 Analysis of Bed level changes

For 10 years, the 2D hydro-morphological model was run. The bed level changes in ten years from 2011 to 2021 are shown in Fig. 5.10. For cross-section at RMJ 13, it is seen that about 13 meters erosion was occurred in left bank (Fig. 5.11).

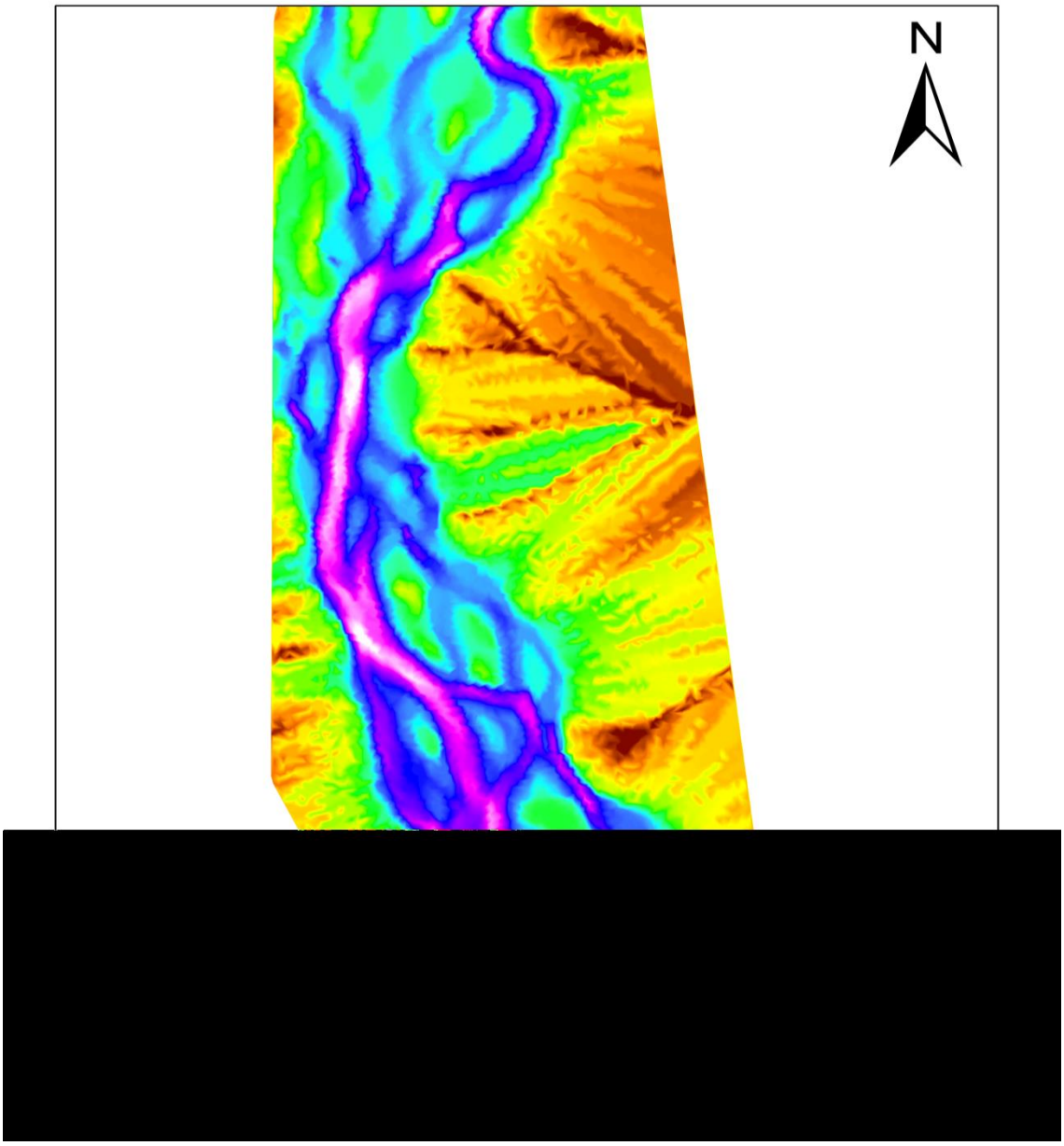

Figure 5.9: Simulation of bed level of the year 2012

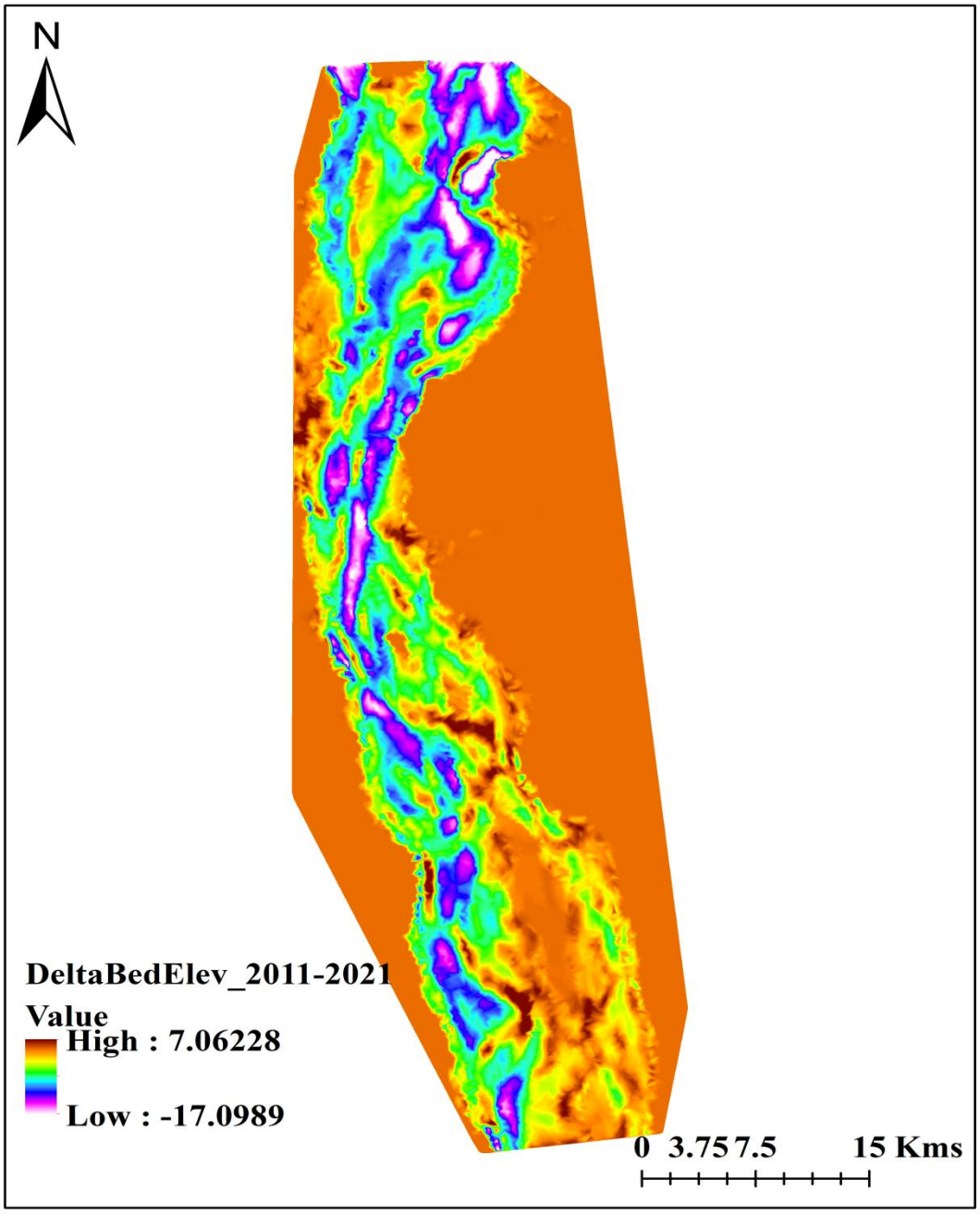

Figure 5.10: Simulation of net bed level changes from 2011-2021

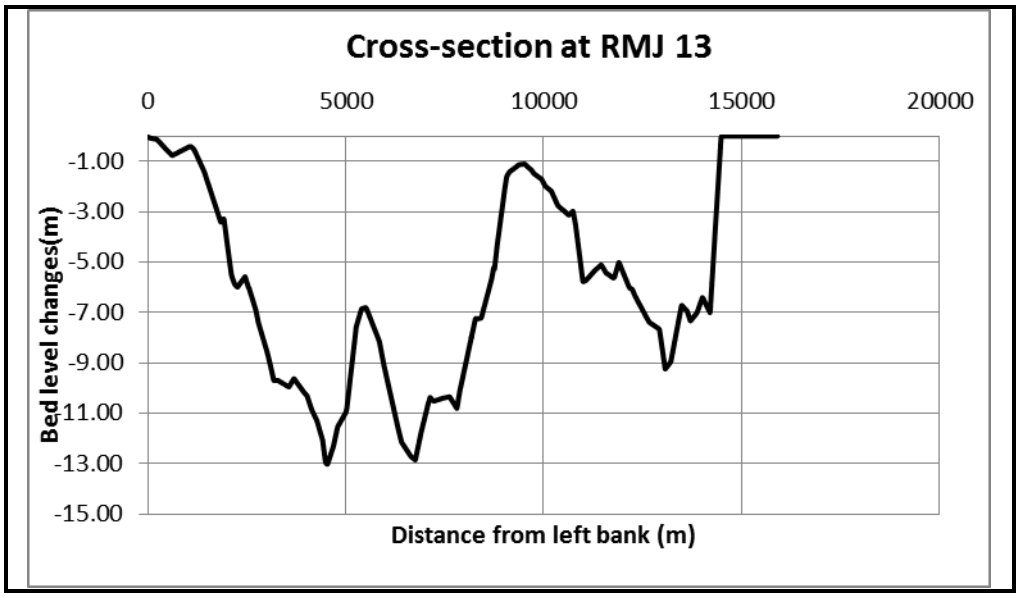

Figure 5.11: Simulation of bed level changes from 2011-2021

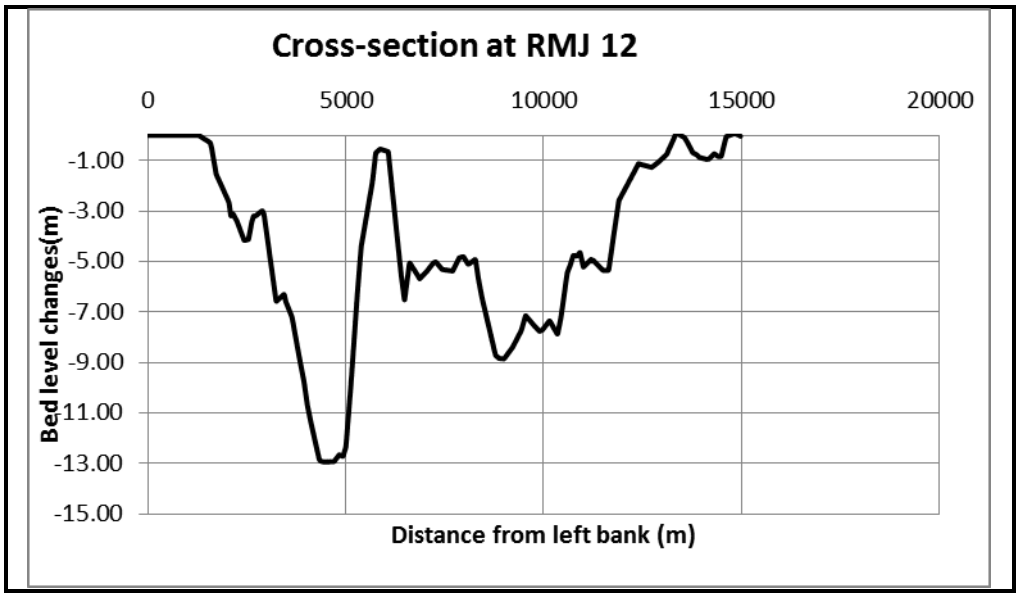

Figure 5.12: Simulation of bed level changes from 2011-2021

For cross-section at RMJ 12, it is seen that about 5-9 meters erosion was occurred in right bank. But the left bank is vulnerable to river bank erosion that right bank as the erosion was observed 13 meters.

For cross-section at RMJ 10, 9 the river bed near to the left bank is less vulnerable to erosion. But the middle of these two sections are more vulnerable to river erosion which is shown in Fig. 5.13 and Fig. 5.14.

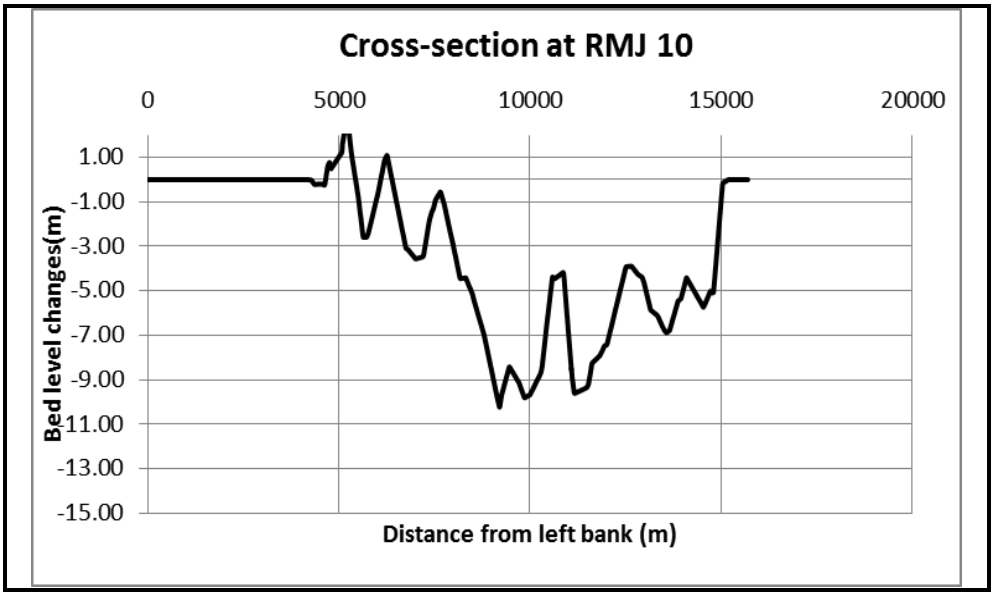

Figure 5.13: Simulation of bed level changes from 2011-2021

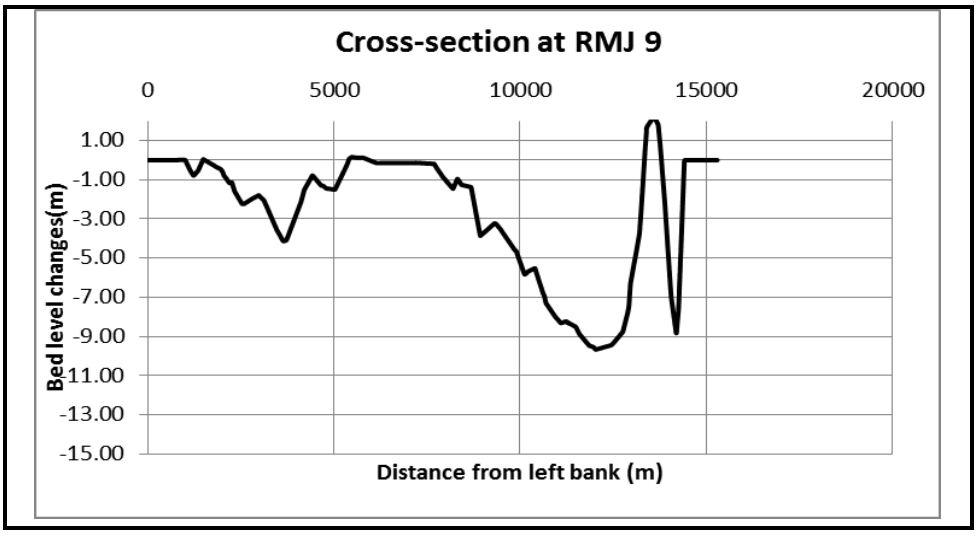

Figure 5.14: Simulation of bed level changes from 2011-2021

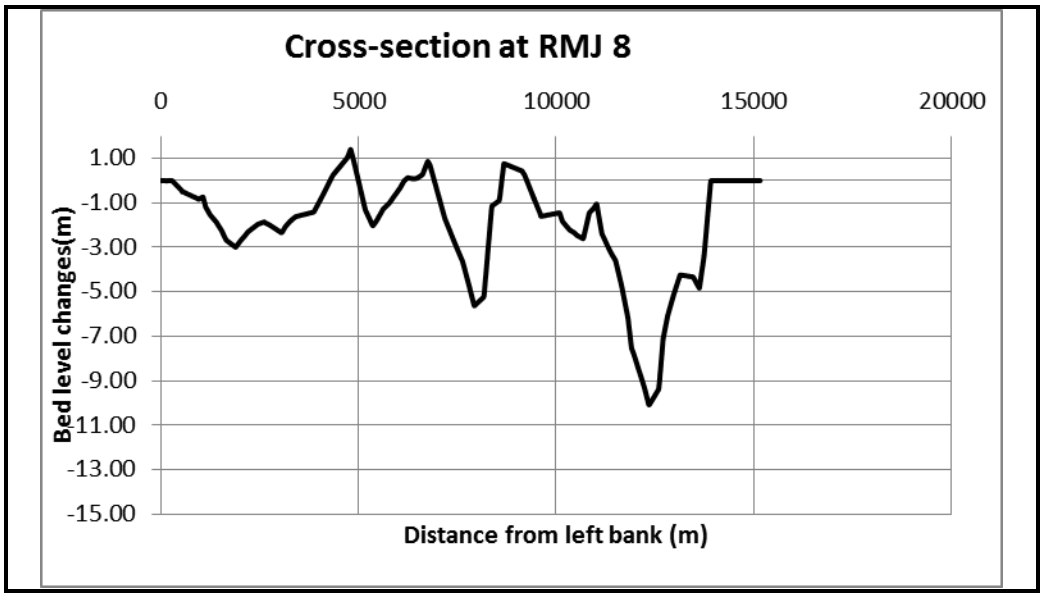

Figure 5.15: Simulation of bed level changes from 2011-2021

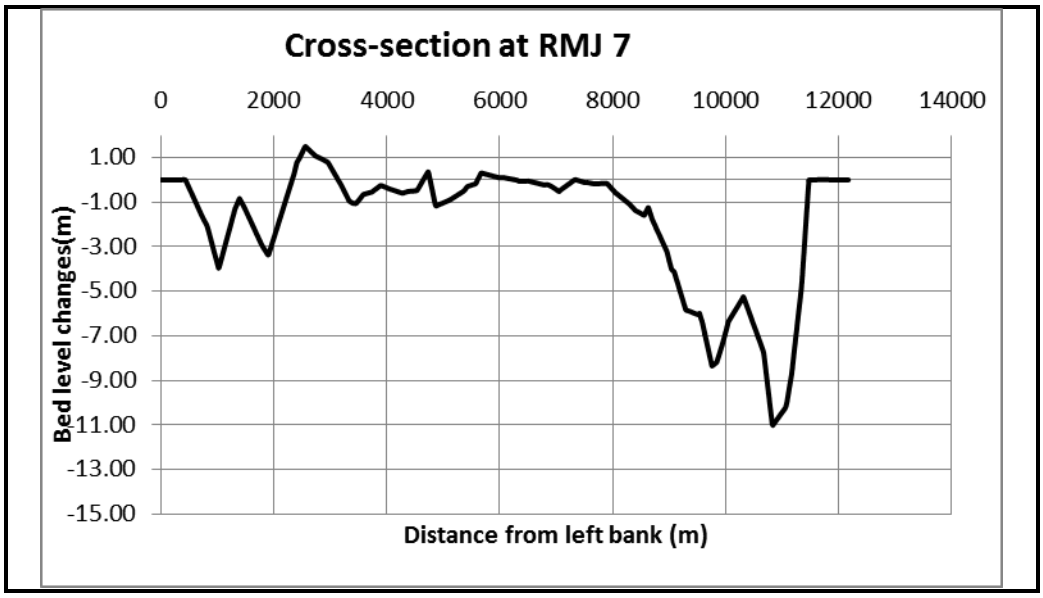

Figure 5.16: Simulation of bed level changes from 2011-2021

Cross-section at 8 is vulnerable to river bed erosion and deposition which is seen in fig. 5.15.

But for cross-section at RMJ 5.16, the river bed near to right bank is more vulnerable to river erosion.

5.3 One dimensional hydrodynamic model calibration, validation and simulation

hydrodynamic model is calibrated for the year of 2018 which is shown in Fig.5.17. The Manning's n was given 0.028. The correlation between observed and simulated water level was found 0.96. Then the model is validated for the year 2019 and the R^2 was found 0.97. The model was also simulated for the year 2020 which is shown in Fig.5.18. Then five variables were extracted to develop multivariate regression model.

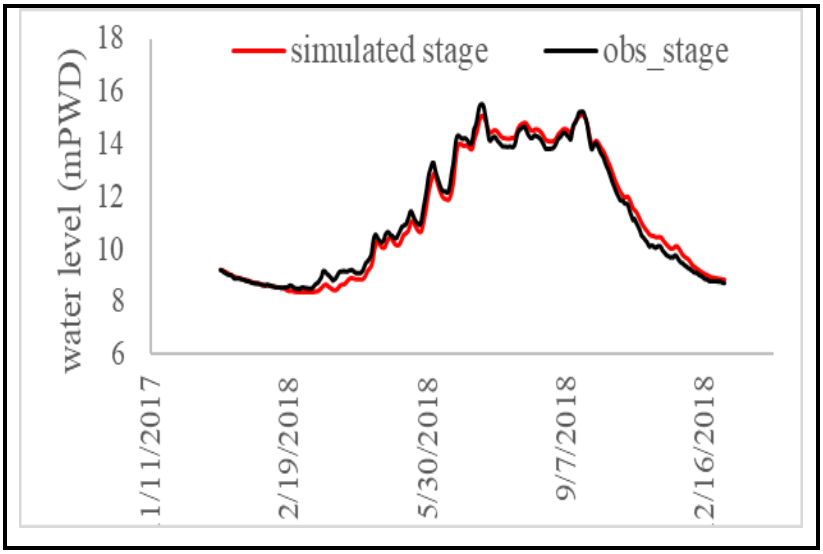

Figure 5.17: Model calibration at Kazipur

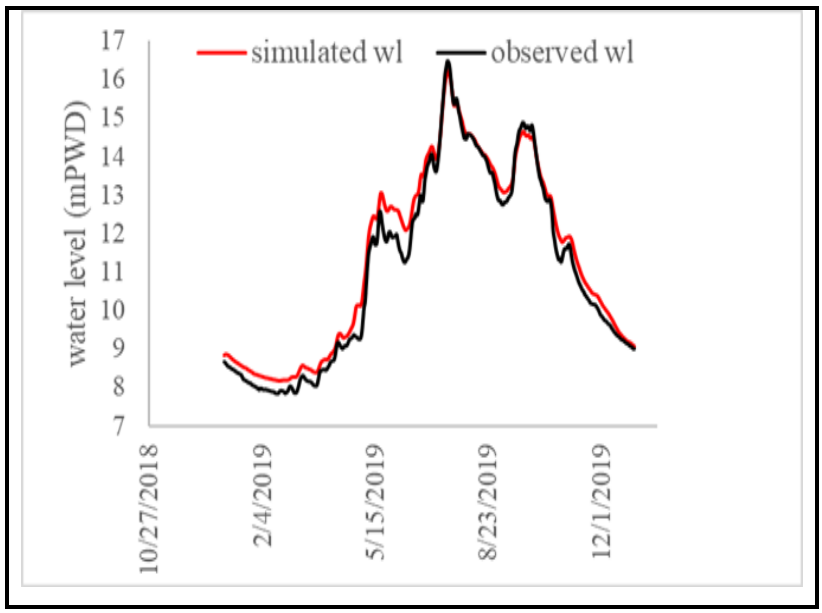

Figure 5.18:Model validation at Kazipur

5.4 2D hydrodynamic model calibration, validation and simulation

2D hydrodynamic model is calibrated for the year of 2018 which is shown in Fig.5.19.The Manning's n was given 0.032. The correlation between observed and simulated water level was found 0.82. Then the model is validated for the year 2019(Fig.5.20) and the R^2 was found 0.86. The model was also simulated for the year 2020. Then three variables such as minimum, maximum water level and maximum velocity were extracted to develop multivariate regression model.

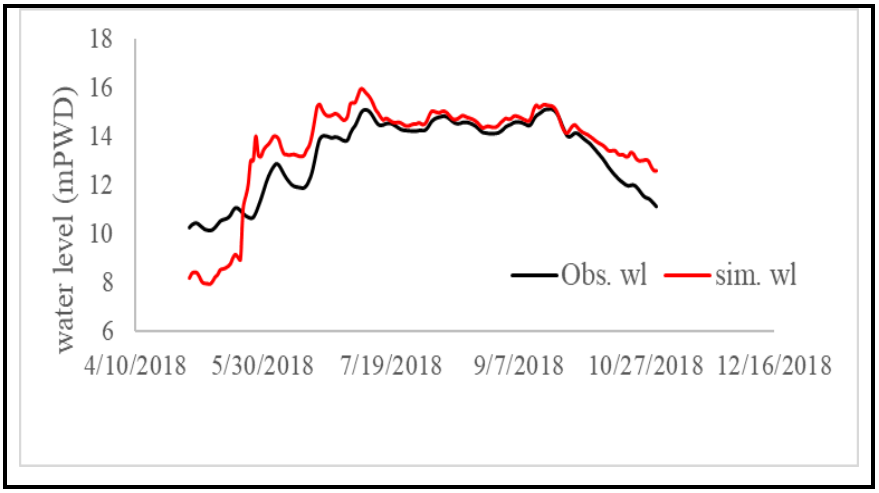

Figure 5.19: Model calibration at Kazipur

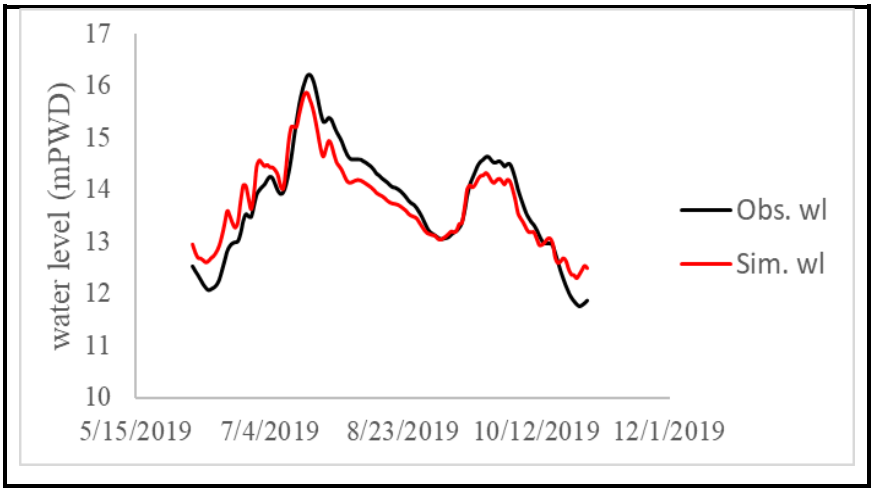

Figure 5.20: Model validation at Kazipur

5.5 Estimation of bank erosion rate

Bank erosion rate was estimated from the google satellite images at 300 meters interval from Bahadurabad station to Sirajganj station (Fig. 5.18).

From the Fig. 5.18, it is seen that for the year 2014 and 2015 the erosion rate is very high and erosion was observed in about every locations. The maximum erosion 600 m was observed for the year 2014 at a distance 28-32 kms from the Baahadurabad station. The maximum erosion 520 m was observed for the year 2015 at a distance 22 kms and 62 kms from the Bahadurabad station. In 2014 and 2015, bank erosion was observed at a fixed interval.

From the Fig. 5.18, it is seen that the erosion rate is same for the year 2016 and 2017. The location of bank erosion is also same. The maximum erosion rate was observed at a distance 28-32 kms from the Bahadurabad station for the year 2016 and 2017.

For the year 2018 the maximum erosion rate was observed upto 350 meter at a distance 40 km from Bahadurabad station The erosion rate was observed lesser in the year of 2018 from other years. But for the year of 2019, the erosion rate was observed very high upto 1000 meter at a distance of 33 kms from Bahadurabad station. Bank erosion up to 300 meters were also observed in other three locations which is located 20-26 kms and 52 kms away from Bahdurabad station.

For the year 2020, the bank erosion rate was observed in one location only. But the magnitude was very high. For the year 2021, the bank erosion was also observed in one location and it was high from previous year. The maginitude of bank erosion of that location was observed 800 meter.

From the analysis of bank erosion, it is found that the bank erosion was seen in every locations such as for the year 2014,2015. But the erosion rate and locations of bank erosion was also reduced in some extent in recent years(Fig. 5.18).

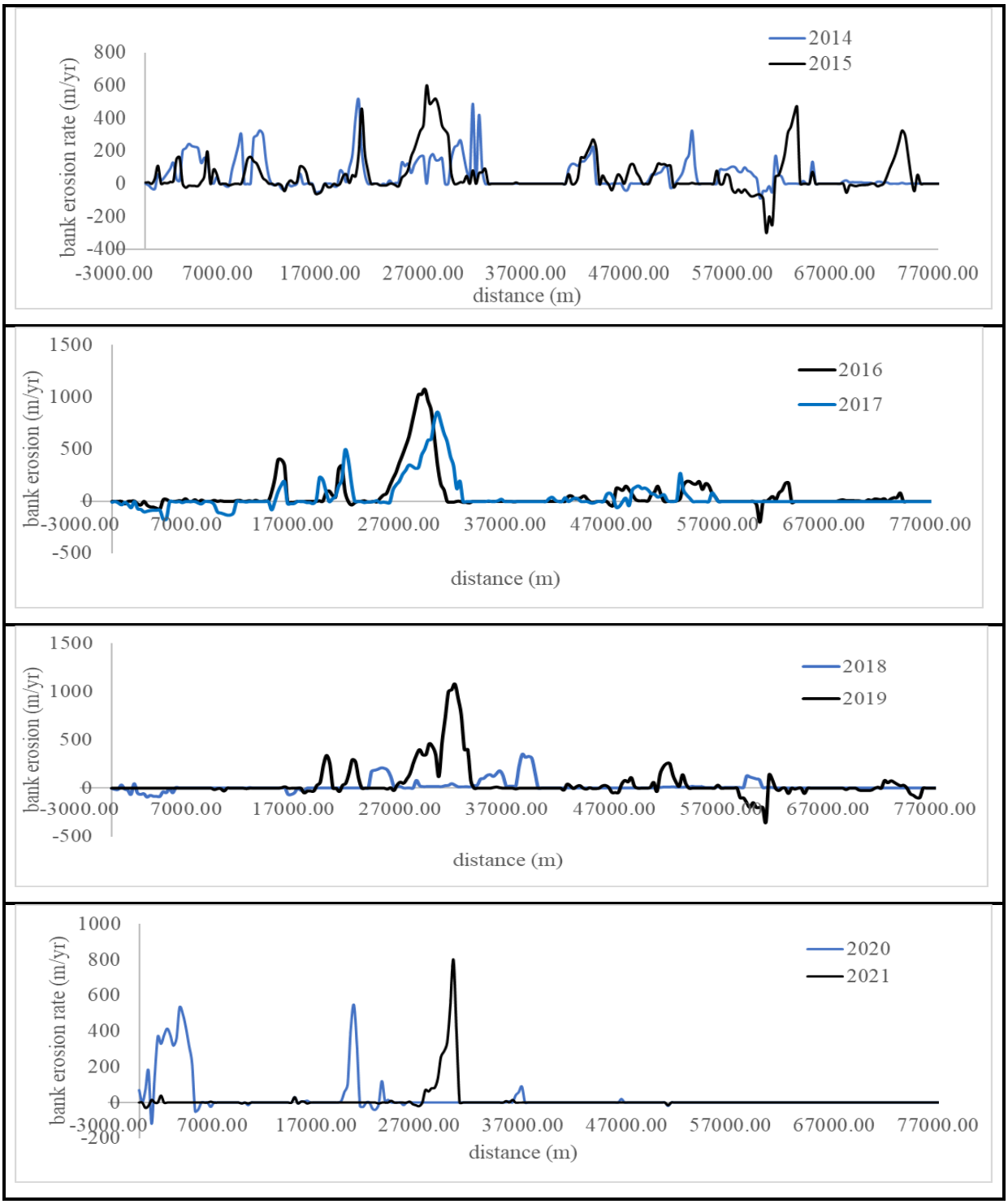

Figure 5.21 : Observed bank erosion rate estimated from satellite images

5.6 Scenario one (HECR-AS 1D and Regression model

5.6.1 Calibration of multi-variate regression model with 1d hydraulic parameters

19 regression models were run under machine learning and deep learning technique. The four statistical parameters such as RMSE, R^2 , MSE and MAE were determined to select suitable regression model which is shown in Table 5.1.

Table 5.1: Performance evaluation of Boosted regression model

SL	Regression Model types	Statistical parameters			
		RMSE	R^2	MSE	MAE
1.	Boosted Ensemble Tree	30	0.70	1050	15

5.6.1.1 Calibration of Ensemble type regression model

For boosted type regression model, the value of four statistical parameters were found in acceptable range. The value of RMSE,R2,MSE,MAE was found 30,0.70,1000 and 15 (Table 5.1).From the Fig.5.23, it is also seen that there is good agreement between simulated and observed bank erosion rate. For the R^2 =0.71, the parameters of regression model such as minimum leaf size, number of learners and learning rate was 8,32,0.1 respectively. Then these parameters were adjusted gradually and evaluated with four statistical parameters. For minimum leaf size of 4,number of learners of 36 and for learning rate of 0.5, the RMSE,R2,MSE,MAE was found 20,650,0.83 and 8 respectively.
The prediction of this type of regression model can be further validated by comparing observed and predicted bank erosion rate.

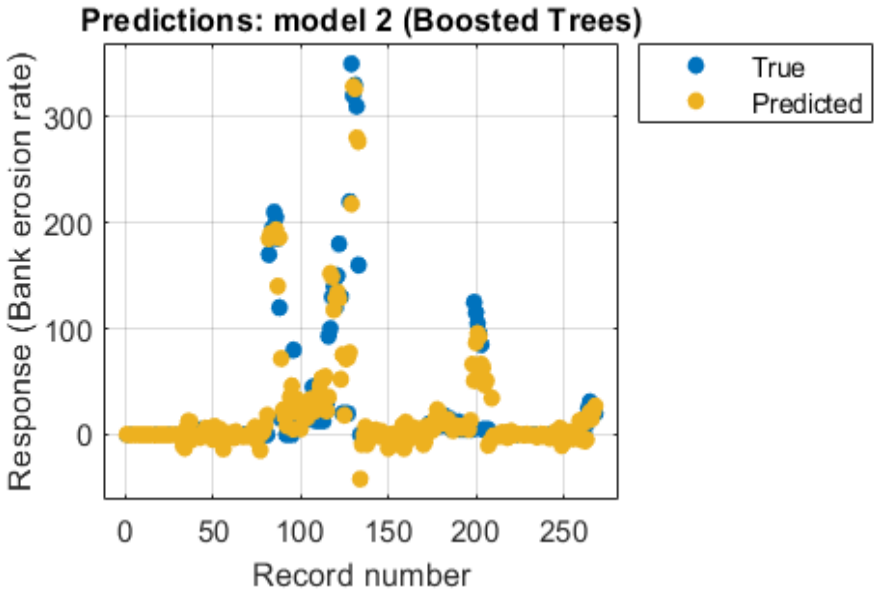

Figure 5.22: Calibration graph of boosted type regression model for Scenario 1

5.6.2 Validation of multi-variate regression model

5.6.2.2 Validation of Ensemble type regression model

From two ensemble regression model, boosted type regression model was selected based on the statistical parameters. Then this model was further validated for the year 2019, 2020 and 2021. From the Fig.5.28, it has seen that the regression model gave bank erosion rate in three location which is well matched with observed bank erosion rate. For the year of 2020, there was good agreement between observed and simulated bank erosion. But for the year 2019, in the upstream locations the model underestimated bank erosion (Fig.5.28). For the year 2021, the output results found satisfactory with observed bank erosion. The calibrated regression model was also simulated for velocity, discharge and water level which is shown in Appendix (Fig. 5.65-5.74). It has been found that the velocity is very important in the prediction of bankline shifting. Discharge and water level is also important parameter as it was found that these parameters effect in bankline shifting (Fig. 5.65-5.74).

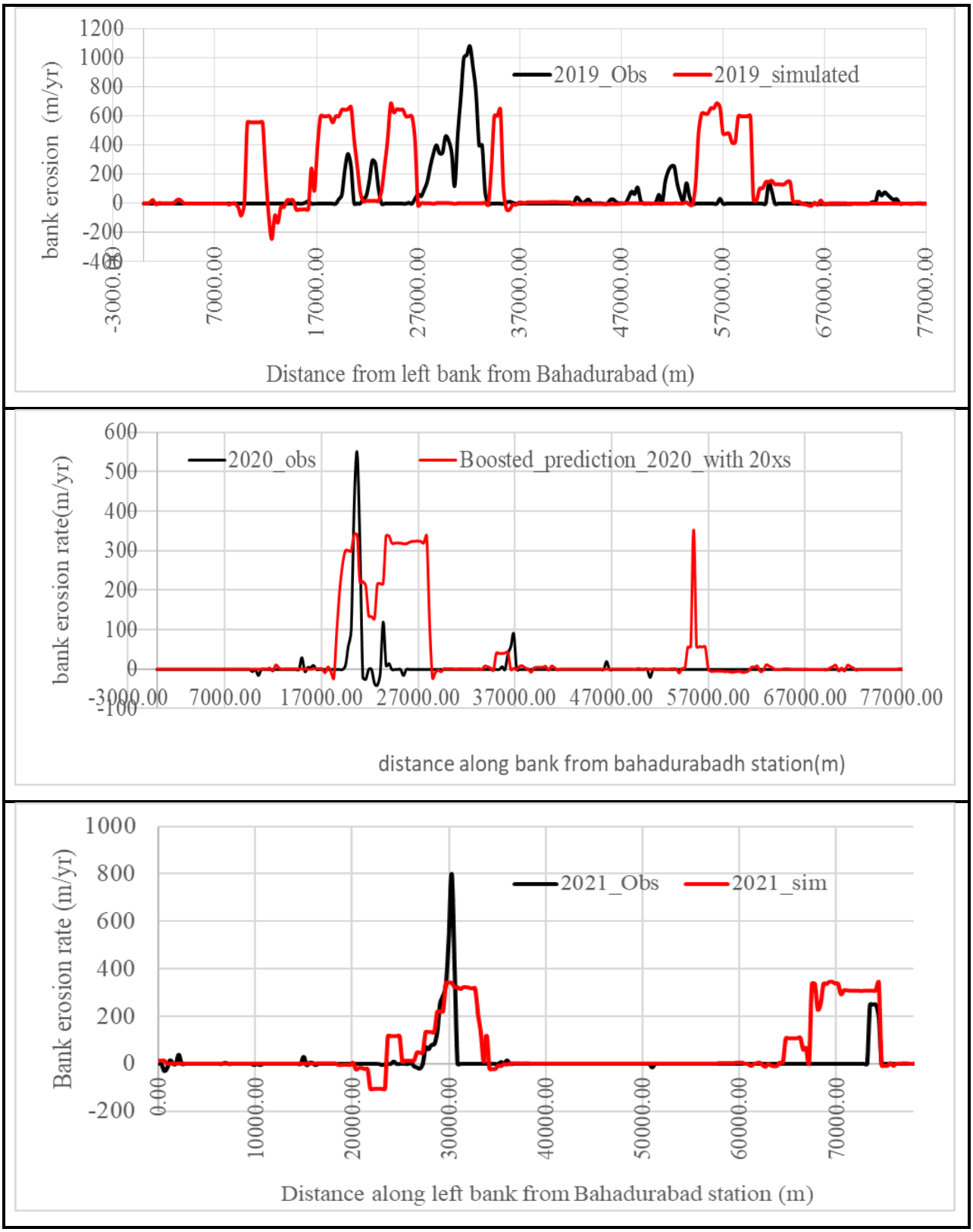

Figure 5.23: Validation graph for boosted type regression model (Scenario 1)

5.6.6 Performance evaluations of the validated regression model

The model further has been validated for the year 2019 and 2020. The performance of five regression model was validated using four statistical parameters such as RMSE, R^2 , MSE and MAE. It was found that linear regression model is not suitable for the prediction of bankline shifting for the long reach as RMSE, R^2 , MSE and MAE was found 300, -0.20, 1000 and 260. Fine tree type regression model can be suitable for estimation of bankline shifting of the long reach. RMSE, R^2 , MSE and MAE was found 65,0.50, 4225 and 27 respectively (Table 5.2). Cubic support vector machines cannot be suitable for the prediction of bankline shifting. Gaussian Exponential GPR process regression model cannot apply for the prediction of bankline shifting as the value RMSE, R^2 ,MSE MASE is very poor. Out of five regression model, the performance of Boosted ensemble tree type regression model is better compared to other regression model. The RMSE, R^2 , MSE and MAE was found 56, 0.60, 3200 and 23 as shown in Table 5.2.

Table 5.2: Performance evaluation of validated regression model

SL	**Regression Model types**	**RMSE**	**R^2**	**MSE**	**MAE**
1.	Boosted Ensemble Tree	56	0.60	3200	23

5.7 Scenario two (HEC-RAS 2D and Regression model)

5.7.1 Calibration of multi-variate regression model with 2D parameters

Boosted ensemble type regression model was calibrated for the year 2018(Fig.5.29). Three variables such as maximum, minimum water depth and maximum velocity were extracted from the 2D hydraulic model. Then these three variables and one output variable were processed in MATLAB. The RMSE,MSE,MAE,R^2 was found 38,1444,13 and 0.60. After that the calibrated model was simulated for the year 2019 and 2020.

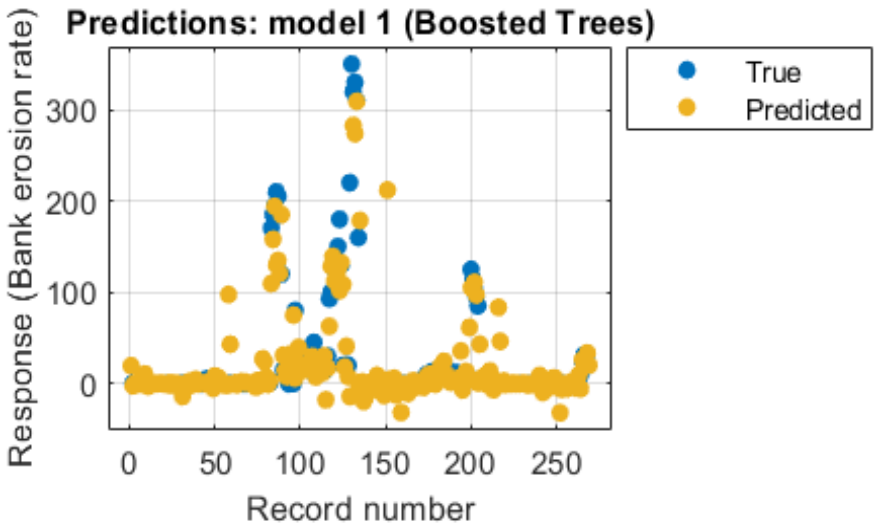

Figure 5.24: Calibration graph of regression model using 2d parameters (Scenario 2)

5.7.2 Simulation of multi-variant regression model with 2D parameters

The calibrated boosted regression model was simulated for the year 2019 and 2020. For the simulation of 2019, it has found that there is a good agreement between simulated and observed erosion rate which is shown in Fig.5.30. However, the calibrated model gives bank erosion rate at a fixed distance interval where this type of scenarios were observed for the year 2014 and 2015 (Fig.5.18). For the year of 2020, the maximum simulated erosion rate was found 1250 meter and the observed erosion rate was found 550 meter (Fig. 5.30). The R^2 , RMSE, MSE, MAE was found 0.65,50,2500 and 20 respectively for the validation of the year 2019 and 2020.

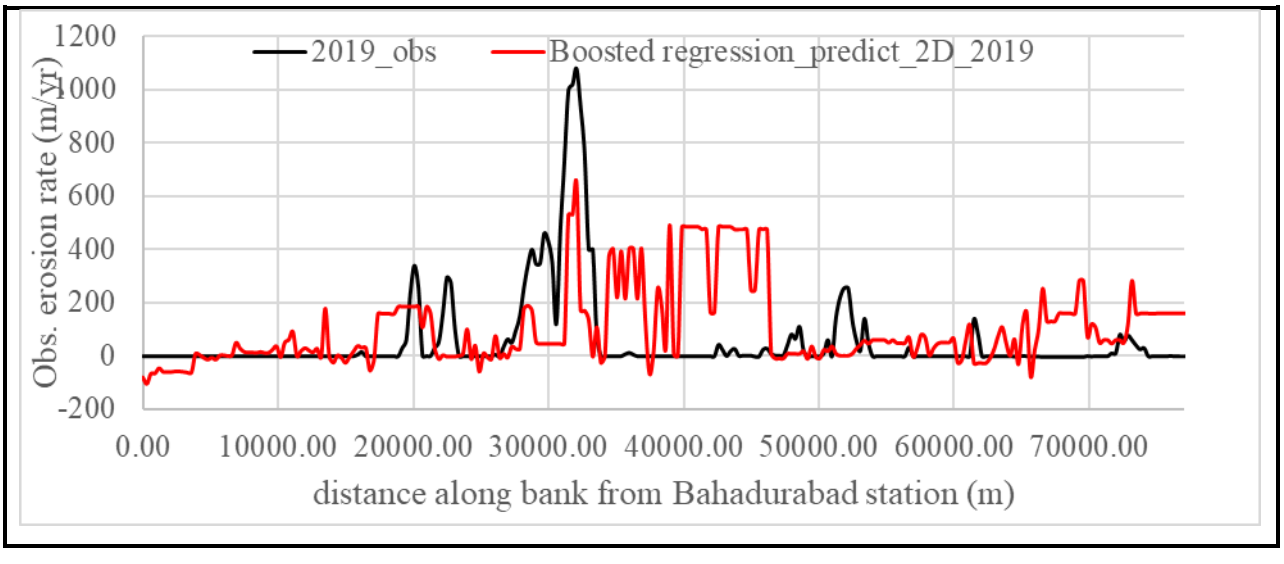

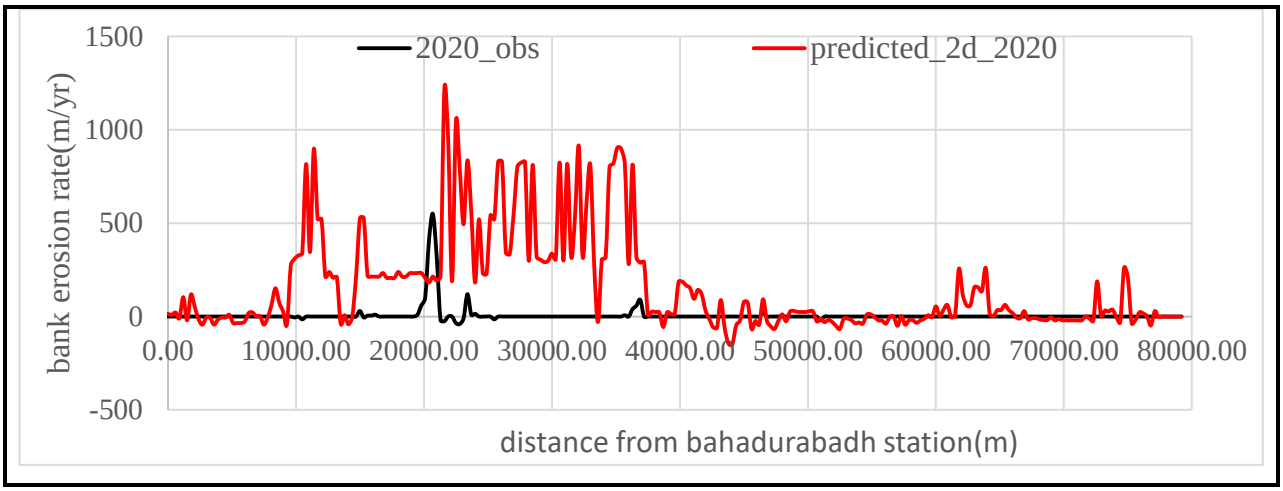

Figure 5.25: Validation graph of the regression model

5.8 Prediction of bankline shifting with and without considering bed level changes

From the Fig.5.31, it is clear that the bathymetry is important parameter to identify the locations which is vulnerable to riverbank erosion. For the year 2019, 2020 and 2021, it has found that using only bathymetry of 2018 the multi-variate regression model predicted bank erosion in same locations and the magnitude is different based upon the magnitude of flow data. But for the prediction of bank erosion of a year and using the bathymetry of that year, the multivariate regression model performed comparatively very well which is shown in Fig.5.31

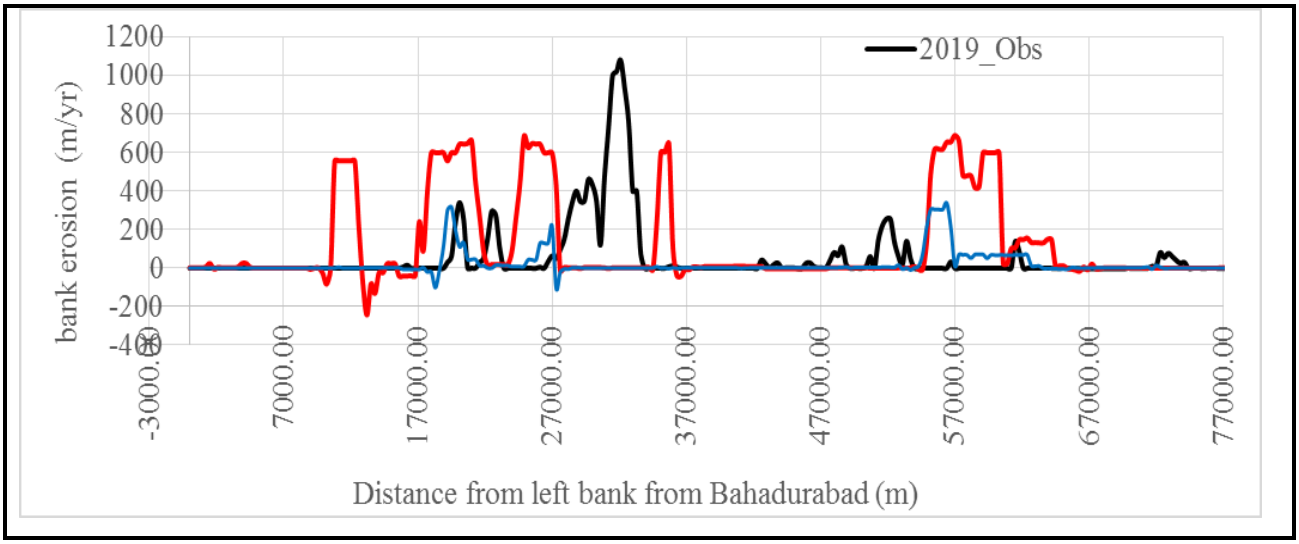

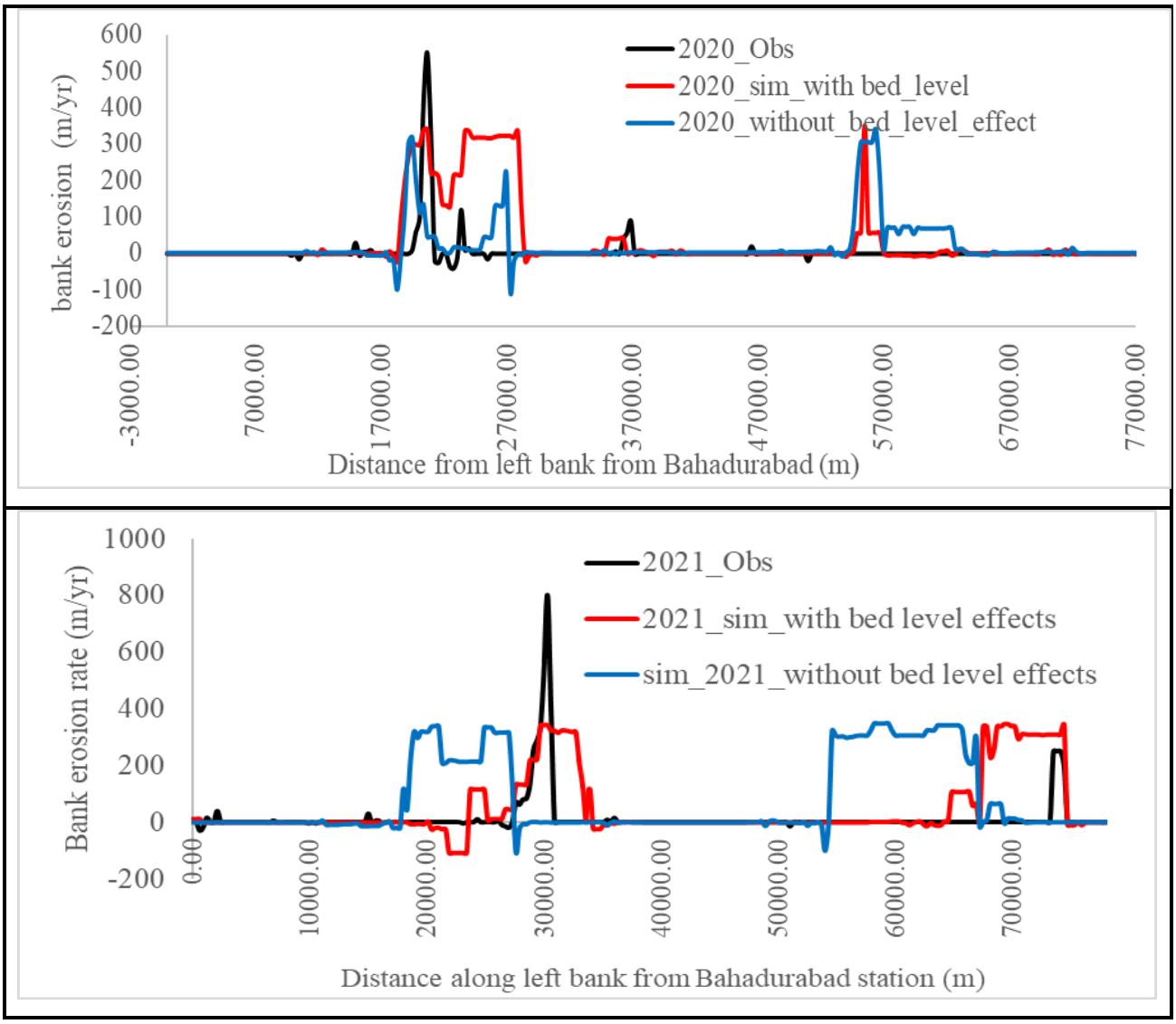

Figure 5.26: Prediction of the regression model with and without bed level effects

5.9 Comparisons between developed multi-variate regression model and CEGIS Bankline shifting prediction Model

CEGIS predicts bank line shifting in three locations within the study area, including Kazla, Bera PanchBaria, and Arjuna. Kazla is located 19 kilometers away from Bahadurabad station. CEGIS predicted 200-300 meters of bank erosion in about 2 kilometers of Kazla in 2019 (Fig. 5.32). The developed regression model also estimated bank erosion for this location, as shown in Fig.5.24 which is well matched with CEGIS prediction. CEGIS predicted 200-300 meter bank erosion at Bera PanchBaria, which is located 25-27 kilometers from Bahadurabad station. The developed regression model also predicted 300 meters of bank erosion for this location (Fig. 5.32). CEGIS also predicted 300 meters of bank erosion for Arjuna, as shown in Figure.5.25. However, the developed

regression model did not predict bank erosion for this location. For the year 2020, CEGIS projected bank erosion of about 150-350 meters for Kazla, Bera PanchBaria and Arjuna which is shown in Fig.5.32.The developed multi-variate regression model also estimated bank erosion on these locations of about 320 meters for Kazla, Bera PanchBaria which is comparatively higher than CEGIS prediction. But for the location Arjuna, the developed model estimated only 10-20 meters bank erosion for the year 2020.

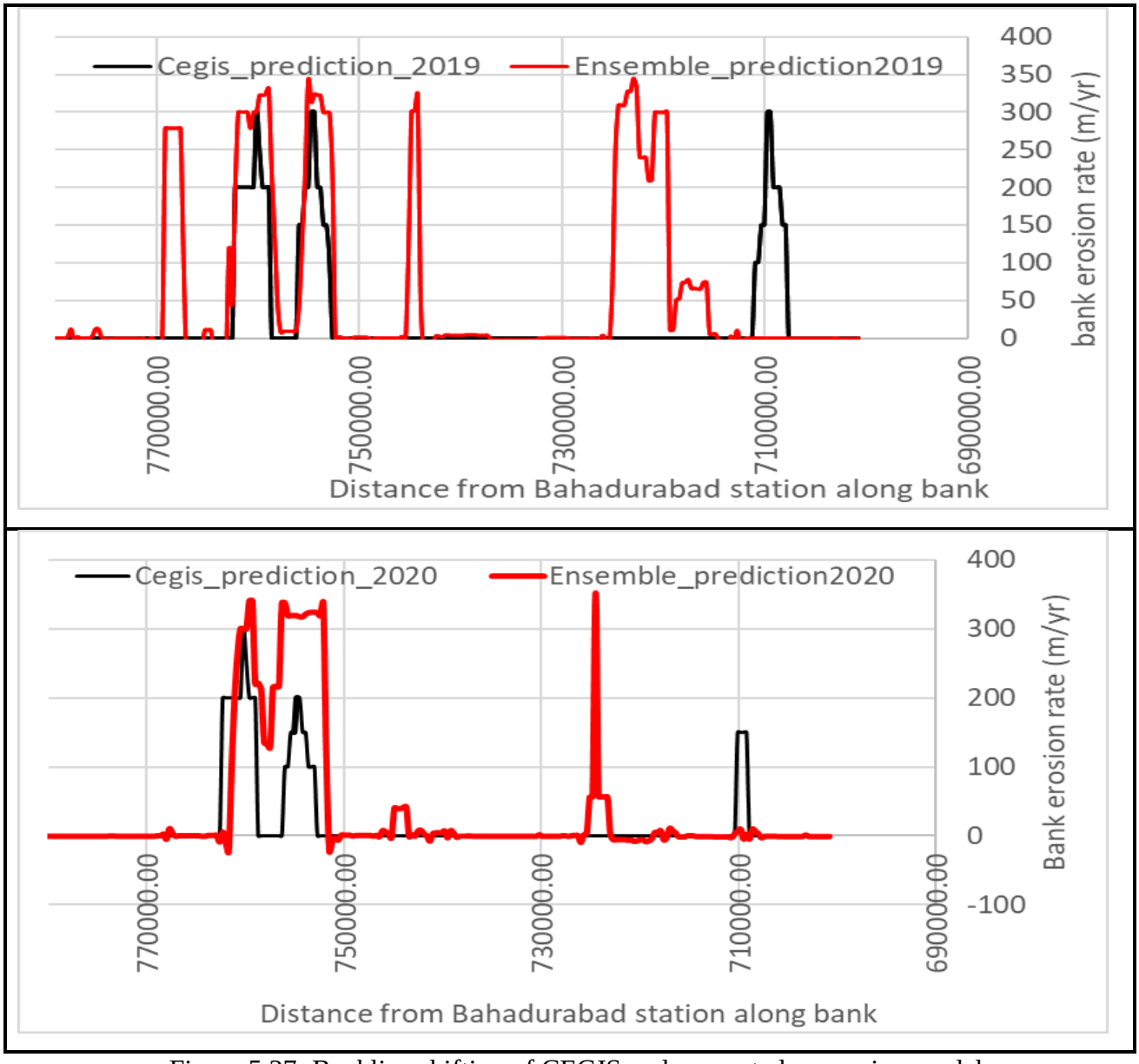

Figure 5.27: Bankline shifting of CEGIS and suggested regression model

5.10 Model performance

The accuracy of the multivariate regression model is evaluated using discrepancy ratio (D.R.) and co-efficient of co-relation (R^2). The discrepancy ratio is the ratio of predicted values to measured values. If the values of D.R. lie between 0.5-2.00, it is considered that the performance of the prediction model is satisfactory. If D.R. ratio is between 0.5-2.00, the D.R. is assigned as 'acceptable' and translated into percentage. The number of remarks 'acceptable' indicates the accuracy of the prediction model relative to the measured values

For Scenario one, about 34 data out of 63 data lies within 0.50-2.00. The accuracy of the prediction model(Scenario 1) is 55% for the D.R. range of 0.50-2.00 which is shown in Figure.5.33 and R^2 was found 0.60. For Scenario two, about 30 data out of 52 data lies with the limit 0.5-2.00 which is shown in Figure. 5.34. Converting into the percentage ,the accuracy of the model is 60% for the D.R range of 0.50-2.00 and R^2 is 0.65.

Table 5.3 : Discrepancy ratio (D.R.) range

Scenario	D.R. range	% of data
01	0.1-0.50	33%
	0.50-2.00	55%
	2.00-4.00	12%
02	0.1-0.50	10%
	0.50-2.00	60%
	2.00-4.00	30%

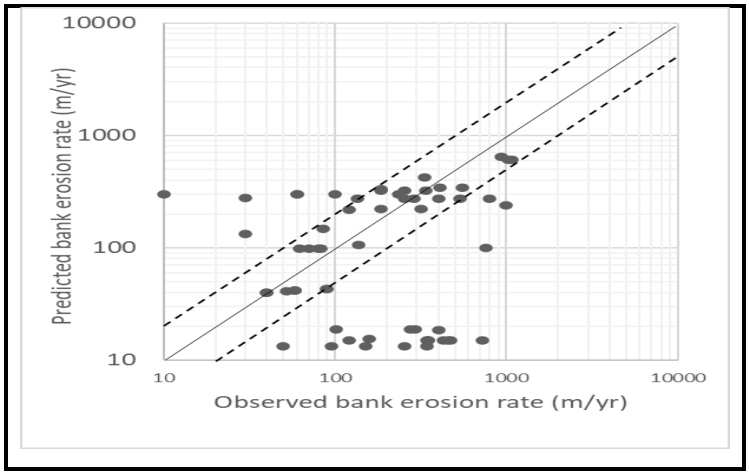

Figure 5.28: Predicted bank erosion rate (m/yr) and measured bank erosion rate (m/yr) for Scenario 1 using 1D hydraulic parameters

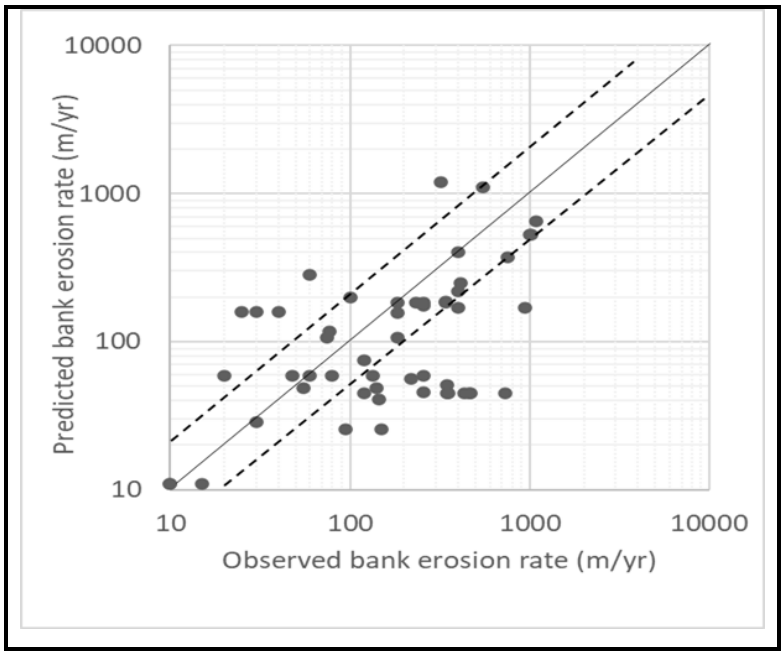

Figure 5.29: Predicted bank erosion rate (m/yr) and measured bank erosion rate (m/yr) for Scenario 2 using 2D hydraulic parameters.

5.11 Summery

Morphological model was run from 2011-2020. Bed level changes has been analyzed using Engelund-hansen transport function. The river bed near right bank was very vulnerable to river erosion. The river bed near right bank was seen both erosion and deposition.

Different regression model was tested. Ensemble boosted regression model was selected for the prediction of Bankline shifting based upon four statistical parameters such as R^2 ,RMSE,MAE,MSE. The best regression model was applied to predict bankline shifting for the year of 2019,2020 and 2021.

The multi-variate regression model was simulated with and without considering bed level changes. It was found that without considering the bed level changes, the multi-variate regression model always gave bank erosion in three locations such as Kazla, Bera PanchBaria and Arjuna and the magnitude of predicted bank erosion is different based upon the magnitude of boundary data.

The output results of the proposed multivariate regression model was compared with CEGIS bank erosion prediction model. CEGIS bank erosion prediction model always predicted bank erosion in three locations such as Kazla, Bera PanchBaria and Arjuna. But the suggested regression model predicted bank erosion based on five hydraulic parameters such as velocity, left over bank discharge, maximum , minimum water level and maximum slope. As the bank erosion is not fixed in three locations, the suggested regression model showed better results compared to CEGIS prediction model.

The accuracy of the developed model was evaluated using R^2 and D.R. Among two models, the models that was developed using 2D hydraulic parameters gave satisfactory results than another model. The R^2 and D.R was found 0.65 and 60% for best predictor regression model.

CHAPTER SIX
CONCLUSIONS AND RECOMMENDATIONS

6.1 General

River erosion is common phenomenon for Bangladesh especially for large rivers. Every year a large area has eroded and causes huge losses for Bangladesh. To ensure early response to river management issues, it is required to predict morphological changes such as bank erosion and bank shifting of the river. Morphological responses of the river like Jamuna can be better analyze using numerical modeling tools. This study attempted to suggest a computational procedure based on hydro-morphological model and machine learning technique to simulate bank erosion.

6.2 Conclusions

The following conclusions have been drawn from the present study are given:

i. River models and machine learning tools have been used to suggest a computational procedure for bankline shifting of the selected reach of the left bank Jamuna river.
ii. In broad category, two Scenarios have been carried out in the present computational procedure. These are Scenario i) use of the output of HEC-RAS 1D and regression tools and Scenario ii) use of results of HEC-RAS 2D and regression tools. In Scenario-i , five variables such as maximum velocity, maximum water level, maximum left over bank discharge, maximum slope and minimum water level were taken from the validated 1D hydro-dynamic model.
iii. The hydro-morphological model like RIVERFLOW 2D has been calibrated and validated for the year 2018 and 2019 respectively for the month May, June and July. The R^2 was found 0.86 and 0.93 respectively for calibration and validation.
iv. Bed level changes has been analyzed for study area. Right bank is very vulnerable to both river bed erosion and deposition. From bed level and cross-sectional analysis, the highest deposition and erosion was observed 16.3 and 13.8 meters respectively using

Engelund-Hansen tansport function.

v. In Scenario-1, 1D hydrodynamic model had been applied in conjunction with machine learning techniques. Prior to application in machine learning tools (Matlab) 1D hydraulic model has been calibrated and validated for the year 2018 and 2019 for the water level with Manning's n respectively. For n=0.028, there found a good agreement between simulated and observed water level and the R^2 was found 0.96 for both calibration and validation. This model is calibrated and validated to extract five variables to use as input variables in MATLAB regression model.2D hydraulic model was also calibrated and validated for the year 2018 and 2019 for monsoon period. The R^2 was found 0.82 and 0.86 respectively for calibration and validation.

vi. In Scenario-1, five input variables and one output variables has been processed using Machine learning technique in MATLAB regression tools. Five different regression models were run and based on four statistical parameters such as R2,RMSE,MSE,MAE boosted ensemble regression model was selected for the prediction of bankline shifting using 1D hydraulic model. The R2, RMSE, MSE, MAE was found 0.80,700,25,20 respectively. The best regression model predicted bank erosion for the year 2019, 2020 and 2021. From the graphical representation, it was found that there is good matched between simulated and observed bank erosion. However, the model underestimated bank erosion in some locations.

vii. In Scenario-2, three variables were extracted to calibrate regression model. The R^2 , RMSE, MSE, MAE was found 0.60, 38, 1444,13. The model was simulated for the year 2019 and 2020. From graphical representation, it was found that there was well matched between observed and simulated bank erosion.

viii. The best regression model was also run for the year 2019 for different morphological conditions such as for bathymetry of year 2018, 2019 and 2020. It has found that bathymetry is important parameter to locate the correct location which is vulnerable to bank erosion.

ix. In Scenario one, R^2 and D.R. was found 0.60 and 55%. In Scenario two, R^2 and D.R. was found 0.65 and 60%.

x. Based on statistical parameters, it revealed that the computational procedure with Scenario-2 performed better than that of Scenario -1 . So the application of RIVEFLOW

2D morphological model and regression model can be used for analyzing river bank shifting.

6.3 Recommendations for future study

Following recommendations can be suggested for further study.These are as follows:

i. The accuracy of Bankline predictions depends on the Bathymetry. It is recommended to survey some cross-sections for the year before the simulation of bank erosion of that year.

ii. 2D hydraulic models can be applied to simulate bank erosion incorporating more input variables such as shear stress, left over bank discharge, slope and others dominant variables.

iii. The model can be calibrated for the more with recent years. The prediction results may be good.

iv. Similar study can be carried out in physical modeling with regression tools.

REFERENCES

Abidin, R. Z., Sulaiman, M. S., & Yusoff, N. (2017). Erosion risk assessment: A case study of the Langat River bank in Malaysia. International Soil and Water Conservation Research, 5(1), 26-35.

Ali, M. M, & Zobeyer, H. (2021). Research on river bank erosion dynamics using numerical modelling and deep learning techniques. Department of Water Resources Engineering, BUET, Dhaka, Bangladesh. Prepared for WARPO, Dhaka, Bangladesh.

Atkinson, P. M., German, S. E., Sear, D. A., and Clark, M. J.: Ex-ploring the relations between riverbank erosion and geomorpho-logical controls using geographically weighted logistic regression, Geogr. Anal., 35, 58–82, 2003.3.

Baruah, A., Deka, P., Deka, R., & Sarma, A. K. (2023). A 2D Hydrodynamic Model Study in Brahmaputra River for Implementation of Bank Protection Work at Nimatighat. In Sustainable Water Resources Management (pp. 92-99). Springer, Singapore.

Buffington, J. M., & Montgomery, D. R. (1997). A systematic analysis of eight decades of incipient motion studies, with special reference to gravel-bedded rivers. Water Resources Research, 33(8), 1993-2029.

Bull, L., & Kirkby, M. (1997). Gully processes and modelling. Progress in Physical Geography, 21(3), 354-374.

CEGIS. (2018). Prediction of river bank erosion along the Jamuna, the Ganges, and the Padma River. Prepared for BWDB, Dhaka, Bangladesh.

Center for Environmental and Geographic Information Services (CEGIS). (2020). River Erosion Prediction Model. https://www.cegisbd.com/DivisionInfo?Div=MOR

Darby, S. E., Trieu, H. Q., Carling, P. A., Sarkkula, J., Koponen, J., Kummu, M., Conlan, I., & Leyland, J. (2010). A physically based model to predict hydraulic erosion of fine-grained riverbanks: The role of form roughness in limiting erosion. Journal of Geophysical Research: Earth Surface, 115(F4).

Davis, L., & Harden, C. (2014). Factors contributing to bank stability in channelized, alluvial streams. River Research and Applications, 30(1), 71-80.

Dey, K.C, Mahmood, S. andd Matin, M.A. (1998). Exponent of flow velocity for the transport of sediments in alluvial rivers. Journal of Civil Engineering, IEB, Bangladesh, Vol. CE 26, No. 01.

Dietrich, W. E., & Gallinatti, J. D. (1991). Fluvial geomorphology. Field Scenarios and measurement programs in geomorphology, 169-220.

Duijsings, J. (1987). A sediment budget for a forested catchment in Luxembourg and its implications for channel development. Earth Surface Processes and Landforms, 12(2), 173-184.

Evans, D., Gibson, C., & Rossell, R. (2006). Sediment loads and sources in heavily modified Irish catchments: A move towards informed management strategies. Geomorphology, 79(1-2), 93-113.

Ghosh, S., & Dwivedi, V. K. (2022). Assessment of Plan Form Development Due to Erosion and Deposition of Soil. In River and Coastal Engineering (pp. 71-79). Springer, Cham.

Green, T. R., Beavis, S. G., Dietrich, C. R., & Jakeman, A. J. (1999). Relating stream-bank erosion to in-stream transport of suspended sediment. Hydrological Processes, 13(5), 777-787.

Group, F. I. S. R. W. (1998). Stream corridor restoration: Principles, processes, and practices. National Technical Info Svc.

Haque, A., & Matin, M. (2022). A Study of Bank Line Shifting of the Selected Reach of Jamuna River Using Multi-Variant Regression Model. Journal of Soft Computing in Civil Engineering, 6(2), 21-34.

Haque, A., Mamoon, W.B., Muhib, K.M., Riham, S.K., Sultana, R. (2020)."Assessment of hydrological and morphological parameters of Kobadak river." 5th International Conference on Advances in Civil Engineering(ICACE-2020), pp. 1-7.

Haque, A., Riham, S.K., Muhib, K.M., Mamoon, W.B.(2020)."Sediment Modeling of Kobadak river by HECRAS." 5th International Conference on Advances in Civil Engineering (ICACE-2020), pp. 1-7.

Hasan, M. (2018). Assessment of hydro-morphological response of selected reach of the Jamuna river due to structural intervention using delft 3D model, M.Sc. Engineering Thesis, Department of Water Resources Engineering, BUET, Dhaka, Bangladesh.

Hydrologic Engineering Center, US Army Corps, "HEC-RAS river analysis System," Hydraulic Reference Manual, 2016.

Hydronia, L. L. C. (2020). RiverFlow2D, Two-Dimensional Flood and River Dynamics Model, Reference Manual.

Islam, M. S., & Matin, M. A. (2022). Prediction of fluvial erosion rate in Jamuna River, Bangladesh. International Journal of River Basin Management, pp. 1-13.

Hooke, J.M. (1979). An analysis of the processes of river bank erosion. , 42(1-2), 0–62. doi:10.1016/0022-1694(79)90005-2

Jana, S. (2021). An automated approach in estimation and prediction of riverbank shifting for flood-prone middle-lower course of the Subarnarekha river, India. International Journal of River Basin Management, 19(3), 359-377.

Julian, J. P., & Torres, R. (2006). Hydraulic erosion of cohesive riverbanks.Geomorphology, 76(1-2), 193-206.

Karmaker, T., & Dutta, S. (2011). Erodibility of fine soil from the composite river bank of Brahmaputra in India. Hydrological Processes, 25(1), 104-111.

Karmaker, T., & Dutta, S. (2015). Stochastic erosion of composite banks in alluvial river bends. Hydrological Processes, 29(6), 1324-1339.

Khan, M. (2015). Modeling the bank erosion of selected reach of Jamuna River, M.Sc. Engineering Thesis, Department of Water Resources Engineering, BUET, Dhaka, Bangladesh.

Khan, S. T., Alam, S., Azam, N., Debnath, M., Mojlish, A. K., Rahman, A., ... & Maliha, M. (2022). A Study on Riverbank Erosion-Accretion and Bar Dynamics of Dharla River Using Multi-temporal Satellite Images. In Advances in Civil Engineering (pp. 407-417). Springer, Singapore.

Lawler, D. M. (1993). The measurement of river bank erosion and lateral channel change: a review. Earth Surface Processes and Landforms, 18(9), 777-821.

Lawler, D., Grove, J., Couperthwaite, J., & Leeks, G. (1999). Downstream change in river bank erosion rates in the Swale–Ouse system, northern England. Hydrological Processes, 13(7), 977-992.

Lawler, D., Grove, J., Couperthwaite, J., & Leeks, G. (1999). Downstream change in river bank erosion rates in the Swale–Ouse system, northern England. Hydrological Processes, 13(7), 977-992.

Lawler, D., Thorne, C., & Hooke, J. (1997). Bank erosion and instability. Applied fluvial geomorphology for river engineering and management,

Majumdar, S., & Mandal, S. (2022). Assessment of geotechnical properties of the bank sediment to investigate the riverbank's stability along the Ganga river within the stretch of Malda district, West Bengal, India. Sustainable Water Resources Management, 8(2), 1-13.

Moody, J. A. (2022). The effects of discharge and bank orientation on the annual riverbank erosion along Powder River in Montana, USA. Geomorphology, 403, 108134.

Mosselman, E., Huisink, M., Koomen, E., & Seijmonsbergen, A. (1995). Morphological changes in a large braided sand-bed river. River geomorphology,

Muramoto, Y., & Fujita, Y. (1992). Recent channel processes of the major rivers in Bangladesh: centering around the bank erosion in the Meghna river. Kyoto Daigaku Bōsai Kenkyūjo nenpō(35), 89-114.

Musa, J. J., Abdulwaheed, S., & Saidu, M. (2010). Effect of surface runoff on Nigerian rural roads (a case study of Offa local government area). AU J. Technol, 13, 242- 248.

Ojile, M. O., & Ogwara, E. O. Vulnerability of communities to flood hazard and riverbank erosion along river Nun in Bayelsa state, Nigeria.

Osman, A. M., & Thorne, C. R. (1988). Riverbank stability analysis. I: Theory. Journal of Hydraulic Engineering, 114(2), 134-150.

Pal, P. K., Rahman, A. and Yunus, A. (2017) 'A Study on Seasonal Variation of Hydro-Morphodynamic Parameters of Jamuna River', 6(6), pp. 307–311.

Paudel, S., Singh, U., Crosato, A., & Franca, M. J. (2022). Effects of initial and boundary conditions on gravel-bed river morphology. Advances in Water Resources, 166, 104256.

Rahman, S. A., Islam, M. M., Salman, M. A., & Rafiq, M. R. (2022). Evaluating bank erosion and identifying possible anthropogenic causative factors of Kirtankhola River in Barishal, Bangladesh: an integrated GIS and Remote Sensing approaches. International Journal of Engineering and Geosciences, 7(2), 179-190.

Saadon, A., Abdullah, J., Muhammad, N. S., & Ariffin, J. (2020). Development of riverbank erosion rate predictor for natural channels using NARX-QR Factorization model: a case study of Sg. Bernam, Selangor, Malaysia. Neural Computing and Applications, 32(18), 14839-14849.

Saadon, A., Abdullah, J., Muhammad, N. S., & Ariffin, J. (2021). Streambank Erosion Prediction. IOP Conf. Ser.: Earth Environ. Sci. 685 012007.

Saadon, A., Abdullah, J., Muhammad, N. S., Ariffin, J., & Julien, P. Y. (2021). Predictive models for the estimation of riverbank s rates. Catena, 196, 104917.

Saha, M., Sauda, S. S., Real, H. R. K., & Mahmud, M. (2022). Estimation of annual rate and spatial distribution of soil erosion in the Jamuna basin using RUSLE model: A geospatial approach. Environmental Challenges, 8, 100524.

Sekely, A. C., Mulla, D., & Bauer, D. W. (2002). Streambank slumping and its contribution to the phosphorus and suspended sediment loads of the Blue Earth River, Minnesota. Journal of Soil and Water Conservation, 57(5), 243-250.

Shields, A. (1936). Application of similarity principles and turbulence research to bed-load movement.

Simon, A., & Collison, A. J. (2001). Pore-water pressure effects on the detachment of cohesive streambeds: seepage forces and matric suction. Earth Surface Processes and Landforms, 26(13), 1421-1442.

Singer, M. J., & Munns, D. N. (2006). Soils: an introduction. Pearson Prentice Hall Upper Saddle River, NJ.

Sultana, M. (2022). Bank Erosion and Sediment Deposition in Teesta River: A Spatiotemporal Analysis. In Anthropogeomorphology (pp. 73-89). Springer, Cham.

SWMC. (2001). Morphological assessment of rivers of Bangladesh. Final report.

Thorne, C. (1982). Processes and mechanisms of river bank erosion. Gravel-bed rivers, 227-271.

Thorne, C. (1992). Bend scour and bank erosion on the meandering Red River, Louisiana.Lowland floodplain rivers. Geomorphological perspectives,

Thorne, C. R. (1990). Effects of vegetation on riverbank erosion and stability.Vegetation and erosion.

Thorne, C. R., & Osman, A. M. (1988). Riverbank stability analysis. II: Applications.Journal of Hydraulic Engineering, 114(2), 151-172.

Thorne, C. R., & Tovey, N. K. (1981). Stability of composite river banks. Earth Surface Processes and Landforms, 6(5), 469-484.

Tingsanchali, T., & Chinnarasri, C. (1997). Design of Mekong river bank protection. Proc. Conf. on Mgmt. of Landscapes Distributed by Channel Incision, University of Mississippi, Miss.

Urmi Laz, O. and Navera, U. K. (2018) ‘Application of Delft3D Mathematical Model in the Jamuna River for Two-Dimensional Simulation’, in 4th International Conference on Civil Engineering for Sustainable Development (ICCESD 2018), pp. 1–7.

Wolman, M. G. (1959). Factors influencing erosion of a cohesive river bank. American Journal of Science, 257(3), 204-216.

Yu, M., Xie, Y., Wu, S., & Tian, H. (2019). Sidewall shear stress distribution effects on cohesive bank erosion in curved channels. Proceedings of the institution of civil engineers-water management.

Yusoff, A. H., Rahman, S. N. A., Sulaiman, M. S., Ideris, M. M., & Goh, Y. C. (2022, June). Determination of erosion risk level at the downstream of Kelantan river. In AIP Conference Proceedings (Vol. 2454, No. 1, p. 050047). AIP Publishing LLC.

Zhang W, Goh AT. Multivariate adaptive regression splines and neural network models for prediction of pile drivability. Geoscience Frontiers. 2016 Jan 1;7(1):45-52.

Zhang W, Li H, Li Y, Liu H, Chen Y, Ding X. Application of deep learning algorithms in geotechnical engineering: a short critical review. Artificial Intelligence Review. 2021 Dec;54(8):5633-73.

Zhang W, Wu C, Zhong H, Li Y, Wang L. Prediction of undrained shear strength using extreme gradient boosting and random forest based on Bayesian optimization. Geoscience Frontiers. 2021 Jan 1;12(1):469-77.

Zhang W, Zhang R, Wu C, Goh AT, Lacasse S, Liu Z, Liu H. State-of-the-art review of soft computing applications in underground excavations. Geoscience Frontiers. 2020 Jul 1;11(4):1095-106.

Zhang W, Zhang R, Wu C, Goh AT, Wang L. Assessment of basal heave stability for braced excavations in anisotropic clay using extreme gradient boosting and random forest regression. Underground Space. 2020 Mar 24.

Zhang WG, Li HR, Wu CZ, Li YQ, Liu ZQ, Liu HL. Soft computing approach for prediction of surface settlement induced by earth pressure balance shield tunneling. Underground Space. 2021 Aug 1;6(4):353-63.

APPENDICES

Morphological analysis

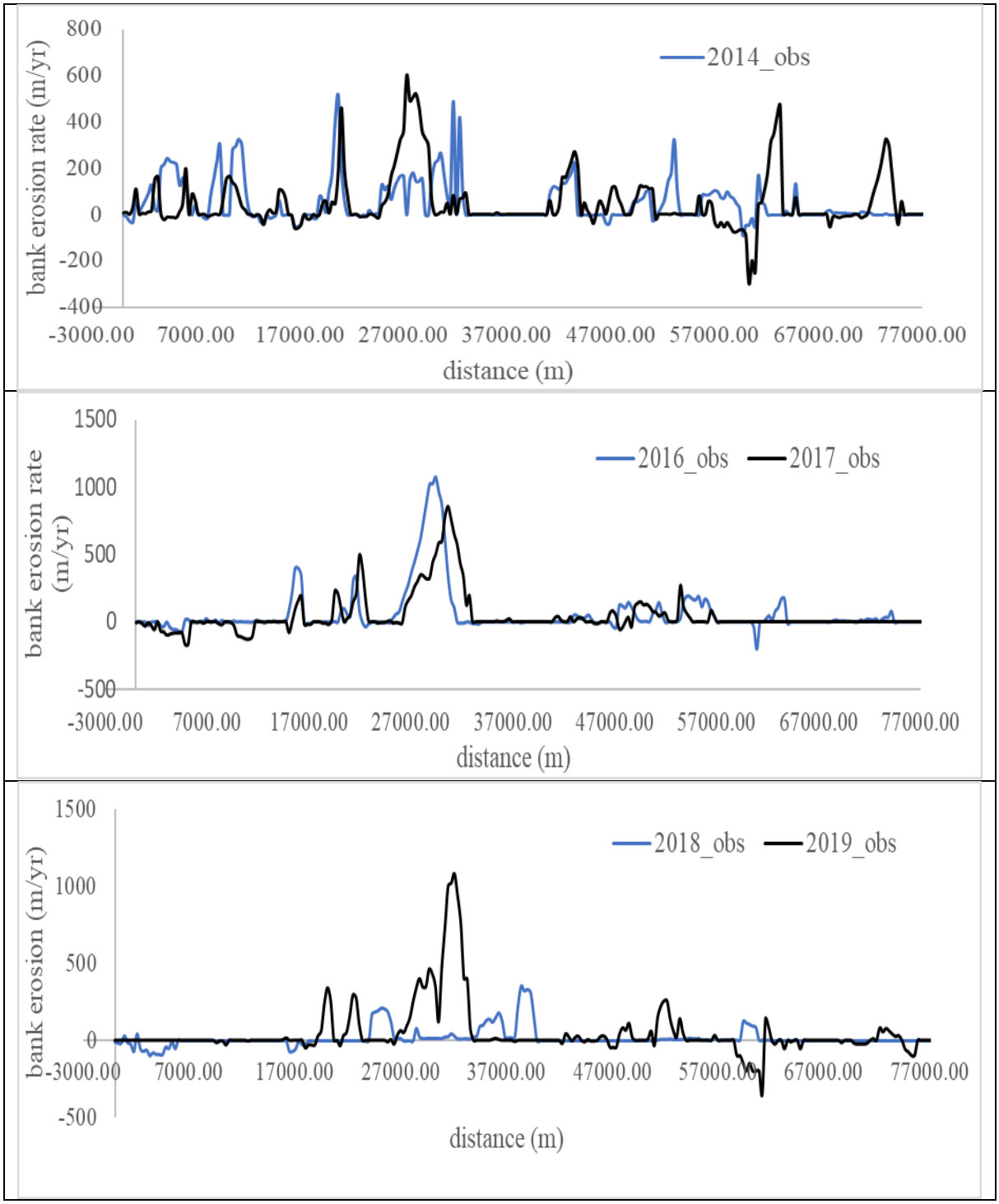

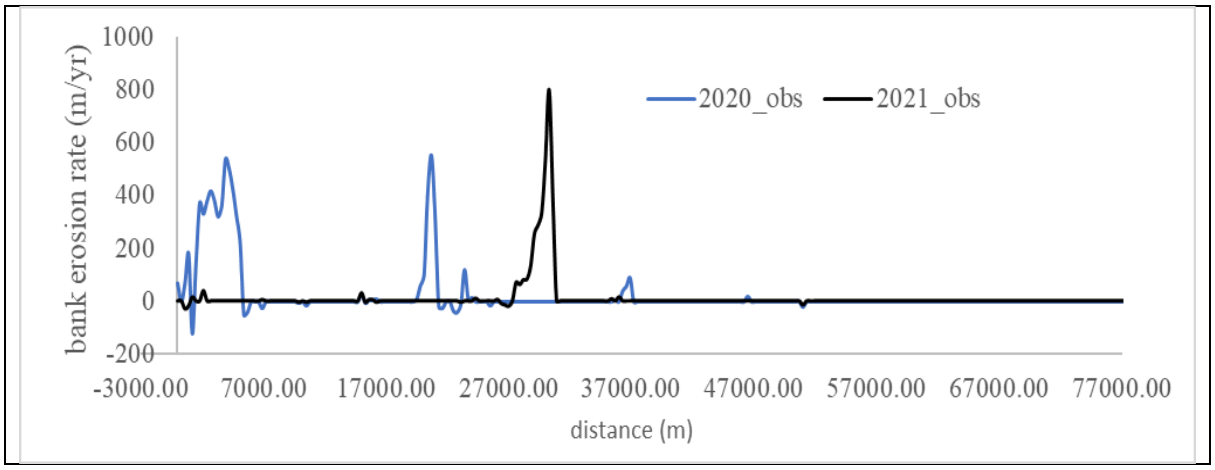

Figure 5.30: Bank erosion rate of the selected reach of the left bank,Jmauna river

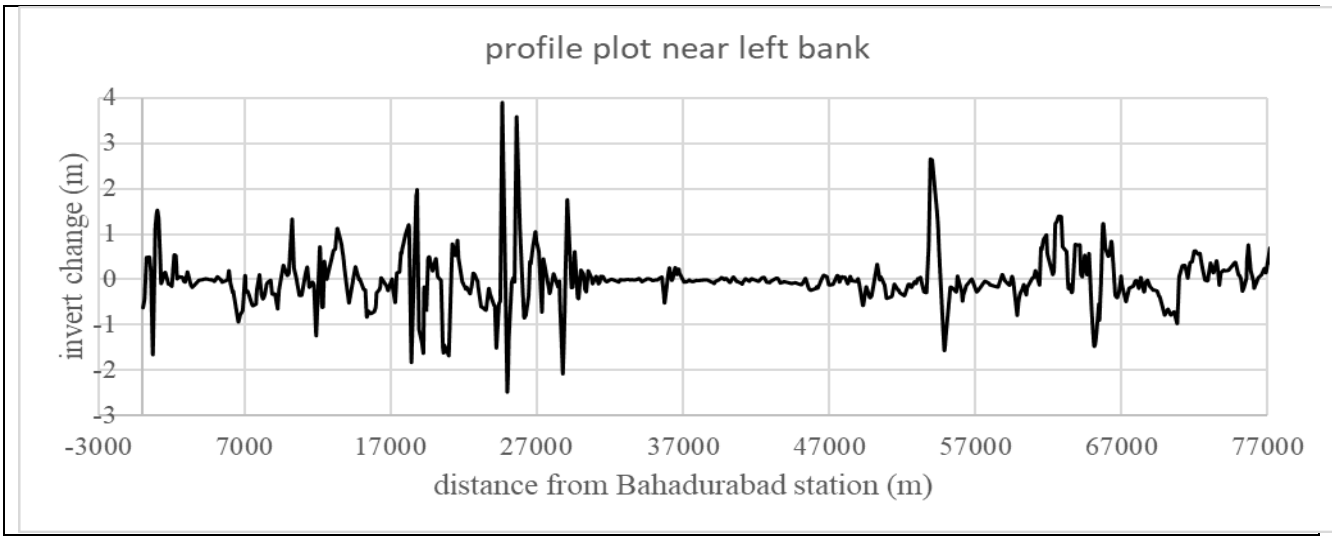

Figure 5.31 : Longitudinal profile of bed level changes from 2018-2021

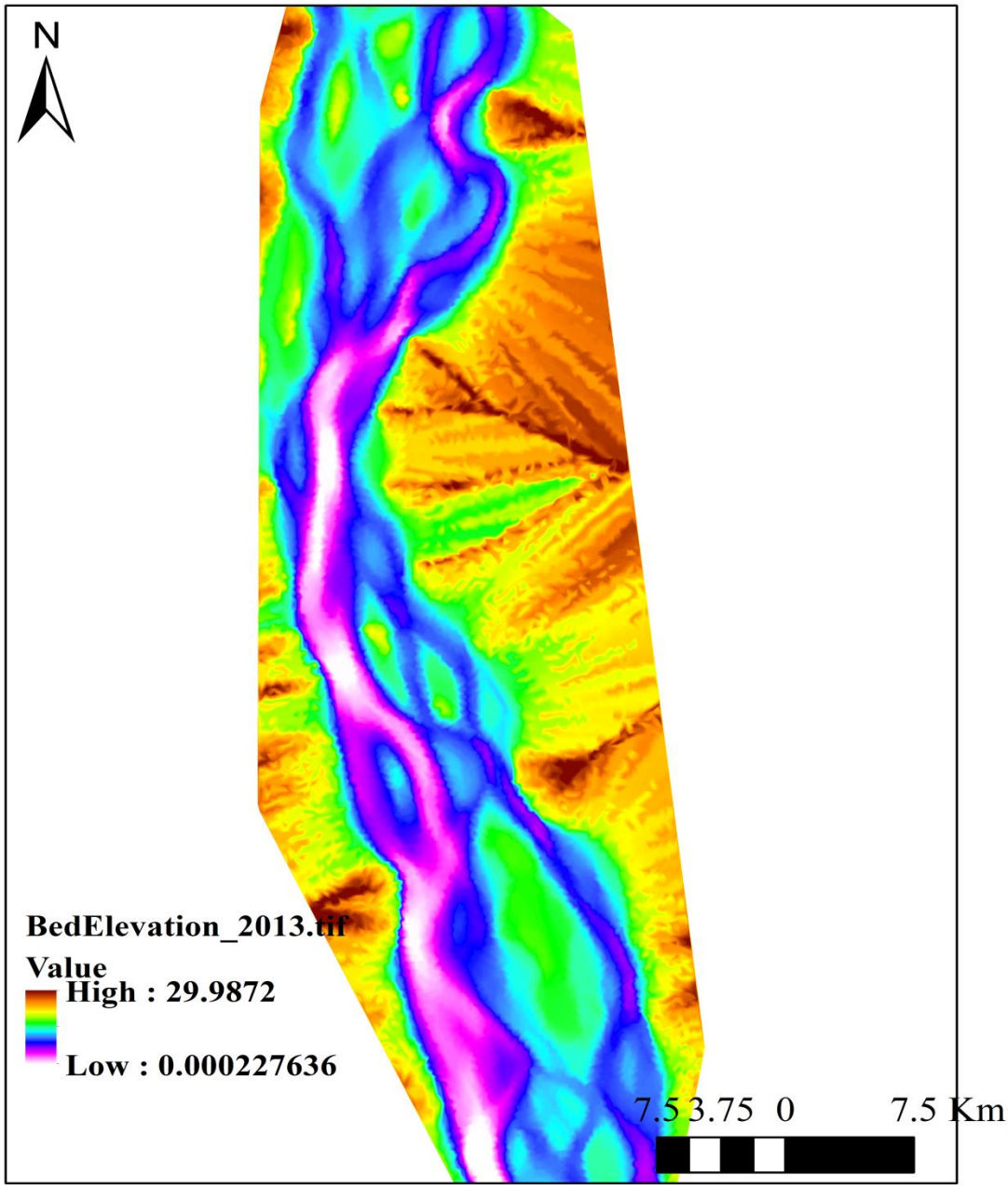

Figure 5.32: simulated bed elevation for the year 2013

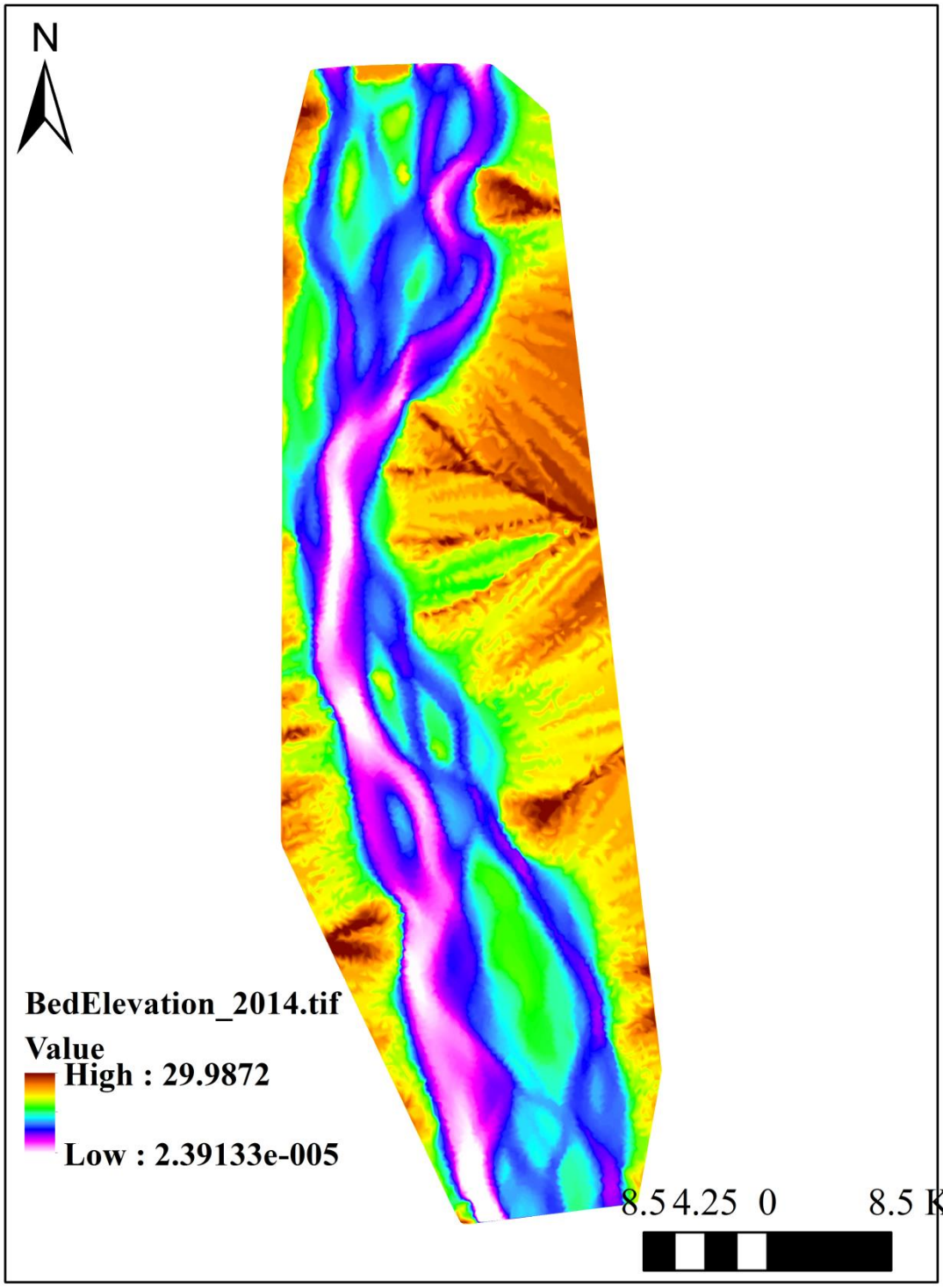

Figure 5.33: simulated bed elevation for the year 2014

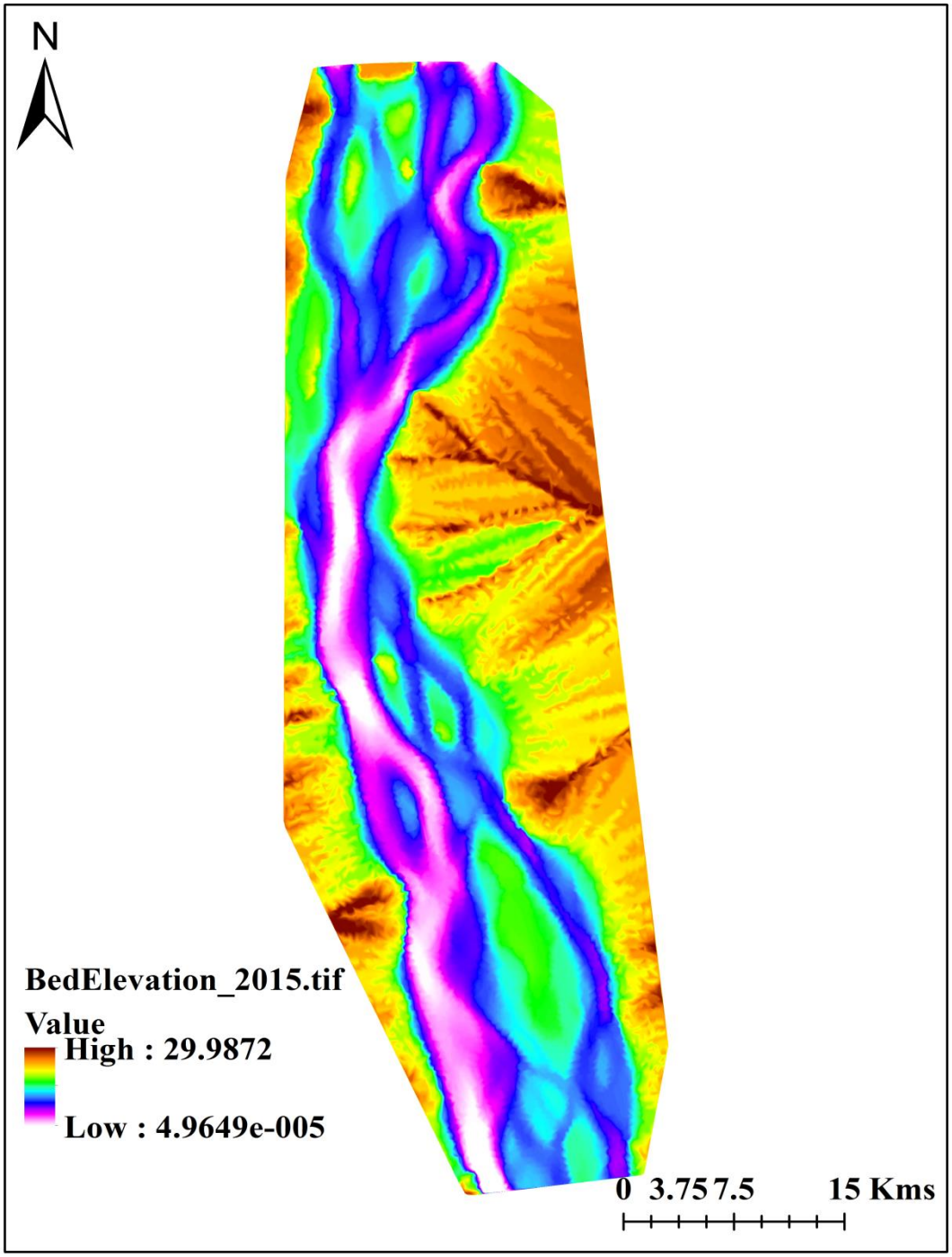

Figure 5.34 : simulated bed elevation for the year 2015

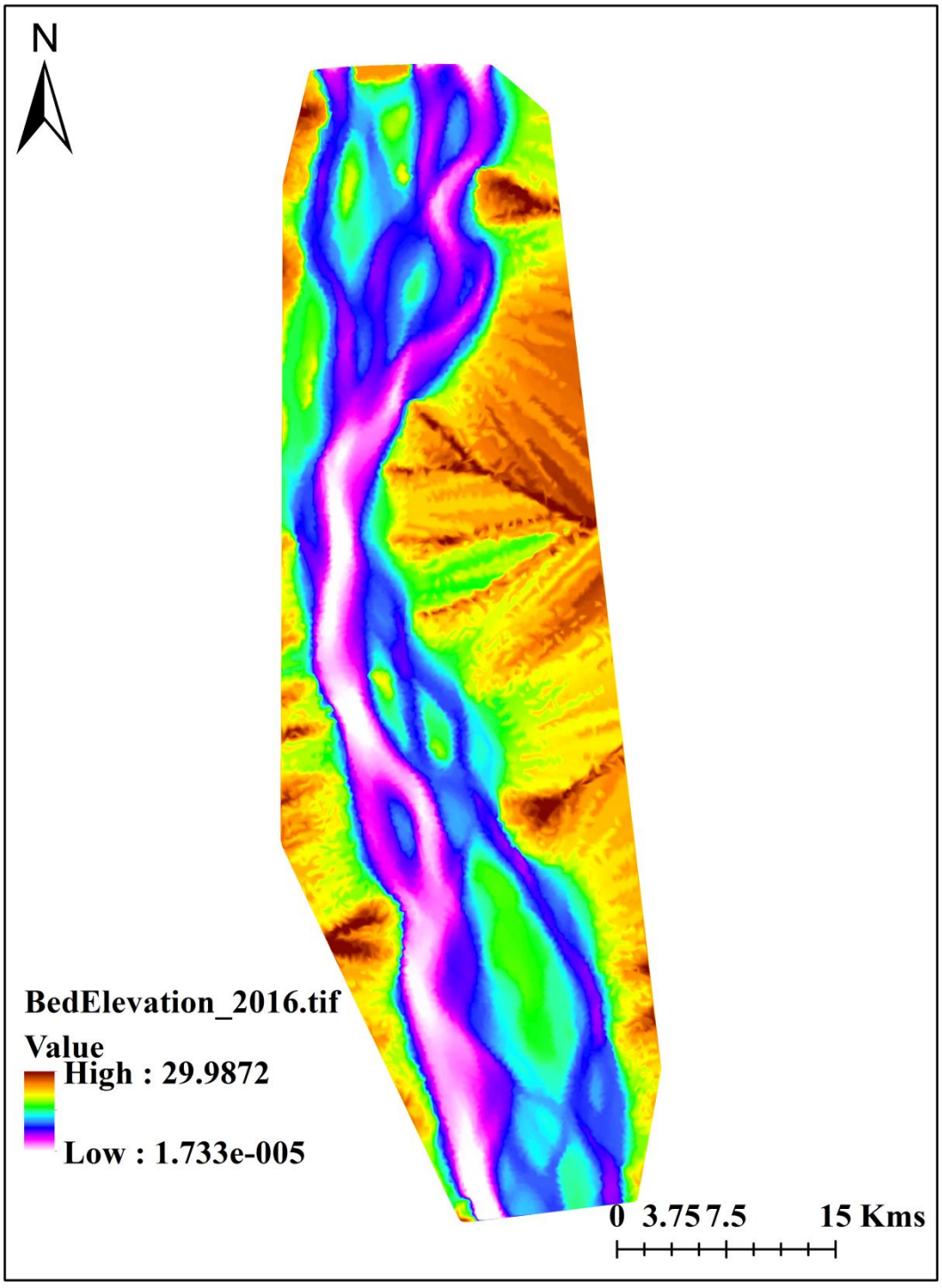

Figure 5.35 : simulated bed elevation for the year 2016

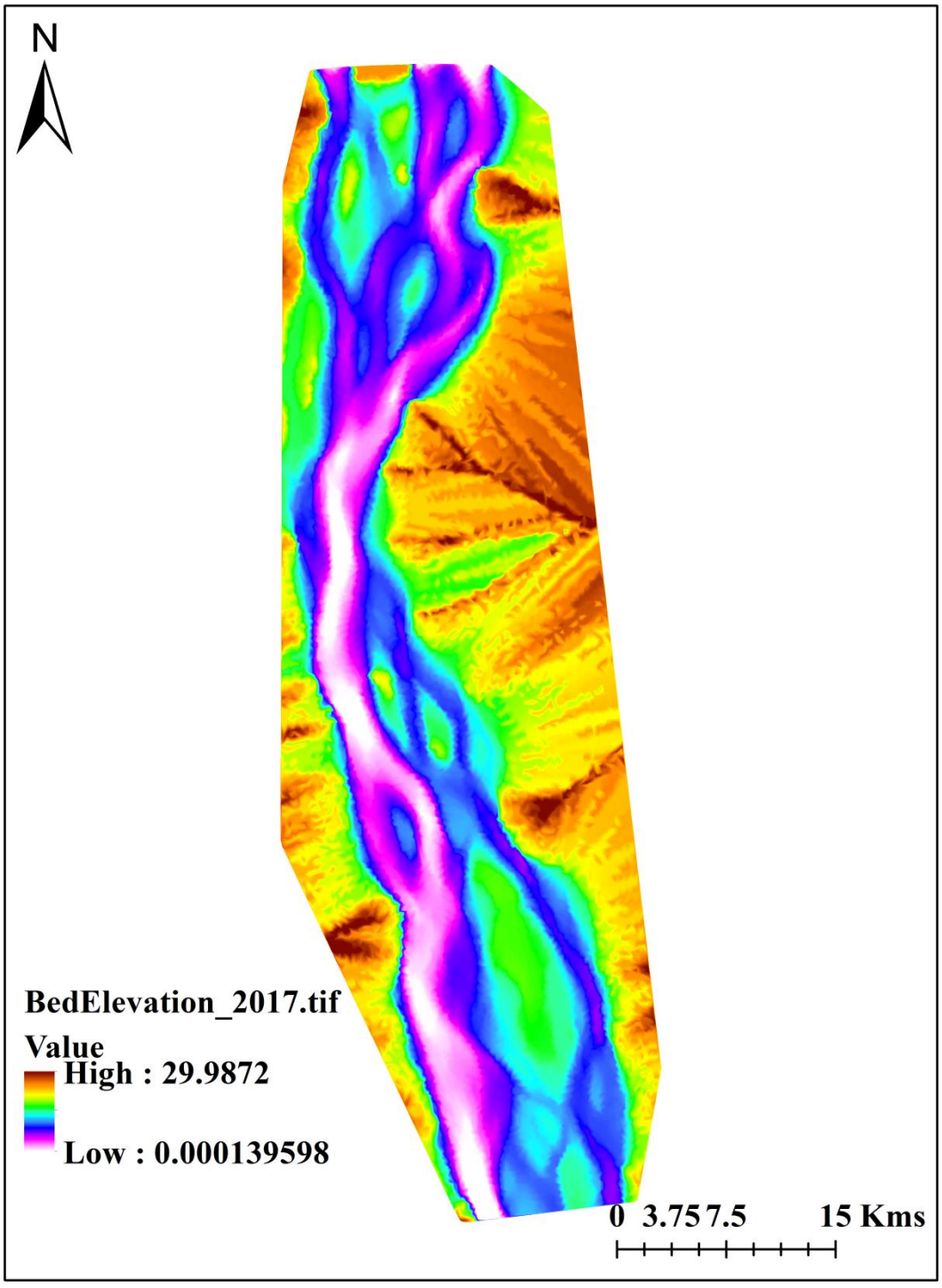

Figure 5.36 : simulated bed elevation for the year 2017

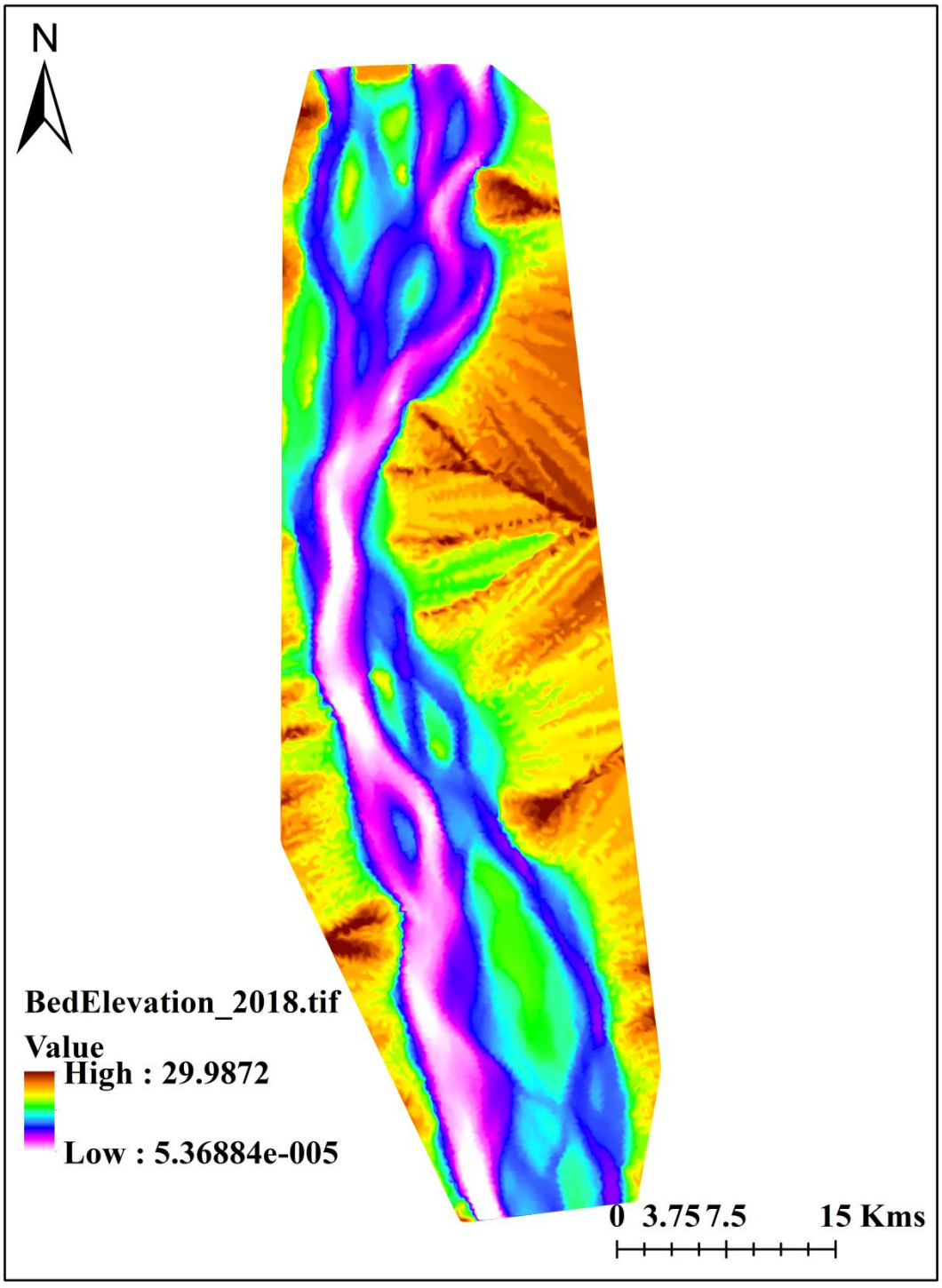

Figure 5.37 : simulated bed elevation for the year 2018

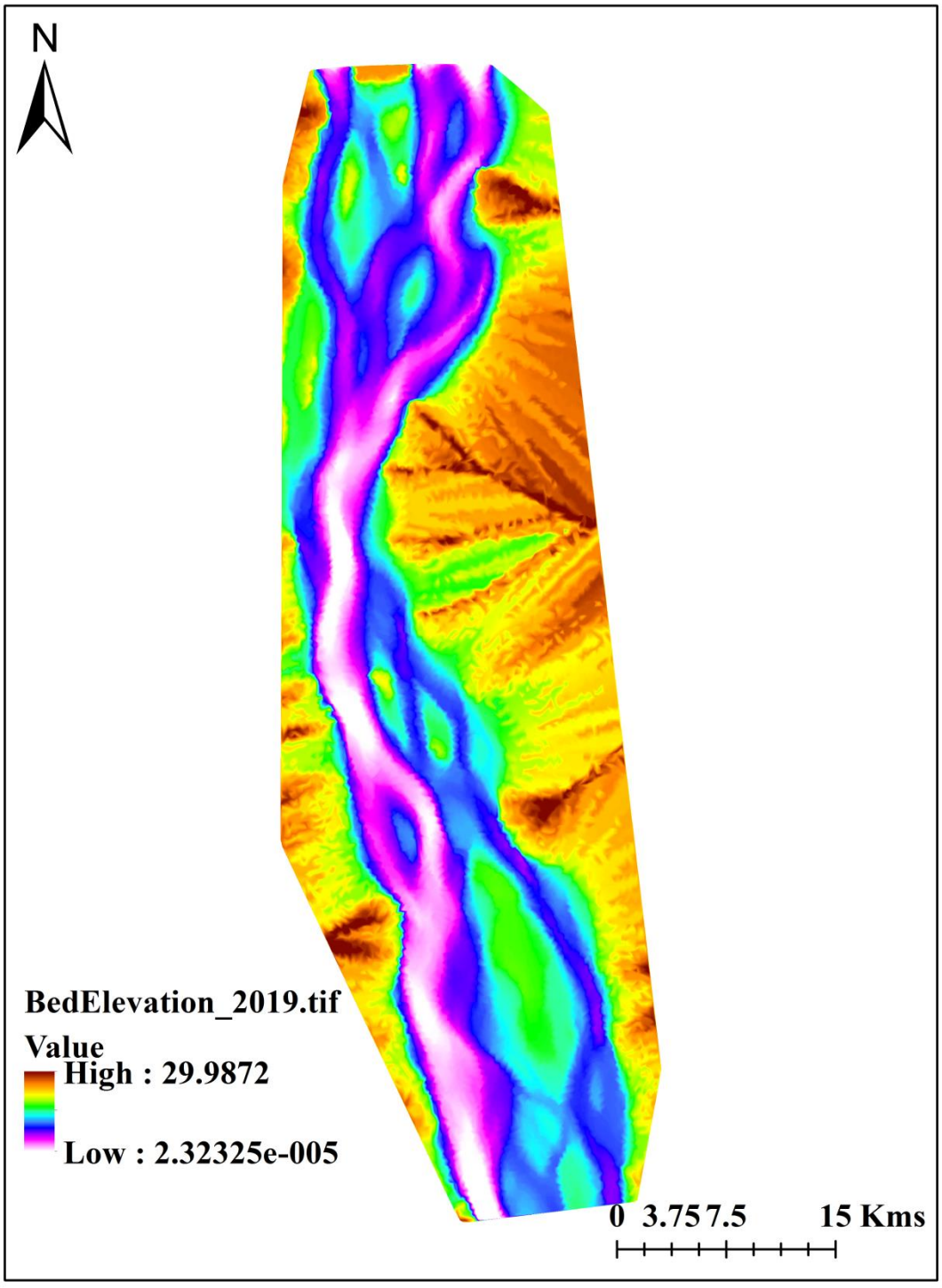

Figure 5.38 : simulated bed elevation for the year 2019

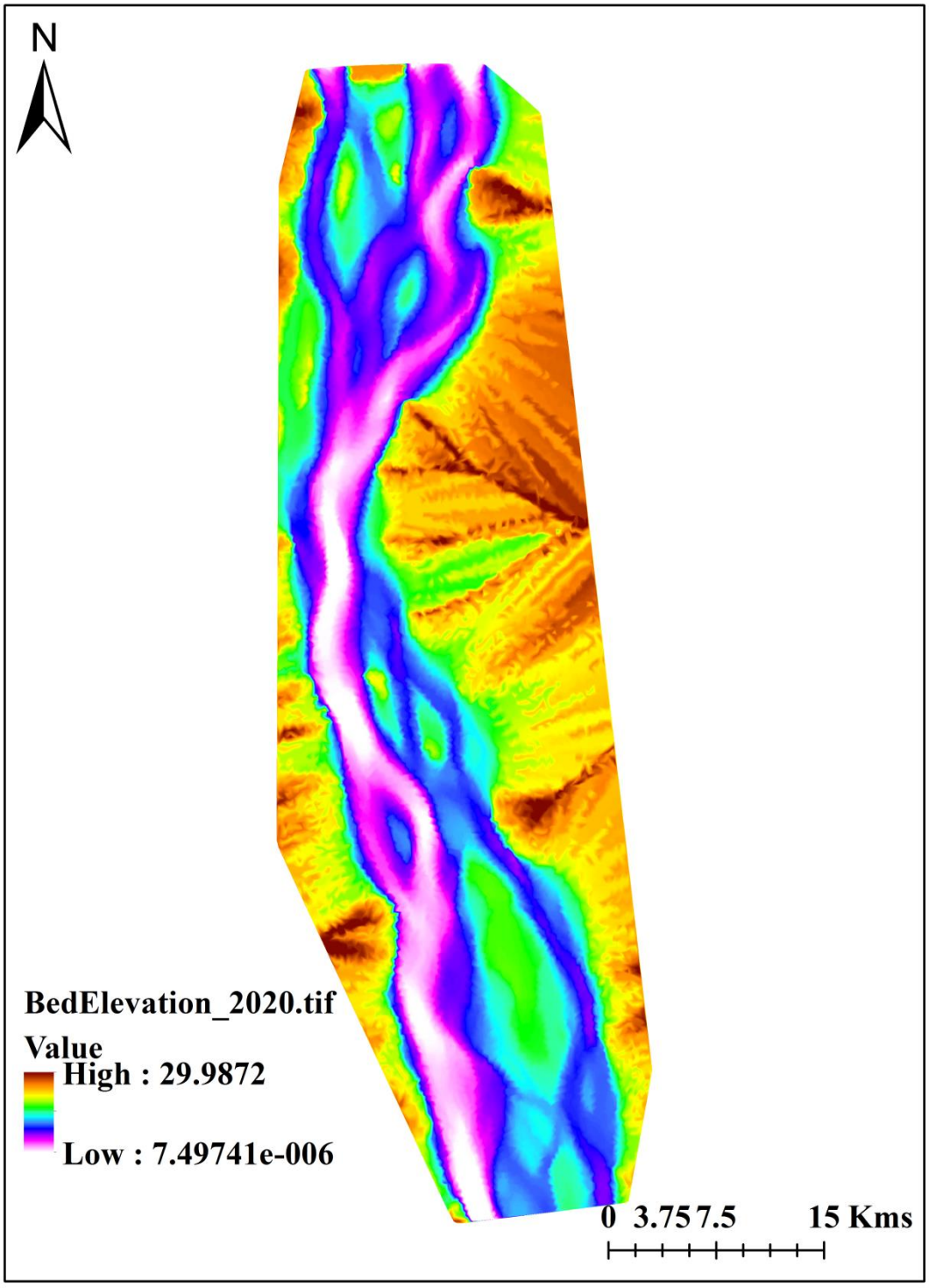

Figure 5.39 : simulated bed elevation for the year 2020

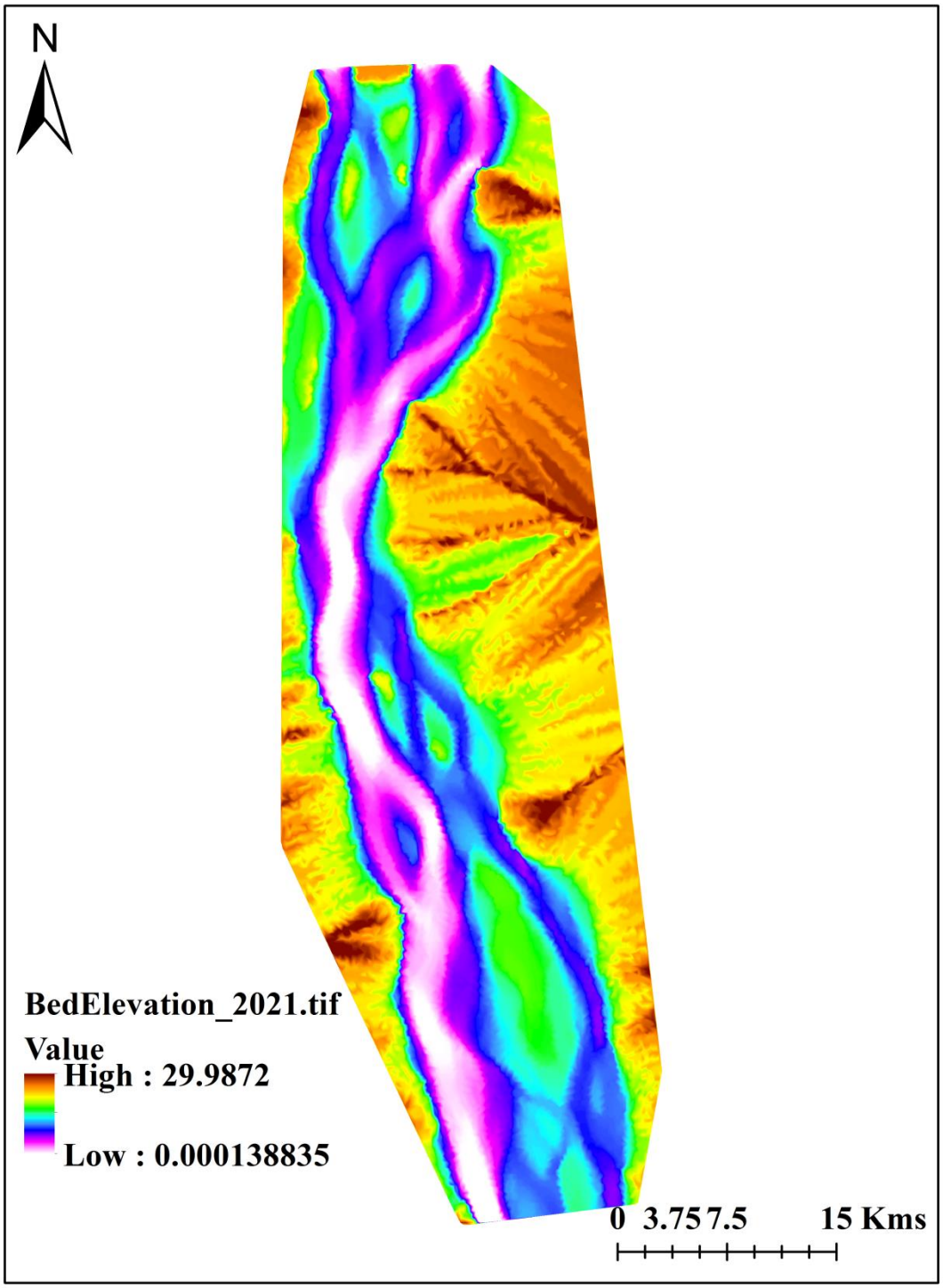

Figure 5.40 : simulated bed elevation for the year 2021

Table 4.3: Data set for calibration of regression model (Scenario-1)

XS ID	MAX LOB discharge	max WSE	max slope	max velocity	min WSE	bank erosion rate
13.00	7420.94	19.56	0.00	0.45	12.70	0
12.98	6782.87	19.56	0.00	0.44	12.70	0
12.95	6197.43	19.56	0.00	0.43	12.70	0
12.93	5672.8	19.55	0.00	0.42	12.70	0
12.91	18328	19.55	0.00	0.33	12.70	0
12.88	19837.87	19.54	0.00	0.31	12.70	0
12.86	21180.47	19.54	0.00	0.30	12.69	0
12.83	4177.44	19.54	0.00	0.39	12.69	0
12.81	3929.9	19.54	0.00	0.38	12.69	0
12.79	3708.28	19.53	0.00	0.38	12.69	0
12.76	3510.2	19.53	0.00	0.37	12.69	0
12.74	2983.08	19.53	0.00	0.37	12.69	0
12.72	2812.4	19.53	0.00	0.37	12.69	0
12.69	2662.14	19.52	0.00	0.37	12.69	0
12.67	2520.87	19.52	0.00	0.36	12.69	0
12.65	2403.29	19.52	0.00	0.36	12.69	0
12.62	582.71	19.52	0.00	0.38	12.69	0
12.60	626.67	19.51	0.00	0.38	12.69	0
12.57	674.9	19.51	0.00	0.38	12.69	0
12.55	729.64	19.51	0.00	0.38	12.69	0
12.53	788.29	19.50	0.00	0.39	12.69	0
12.50	852.14	19.50	0.00	0.39	12.69	0
12.48	922.87	19.50	0.00	0.39	12.69	0
12.455*	1001.45	19.49	0.00	0.40	12.69	0
12.432*	1089	19.49	0.00	0.40	12.69	0
12.408*	1187.79	19.49	0.00	0.41	12.68	0
12.384*	1297.99	19.48	0.00	0.42	12.68	0
12.361*	1422.93	19.48	0.00	0.43	12.68	0
12.337*	1564.99	19.47	0.00	0.44	12.67	0
12.313*	1724.68	19.47	0.00	0.45	12.66	0
12.289*	1911.49	19.46	0.00	0.47	12.65	0
12.266*	2127.22	19.45	0.00	0.49	12.64	0
12.242*	2381.26	19.44	0.00	0.51	12.64	0

12.218*	2677.66	19.43	0.00	0.53	12.63	0
12.195*	3034.4	19.42	0.00	0.56	12.62	0
12.171*	3461.83	19.41	0.00	0.59	12.62	0
12.147*	3977.68	19.39	0.00	0.63	12.61	0
12.124*	4610.36	19.37	0.00	0.67	12.60	0
12.10	5308.7	19.33	0.00	0.73	12.59	0
12.096*	5114.32	19.30	0.00	0.74	12.58	0
12.092*	4915.68	19.27	0.00	0.74	12.56	0
12.088*	4712.37	19.23	0.00	0.75	12.55	0
12.085*	4516.04	19.20	0.00	0.75	12.52	0
12.081*	4326.46	19.17	0.00	0.76	12.50	0
12.077*	4133.93	19.13	0.00	0.76	12.47	5
12.073*	3957.86	19.10	0.00	0.77	12.43	0
12.069*	3777.82	19.07	0.00	0.77	12.39	0
12.062*	3606.73	19.03	0.00	0.78	12.34	0
12.058*	3439.38	19.00	0.00	0.79	12.29	0
12.054*	3274.96	18.97	0.00	0.79	12.23	0
12.050*	3118.31	18.93	0.00	0.80	12.17	0
12.046*	2965.75	18.90	0.00	0.81	12.10	0
12.042*	2818.26	18.87	0.00	0.81	12.04	0
12.038*	2673.91	18.83	0.00	0.82	11.98	0
12.035*	2532.76	18.80	0.00	0.83	11.91	0
12.031*	2779.48	18.77	0.00	0.83	11.84	0
12.027*	2679.37	18.73	0.00	0.84	11.78	0
12.02	2545.66	18.70	0.00	0.84	11.71	0
12.02	2449.96	18.67	0.00	0.84	11.65	0
12.015*	2362.58	18.64	0.00	0.85	11.59	0
12.012*	2276.85	18.61	0.00	0.86	11.54	0
12.008*	2198.56	18.57	0.00	0.87	11.49	0
12.004*	2119.63	18.54	0.00	0.88	11.46	0
12.00	2048.4	18.51	0.00	0.89	11.43	0
11.965*	1985.37	18.48	0.00	0.90	11.40	0
11.931*	1845.23	18.44	0.00	0.92	11.38	0
11.896*	1706.72	18.40	0.00	0.94	11.35	0
11.862*	1573.13	18.37	0.00	0.96	11.32	0

11.827*	1447.35	18.33	0.00	0.98	11.28	0
11.792*	1339.32	18.29	0.00	1.00	11.25	250
11.758*	1243.49	18.25	0.00	1.01	11.21	300
11.723*	1190.07	18.22	0.00	1.03	11.17	320
11.688*	1140.3	18.18	0.00	1.03	11.12	330
11.654*	1098.6	18.15	0.00	1.02	11.07	320
11.619*	1057.43	18.11	0.00	1.02	11.02	300
11.585*	1017.99	18.08	0.00	1.01	10.96	280
11.550*	981.28	18.05	0.00	1.01	10.91	280
11.515*	945.99	18.02	0.00	1.00	10.86	0
11.481*	913.29	17.99	0.00	1.00	10.80	0
11.446*	882.49	17.96	0.00	0.99	10.75	0
11.412*	943.57	17.94	0.00	0.99	10.69	0
11.377*	955.62	17.91	0.00	0.98	10.63	0
11.342*	945.78	17.89	0.00	0.98	10.58	0
11.308*	937.62	17.86	0.00	0.97	10.52	0
11.273*	930.05	17.84	0.00	0.97	10.48	0
11.238*	924.25	17.81	0.00	0.97	10.45	0
11.204*	921.83	17.79	0.00	0.96	10.42	400
11.169*	948.77	17.77	0.00	0.96	10.40	400
11.135*	949.06	17.75	0.00	0.96	10.38	400
11.10	949.66	17.73	0.00	0.95	10.37	0
11.096*	951.41	17.71	0.00	0.95	10.36	0
11.093*	834.51	17.69	0.00	0.90	10.35	0
11.089*	738.73	17.68	0.00	0.86	10.34	0
11.085*	659.3	17.67	0.00	0.82	10.33	0
11.081*	592.22	17.66	0.00	0.79	10.32	0
11.078*	534.57	17.65	0.00	0.76	10.32	0
11.074*	485.16	17.64	0.00	0.74	10.31	0
11.070*	441.68	17.63	0.00	0.72	10.31	0
11.067*	403.63	17.62	0.00	0.71	10.30	0
11.063*	369.83	17.61	0.00	0.69	10.30	0
11.059*	339.08	17.60	0.00	0.68	10.30	0
11.056*	301.95	17.59	0.00	0.67	10.30	0
11.052*	278.03	17.58	0.00	0.67	10.30	0

11.048*	255.73	17.57	0.00	0.66	10.30	0
11.044*	235.85	17.56	0.00	0.66	10.30	0
11.041*	217.89	17.55	0.00	0.66	10.30	0
11.037*	200.5	17.54	0.00	0.67	10.30	0
11.033*	184.45	17.53	0.00	0.67	10.30	0
11.030*	169.12	17.51	0.00	0.68	10.29	0
11.026*	154.35	17.50	0.00	0.69	10.29	0
11.022*	138.96	17.48	0.00	0.70	10.29	0
11.019*	114.41	17.46	0.00	0.71	10.29	0
11.015*	104.19	17.44	0.00	0.73	10.29	0
11.011*	93.52	17.42	0.00	0.75	10.28	0
11.007*	106.34	17.40	0.00	0.79	10.28	0
11.004*	87.69	17.36	0.00	0.82	10.28	0
11.00	68.86	17.31	0.00	0.86	10.27	0
10.980*	47.88	17.25	0.00	0.92	10.26	200
10.961*	47.05	17.21	0.00	0.83	10.26	0
10.941*	49.84	17.17	0.00	0.80	10.26	0
10.922*	53.25	17.14	0.00	0.77	10.25	0
10.902*	57.5	17.11	0.00	0.74	10.25	0
10.883*	62.72	17.08	0.00	0.72	10.25	0
10.863*	68.85	17.06	0.00	0.70	10.25	0
10.843*	75.72	17.04	0.00	0.68	10.25	0
10.824*	83.33	17.03	0.00	0.66	10.25	0
10.804*	82.66	17.01	0.00	0.64	10.25	0
10.785*	92.34	17.00	0.00	0.63	10.25	0
10.765*	102.5	16.98	0.00	0.61	10.25	0
10.746*	112.79	16.97	0.00	0.60	10.25	0
10.726*	123.48	16.96	0.00	0.59	10.25	0
10.707*	134.59	16.95	0.00	0.58	10.25	0
10.687*	147.25	16.94	0.00	0.57	10.25	0
10.667*	162.02	16.93	0.00	0.56	10.25	0
10.648*	179.71	16.92	0.00	0.55	10.25	0
10.628*	201.08	16.91	0.00	0.55	10.25	0
10.609*	226.21	16.90	0.00	0.54	10.25	0
10.589*	258.17	16.90	0.00	0.54	10.25	0

10.570*	296.54	16.89	0.00	0.53	10.25	0
10.550*	326.21	16.88	0.00	0.53	10.25	0
10.530*	373.02	16.87	0.00	0.53	10.24	0
10.511*	394.01	16.86	0.00	0.52	10.24	0
10.491*	450.59	16.86	0.00	0.52	10.24	0
10.472*	511.02	16.85	0.00	0.52	10.24	0
10.452*	575.09	16.84	0.00	0.52	10.24	0
10.433*	644.83	16.83	0.00	0.52	10.24	0
10.413*	720.06	16.82	0.00	0.52	10.24	0
10.393*	801.15	16.82	0.00	0.53	10.24	0
10.374*	886.88	16.81	0.00	0.53	10.24	0
10.354*	979.31	16.80	0.00	0.53	10.24	0
10.335*	1080.87	16.79	0.00	0.54	10.24	0
10.315*	1187.95	16.78	0.00	0.54	10.23	0
10.296*	1304.06	16.77	0.00	0.55	10.23	0
10.276*	1428.99	16.76	0.00	0.55	10.23	0
10.257*	1566.8	16.75	0.00	0.56	10.22	0
10.237*	1711.09	16.74	0.00	0.57	10.22	0
10.217*	1872.06	16.73	0.00	0.58	10.21	0
10.198*	2046.74	16.72	0.00	0.59	10.20	0
10.178*	2238.54	16.70	0.00	0.60	10.19	0
10.159*	2448.36	16.69	0.00	0.61	10.18	0
10.139*	2676.67	16.67	0.00	0.63	10.17	0
10.120*	2920.37	16.65	0.00	0.65	10.16	0
10.10	3136.77	16.64	0.00	0.66	10.14	0
10.095*	3239.91	16.61	0.00	0.68	10.12	0
10.091*	3210.82	16.60	0.00	0.68	10.10	0
10.086*	3054.81	16.58	0.00	0.67	10.07	0
10.082*	2869.34	16.56	0.00	0.66	10.05	0
10.077*	2699.21	16.54	0.00	0.65	10.01	0
10.073*	2547.71	16.52	0.00	0.65	9.98	0
10.068*	2413.58	16.50	0.00	0.64	9.94	0
10.064*	2308.75	16.49	0.00	0.64	9.89	0
10.059*	2201.43	16.47	0.00	0.64	9.84	0
10.055*	2103.27	16.45	0.00	0.64	9.79	0

10.050*	2021.15	16.43	0.00	0.65	9.74	0
10.045*	1938.15	16.42	0.00	0.65	9.71	0
10.041*	1859.89	16.40	0.00	0.65	9.68	0
10.036*	1812.82	16.38	0.00	0.66	9.65	0
10.032*	1750.8	16.36	0.00	0.67	9.63	0
10.027*	1690.93	16.34	0.00	0.68	9.61	0
10.023*	1630.1	16.31	0.00	0.69	9.60	0
10.018*	1543.78	16.29	0.00	0.70	9.58	0
10.014*	1482.61	16.26	0.00	0.72	9.57	0
10.009*	1404.72	16.23	0.00	0.73	9.55	0
10.005*	1306.64	16.19	0.00	0.75	9.54	0
10.00	1176.55	16.15	0.00	0.78	9.52	0
9.9438*	1008.56	16.10	0.00	0.81	9.49	0
9.8875*	1071.66	16.05	0.00	0.82	9.47	0
9.8313*	1143.76	16.00	0.00	0.83	9.45	0
9.7750*	1227.58	15.95	0.00	0.84	9.43	0
9.7188*	1312.96	15.91	0.00	0.85	9.40	0
9.6625*	1406.1	15.86	0.00	0.85	9.37	0
9.6063*	1621.52	15.82	0.00	0.86	9.34	0
9.5500*	1758.45	15.77	0.00	0.86	9.32	0
9.4938*	1891.69	15.73	0.00	0.87	9.29	0
9.4375*	2014.59	15.68	0.00	0.87	9.26	0
9.3813*	2181.72	15.64	0.00	0.88	9.21	0
9.3250*	2318.77	15.60	0.00	0.88	9.17	0
9.2688*	2491.93	15.57	0.00	0.88	9.14	0
9.2125*	2695.31	15.53	0.00	0.88	9.11	0
9.1563*	2898.08	15.49	0.00	0.88	9.09	0
9.10	2992.72	15.46	0.00	0.88	9.07	0
9.0941*	3215.36	15.42	0.00	0.88	9.05	0
9.0882*	3217.32	15.39	0.00	0.88	9.03	0
9.0824*	3222.2	15.36	0.00	0.88	9.01	0
9.0765*	3267.36	15.33	0.00	0.88	8.98	0
9.0706*	3354.33	15.29	0.00	0.87	8.94	0
9.0647*	3325.03	15.25	0.00	0.87	8.91	0
9.0588*	3272.98	15.22	0.00	0.86	8.87	0

9.0529*	3279.02	15.18	0.00	0.86	8.83	0
9.0471*	3240.08	15.14	0.00	0.85	8.79	0
9.0412*	3183.41	15.11	0.00	0.85	8.76	0
9.0353*	3128.13	15.07	0.00	0.84	8.72	0
9.0294*	3078.6	15.04	0.00	0.84	8.68	0
9.0235*	3027.02	15.00	0.00	0.84	8.66	0
9.0176*	2983.68	14.97	0.00	0.83	8.63	0
9.0118*	2944.29	14.94	0.00	0.83	8.62	0
9.0059*	2905.13	14.90	0.00	0.82	8.60	0
9.00	2859.35	14.87	0.00	0.82	8.59	0
8.9500*	2864.7	14.84	0.00	0.81	8.58	0
8.9000*	3385	14.82	0.00	0.79	8.57	0
8.8500*	3999.48	14.79	0.00	0.78	8.56	0
8.8000*	4630.08	14.76	0.00	0.76	8.55	0
8.7500*	5304.28	14.74	0.00	0.74	8.53	0
8.7000*	6048.56	14.72	0.00	0.72	8.50	0
8.65	6777.36	14.69	0.00	0.71	8.47	0
8.6000*	7527.89	14.67	0.00	0.69	8.43	0
8.55	8395.17	14.65	0.00	0.67	8.39	0
8.5000*	9271.98	14.63	0.00	0.66	8.35	0
8.45	9991.19	14.61	0.00	0.64	8.31	0
8.4000*	10669.01	14.59	0.00	0.62	8.27	0
8.3500*	11329.32	14.57	0.00	0.60	8.24	0
8.3000*	11973.77	14.55	0.00	0.58	8.21	0
8.2500*	12598.33	14.53	0.00	0.56	8.19	0
8.2000*	13232.27	14.52	0.00	0.55	8.17	0
8.1500*	13854.87	14.50	0.00	0.53	8.14	0
8.10	14469.69	14.49	0.00	0.51	8.12	0
8.0960*	15068.48	14.48	0.00	0.50	8.11	0
8.0920*	14217.64	14.46	0.00	0.50	8.09	0
8.0880*	13389.72	14.45	0.00	0.51	8.07	0
8.0840*	12378.96	14.44	0.00	0.51	8.05	0
8.0800*	11576	14.43	0.00	0.52	8.03	0
8.0760*	10789.23	14.41	0.00	0.52	8.01	0
8.0720*	10025.88	14.40	0.00	0.52	7.99	0

8.0680*	9288.86	14.39	0.00	0.53	7.96	0
8.0640*	8566.08	14.37	0.00	0.53	7.93	0
8.0600*	7871.88	14.36	0.00	0.53	7.90	0
8.0560*	7196.66	14.35	0.00	0.54	7.87	0
8.0520*	6544.1	14.33	0.00	0.54	7.83	0
8.0480*	5919.49	14.32	0.00	0.54	7.79	0
8.0440*	5318.73	14.31	0.00	0.54	7.75	0
8.0400*	4747.14	14.29	0.00	0.54	7.70	0
8.0360*	4196.87	14.28	0.00	0.54	7.66	0
8.0320*	3673.3	14.27	0.00	0.54	7.60	0
8.0280*	3180.71	14.26	0.00	0.54	7.54	0
8.0240*	3448.19	14.24	0.00	0.53	7.47	0
8.0200*	3086.87	14.23	0.00	0.53	7.40	0
8.0160*	2761.64	14.22	0.00	0.53	7.34	0
8.0120*	2473.81	14.21	0.00	0.53	7.29	0
8.0080*	2483.07	14.19	0.00	0.53	7.24	0
8.0040*	2302.37	14.18	0.00	0.52	7.19	0
8.00	2171.04	14.17	0.00	0.52	7.15	0
7.9250*	2109.24	14.16	0.00	0.52	7.12	0
7.8500*	2170.29	14.15	0.00	0.53	7.08	0
7.7750*	2323.12	14.13	0.00	0.54	7.04	10
7.7000*	2325.21	14.12	0.00	0.56	6.99	25
7.6250*	2653.11	14.11	0.00	0.57	6.95	31
7.5500*	2292.7	14.09	0.00	0.59	6.90	22

Table 4.4: Data set for calibration of regression model (Scenario-2)

XS ID	max WSE	max velocity	min WSE	bank erosion rate
12.83	21.963	0.518	7.253	0
12.81	20.729	0.501	6.697	0
12.79	19.545	0.487	6.177	0
12.76	19.644	0.484	6.862	0
12.74	19.507	0.484	8.324	0
12.72	20.199	0.481	8.5334	0
12.69	19.232	0.464	8.046	0
12.67	18.53	0.444	7.619	0
12.65	16.81	0.429	6.82	0
12.62	15.346	0.421	4.581	0
12.60	12.221	0.424	2.215	0
12.57	10.377	0.421	0.704	0
12.55	8.634	0.407	0.732	0
12.53	7.532	0.393	0.606	0
12.50	6.57	0.409	0.674	0
12.48	5.703	0.441	1.953	0
12.455*	5.327	0.447	5.25	0
12.432*	4.77	0.423	3.206	0
12.408*	3.66	0.516	2.549	0
12.384*	9.993	0.62	1.062	0
12.361*	11.239	0.735	3.411	0
12.337*	11.751	0.812	3.529	0
12.313*	10.935	0.813	3.042	0
12.289*	10.804	0.837	2.853	0
12.266*	10.66	0.9	2.525	0
12.242*	10.556	0.99	2.832	0
12.218*	10.38	0.993	2.287	0
12.195*	9.987	1.061	1.96	0
12.171*	9.887	1.1105	2.018	0
12.147*	9.959	1.175	2.021	0

12.124*	9.942	1.187	1.94	0
12.10	9.73	1.261	1.793	0
12.096*	9.694	1.347	1.782	0
12.092*	9.7	1.315	1.763	0
12.088*	9.343	1.31	1.474	0
12.085*	9.01	1.304	1.2	0
12.081*	8.489	1.299	0.636	0
12.077*	7.034	1.261	0.105	5
12.073*	6.808	1.23	0.366	0
12.069*	6.789	1.243	0.41	0
12.062*	6.754	1.238	0.589	0
12.058*	6.752	1.236	0.557	0
12.054*	6.72	1.249	0.414	0
12.050*	6.659	1.257	0.379	0
12.046*	6.592	1.251	0.387	0
12.042*	6.52	1.248	0.3	0
12.038*	6.529	1.239	0.258	0
12.035*	6.58	1.254	0.046	0
12.031*	6.654	1.254	0	0
12.027*	6.8	1.252	0	0
12.02	6.926	1.267	0	0
12.02	6.9	1.339	0	0
12.015*	7.011	1.391	0.3	0
12.012*	7.163	1.404	0.4	0
12.008*	7.338	1.454	0.163	0
12.004*	7.541	1.501	0.438	0
12.00	7.692	1.55	0.609	0
11.965*	7.8	1.586	0.774	0
11.931*	8.178	1.628	1.027	0
11.896*	8.342	1.703	1.222	0
11.862*	8.662	1.712	1.598	0
11.827*	8.875	1.74	1.872	0
11.792*	9.054	1.768	2.029	250
11.758*	9.358	1.793	2.393	300
11.723*	9.61	1.841	2.638	320

11.688*	9.825	1.891	2.84	330
11.654*	10.108	1.963	3.161	320
11.619*	10.359	2.057	3.353	300
11.585*	10.603	2.069	3.588	280
11.550*	10.909	2.059	3.95	280
11.515*	11.127	2.078	4.176	0
11.481*	11.425	2.085	4.45	0
11.446*	11.707	2.103	4.729	0
11.412*	11.997	2.125	5.005	0
11.377*	12.159	2.179	5.198	0
11.342*	12.307	2.268	5.333	0
11.308*	12.477	2.183	5.484	0
11.273*	12.629	2.178	5.629	0
11.238*	12.854	2.179	5.9046	0
11.204*	12.974	2.147	5.09	400
11.169*	11.981	2.123	6.469	400
11.135*	13.32	2.07	6.332	400
11.10	11.01	2.205	3.358	0
11.096*	10.831	2.419	3.667	0
11.093*	6.076	2.79	1.324	0
11.089*	11.399	2.969	4.633	0
11.085*	11.417	2.802	4.48	0
11.081*	11.663	3.066	4.732	0
11.078*	11.8	2.608	4.946	0
11.074*	6.152	2.279	1.897	0
11.070*	5.832	1.747	3.812	0
11.067*	5.911	1.46	3.836	0
11.063*	6.1	1.274	1.753	0
11.059*	6.291	1.181	1.678	0
11.056*	6.213	1.12	2.23	0
11.052*	6.405	1.095	1.2	0
11.048*	7.507	1.096	1.2	0
11.044*	9.76	1.07	2.96	0
11.041*	7.066	0.994	0.567	0
11.037*	8.182	1.11	1.264	0

11.033*	9.743	1.156	3.054	0
11.030*	9.579	0.986	2.754	0
11.026*	9.268	0.893	2.566	0
11.022*	9.157	0.804	2.439	0
11.019*	8.947	0.721	2.267	0
11.015*	8.351	0.647	1.662	0
11.011*	7.91	0.603	1.385	0
11.007*	8.031	0.587	1.458	0
11.004*	7.415	0.581	0.653	0
11.00	8.602	0.55	1.985	0
10.980*	5.79	0.545	0	200
10.961*	6.368	0.498	0.177	0
10.941*	6.39	0.556	0.193	0
10.922*	6.317	0.549	0.606	0
10.902*	6.446	0.54	0.719	0
10.883*	6.63	0.545	0.32	0
10.863*	6.533	0.565	0.072	0
10.843*	4.567	0.626	0	0
10.824*	6.649	0.698	0.03	0
10.804*	6.812	0.69	0.226	0
10.785*	6.691	0.642	0.106	0
10.765*	6.658	0.601	0.04	0
10.746*	7.013	0.556	0.403	0
10.726*	6.979	0.511	0.229	0
10.707*	7.135	0.555	0	0
10.687*	6.624	0.678	0	0
10.667*	6.509	0.584	0	0
10.648*	6.192	0.49	0	0
10.628*	6.312	0.46	0	0
10.609*	6.377	0.444	0	0
10.589*	6.404	0.447	0	0
10.570*	6.432	0.491	0	0
10.550*	6.461	0.504	0	0
10.530*	6.493	0.537	0	0
10.511*	6.53	0.56	0	0

10.491*	6.556	0.59	0	0
10.472*	6.575	0.596	0.022	0
10.452*	6.573	0.648	0.057	0
10.433*	6.569	0.648	0.08	0
10.413*	6.557	0.678	0.04	0
10.393*	6.575	0.676	0.11	0
10.374*	6.58	0.723	0.124	0
10.354*	6.6	0.733	0.137	0
10.335*	6.618	0.734	0.1	0
10.315*	6.636	0.744	0.131	0
10.296*	6.665	0.71	0.137	0
10.276*	6.687	0.661	0.176	0
10.257*	6.722	0.444	0.198	0
10.237*	6.712	0.651	0.2	0
10.217*	6.708	0.745	0.125	0
10.198*	6.75	0.991	0.222	0
10.178*	6.704	1.344	0.222	0
10.159*	6.649	1.431	0.23	0
10.139*	6.716	2.458	0.213	0
10.120*	6.661	11.34	0.131	0
10.10	6.68	28.341	0.335	0
10.095*	6.743	18.273	0.276	0
10.091*	6.72	14.664	0.335	0
10.086*	6.589	13.67	0.293	0
10.082*	6.685	11.566	0.22	0
10.077*	6.684	9.254	0.318	0
10.073*	6.732	8.12	0.204	0
10.068*	6.769	7.125	0.269	0
10.064*	6.777	6.298	0.342	0
10.059*	6.857	6.368	0.306	0
10.055*	6.914	6	0.405	0
10.050*	6.925	5.66	0.465	0
10.045*	7.053	5.25	0.583	0
10.041*	7.122	4.802	0.693	0
10.036*	7.207	4.506	0.721	0

10.032*	7.273	4.059	0.792	0
10.027*	7.382	3.575	0.876	0
10.023*	7.424	3.085	0.957	0
10.018*	7.44	2.687	0.947	0
10.014*	6.372	2.509	0.57	0
10.009*	5.22	2.436	0	0
10.005*	4.338	1.168	0	0
10.00	4.261	1.301	0	0
9.9438*	3.83	1.241	0	0
9.8875*	3.842	1.304	0	0
9.8313*	3.868	0.643	0	0
9.7750*	3.891	0.96	0	0
9.7188*	3.912	0.325	0	0
9.6625*	4	0.39	0	0
9.6063*	4.274	0.424	0	0
9.5500*	4.601	0.318	0	0
9.4938*	4.543	0.335	0	0
9.4375*	4.503	0.351	0	0
9.3813*	4.475	0.358	0	0
9.3250*	4.309	0.368	0	0
9.2688*	4.085	0.374	0	0
9.2125*	4.067	0.375	0	0
9.1563*	4.074	0.386	0	0
9.10	4.043	0.4	0	0
9.0941*	4.052	0.42	0	0
9.0882*	4.305	0.48	0	0
9.0824*	4.567	0.587	0	0
9.0765*	6.614	1.049	0.2	0
9.0706*	6.402	0.921	0	0
9.0647*	5.935	0.694	0	0
9.0588*	5.421	0.557	0	0
9.0529*	5.228	0.5	0	0
9.0471*	5.153	1.341	0	0
9.0412*	5.274	7.505	0	0
9.0353*	7.042	4.554	0	0

9.0294*	5.644	3.401	0	0
9.0235*	6.392	4.446	0	0
9.0176*	6.532	3.689	0	0
9.0118*	6.666	2.016	0	0
9.0059*	6.442	1.279	0	0
9.00	6.583	1.023	0	0
8.9500*	7.023	1.119	0	0
8.9000*	7.43	1.267	0.203	0
8.8500*	7.82	1.504	0.586	0
8.8000*	8.415	1.525	1.245	0
8.7500*	9.292	1.654	2.09	0
8.7000*	10.047	1.599	2.856	0
8.65	10.468	1.652	3.25	0
8.6000*	10.849	1.626	3.644	0
8.55	11.378	1.567	4.169	0
8.5000*	11.793	1.533	4.533	0
8.45	12.203	1.48	4.721	0
8.4000*	12.059	1.41	4.74	0
8.3500*	11.917	1.362	4.742	0
8.3000*	12.112	1.271	4.939	0
8.2500*	12.461	1.19	5.221	0
8.2000*	12.7	1.128	5.524	0
8.1500*	13.058	1.07	5.833	0
8.10	13.319	0.979	6.085	0
8.0960*	13.519	0.908	6.305	0
8.0920*	13.492	0.831	6.343	0
8.0880*	13.022	0.723	5.861	0
8.0840*	11.182	0.603	4.227	0
8.0800*	8.706	0.524	1.537	0
8.0760*	8.299	0.516	1.171	0
8.0720*	8.299	0.514	1.122	0
8.0680*	7.863	0.511	0.698	0
8.0640*	7.974	0.508	0.797	0
8.0600*	6.343	0.66	0	0
8.0560*	6.23	0.8	0	0

8.0520*	6.585	0.829	0	0
8.0480*	7.858	0.522	0.546	0
8.0440*	7.366	0.396	0.072	0
8.0400*	10.773	0.449	3.44	0
8.0360*	10.389	0.538	3.064	0
8.0320*	10.764	0.537	3.475	0
8.0280*	10.894	0.577	3.57	0
8.0240*	12.404	0.614	5.335	0
8.0200*	12.733	0.603	5.431	0
8.0160*	13.069	0.592	5.682	0

Hydrodynamic analysis

Table 5.4: Hydraulic properties at different section for the year 2018

max LOB discharge	max WSE	max slope	max velocity	min WSE
7207.27	19.71	0.00002	0.45	12.66
6871.65	19.7	0.000017	0.43	12.66
6568.09	19.7	0.000015	0.42	12.66
6318.59	19.7	0.000014	0.4	12.66
6072.54	19.69	0.000013	0.39	12.66
5755.17	19.69	0.000012	0.38	12.66
5561.4	19.69	0.000011	0.38	12.66
5380.94	19.69	0.00001	0.37	12.66
6743.48	19.68	0.000009	0.36	12.66
5067.2	19.68	0.000009	0.36	12.66
4922.78	19.68	0.000009	0.36	12.66
4731.67	19.68	0.000008	0.35	12.66
4319.83	19.67	0.000008	0.35	12.66
4191.3	19.67	0.000008	0.35	12.66
4071.6	19.67	0.000008	0.35	12.66
3957.27	19.67	0.000008	0.35	12.66
3851.78	19.66	0.000008	0.35	12.66
3750.68	19.66	0.000008	0.35	12.66
3653.47	19.66	0.000008	0.35	12.66
3561.24	19.66	0.000008	0.36	12.66
3472.89	19.65	0.000009	0.36	12.66
3386.96	19.65	0.000009	0.36	12.65

3178.71	19.65	0.000009	0.37	12.65
3107.09	19.65	0.00001	0.38	12.65
3037.1	19.64	0.000011	0.38	12.65
2968.6	19.64	0.000012	0.39	12.65
2901.7	19.64	0.000013	0.4	12.65
2835.89	19.63	0.000014	0.42	12.64
2770.4	19.63	0.000015	0.43	12.63
2704.77	19.62	0.000017	0.45	12.62
2638.57	19.61	0.00002	0.46	12.61
2571.73	19.61	0.000023	0.49	12.61
2503.37	19.6	0.000028	0.51	12.6
2429.84	19.59	0.000034	0.54	12.59
2351.6	19.57	0.000042	0.58	12.59
2264.59	19.56	0.000054	0.62	12.58
2164.2	19.54	0.000072	0.68	12.57
2042.52	19.51	0.000101	0.75	12.56
1856.11	19.46	0.000147	0.85	12.55
1754.84	19.42	0.000141	0.83	12.54
1663.92	19.38	0.000136	0.82	12.52
1580.76	19.34	0.000132	0.82	12.51
1506.17	19.3	0.000128	0.81	12.49
1440.93	19.27	0.000125	0.81	12.47
1383.19	19.23	0.000123	0.8	12.45
1312.51	19.2	0.000118	0.8	12.42
1259.1	19.16	0.000116	0.8	12.39
1210.5	19.13	0.000115	0.8	12.35
1165.69	19.1	0.000114	0.8	12.3
1124.11	19.06	0.000113	0.81	12.24
1083.9	19.03	0.000113	0.81	12.17
1047.92	19	0.000113	0.82	12.1
1072.82	18.96	0.000113	0.83	12.04
1036.95	18.93	0.000112	0.83	11.97
1010.46	18.9	0.000114	0.85	11.91
984.99	18.86	0.000116	0.86	11.85
959.1	18.83	0.000118	0.88	11.79
933.62	18.79	0.000121	0.89	11.73

908.04	18.75	0.000124	0.91	11.67
882.62	18.72	0.000128	0.93	11.62
850.31	18.68	0.00013	0.95	11.57
824.71	18.64	0.000135	0.97	11.53
788.53	18.59	0.000137	0.98	11.49
761.79	18.55	0.000142	1.01	11.46
729.04	18.51	0.000145	1.03	11.44
790.18	18.47	0.00014	1.02	11.41
831.42	18.43	0.000135	1.02	11.38
856.71	18.39	0.00013	1.01	11.36
863.71	18.35	0.000125	1.01	11.32
860.18	18.31	0.000121	1	11.29
845.15	18.28	0.000117	1	11.25
820.09	18.24	0.000113	0.99	11.21
788.37	18.21	0.000109	0.99	11.17
758.23	18.18	0.000108	1	11.12
716.01	18.15	0.000104	0.99	11.07
696.01	18.12	0.000101	0.99	11.01
655.75	18.09	0.000097	0.98	10.96
618.45	18.06	0.000094	0.98	10.9
579.56	18.03	0.000091	0.98	10.84
538.88	18	0.000089	0.97	10.78
577.94	17.98	0.000086	0.97	10.72
690.29	17.95	0.000083	0.96	10.66
700.6	17.93	0.00008	0.96	10.61
717.11	17.91	0.000078	0.96	10.56
738.66	17.88	0.000076	0.95	10.52
763.33	17.86	0.000074	0.95	10.49
792.26	17.84	0.000072	0.95	10.46
825.91	17.82	0.00007	0.95	10.44
887.48	17.8	0.000068	0.95	10.42
931.96	17.78	0.000067	0.95	10.41
976.16	17.76	0.000065	0.95	10.4
876.38	17.74	0.000058	0.91	10.39
791.42	17.73	0.000052	0.88	10.38
718.79	17.72	0.000048	0.85	10.37

655.32	17.71	0.000044	0.82	10.36
598.73	17.7	0.000041	0.8	10.36
536.13	17.69	0.000039	0.79	10.35
497.84	17.68	0.000037	0.77	10.35
466.94	17.67	0.000036	0.76	10.35
440.79	17.66	0.000034	0.75	10.35
420.76	17.65	0.000034	0.74	10.34
404.05	17.64	0.000033	0.73	10.34
394.31	17.63	0.000033	0.73	10.34
387.92	17.62	0.000033	0.72	10.34
384.5	17.61	0.000033	0.72	10.34
359.46	17.6	0.000034	0.72	10.34
373.45	17.59	0.000034	0.72	10.34
405.72	17.58	0.000036	0.73	10.34
429.72	17.57	0.000037	0.73	10.33
480.31	17.56	0.000039	0.74	10.33
562.53	17.55	0.000041	0.75	10.33
622.74	17.53	0.000044	0.76	10.33
693.81	17.52	0.000048	0.78	10.33
781.34	17.5	0.000053	0.8	10.32
875.2	17.48	0.000059	0.82	10.32
1036.12	17.46	0.000066	0.85	10.32
1183.9	17.44	0.000076	0.88	10.31
1331.95	17.41	0.000089	0.92	10.3
1248.92	17.39	0.000075	0.87	10.3
1183.65	17.37	0.000064	0.83	10.3
1133.08	17.35	0.000056	0.79	10.3
1084.92	17.34	0.000049	0.76	10.29
1038.31	17.33	0.000043	0.73	10.29
1022.34	17.32	0.000039	0.7	10.29
1011.93	17.31	0.000035	0.68	10.29
1005.12	17.3	0.000032	0.65	10.29
1000.92	17.29	0.00003	0.64	10.29
995.83	17.28	0.000027	0.62	10.29
995.76	17.28	0.000026	0.6	10.29
953.75	17.27	0.000024	0.59	10.29

953.14	17.26	0.000023	0.58	10.29
960.55	17.26	0.000022	0.56	10.29
969.66	17.25	0.000021	0.55	10.29
979.95	17.25	0.00002	0.55	10.29
990.61	17.24	0.00002	0.54	10.29
1001.96	17.23	0.000019	0.53	10.29
1013.74	17.23	0.000019	0.52	10.29
1025.52	17.22	0.000018	0.52	10.29
1037.85	17.22	0.000018	0.52	10.29
1051.43	17.21	0.000018	0.51	10.29
1064.8	17.21	0.000018	0.51	10.29
1078.25	17.2	0.000018	0.51	10.29
1091.36	17.2	0.000018	0.5	10.28
1105.33	17.19	0.000018	0.5	10.28
1119.48	17.19	0.000019	0.5	10.28
1133.33	17.18	0.000019	0.5	10.28
1145.94	17.18	0.000019	0.51	10.28
1159.09	17.17	0.00002	0.51	10.28
1172.63	17.16	0.00002	0.51	10.28
1186.06	17.16	0.000021	0.51	10.28
1198.95	17.15	0.000022	0.52	10.28
1211.3	17.14	0.000023	0.52	10.27
1222.68	17.14	0.000024	0.53	10.27
1234.7	17.13	0.000026	0.53	10.27
1245.19	17.12	0.000028	0.54	10.26
1254.77	17.11	0.000029	0.55	10.26
1262.58	17.1	0.000032	0.56	10.25
1268.05	17.09	0.000034	0.57	10.24
1271.96	17.08	0.000038	0.59	10.23
1272.5	17.07	0.000041	0.6	10.22
1270.17	17.05	0.000046	0.62	10.21
1263.69	17.04	0.000052	0.64	10.2
1246.41	17.02	0.000058	0.66	10.18
1190.75	17	0.000062	0.68	10.16
1114.43	16.98	0.000063	0.67	10.14
1017.85	16.96	0.00006	0.66	10.11

927.88	16.95	0.000058	0.66	10.09
847.32	16.93	0.000056	0.65	10.05
774.54	16.92	0.000055	0.65	10.02
708.65	16.9	0.000055	0.65	9.97
649.51	16.88	0.000055	0.65	9.93
595.01	16.87	0.000055	0.65	9.87
544.71	16.85	0.000056	0.65	9.83
497.93	16.83	0.000058	0.66	9.79
454.18	16.82	0.00006	0.66	9.75
420.65	16.8	0.000063	0.67	9.72
379.8	16.78	0.000067	0.68	9.69
340.6	16.76	0.000072	0.7	9.67
302.77	16.73	0.000079	0.72	9.66
265.38	16.71	0.000088	0.74	9.64
229.44	16.68	0.000099	0.77	9.63
194.33	16.64	0.000114	0.8	9.61
164.9	16.6	0.000134	0.83	9.6
135.16	16.56	0.000162	0.88	9.58
108.64	16.5	0.000204	0.94	9.57
78.94	16.42	0.000268	1.01	9.54
109.44	16.35	0.000241	0.98	9.52
141.16	16.28	0.000218	0.96	9.5
176.73	16.22	0.000199	0.93	9.48
214.75	16.17	0.000183	0.91	9.46
242.64	16.12	0.00017	0.9	9.43
286.44	16.07	0.00016	0.88	9.4
328.7	16.03	0.000152	0.87	9.38
371.02	15.98	0.000146	0.86	9.35
409.7	15.94	0.000139	0.86	9.32
444.82	15.9	0.000132	0.85	9.28
477.31	15.87	0.000127	0.85	9.23
499.2	15.83	0.000121	0.85	9.2
520.38	15.79	0.000117	0.85	9.18
540.35	15.76	0.000117	0.86	9.15
539.27	15.73	0.00011	0.87	9.13
530.51	15.69	0.000105	0.87	9.12

562.89	15.66	0.000104	0.87	9.1
602.98	15.63	0.000107	0.87	9.07
657.38	15.6	0.000116	0.87	9.04
690.91	15.56	0.000117	0.86	9.01
724.35	15.53	0.000119	0.86	8.97
707.03	15.49	0.000118	0.85	8.94
727.92	15.46	0.000116	0.85	8.89
746.56	15.42	0.000114	0.84	8.86
836.2	15.39	0.000113	0.84	8.82
852.5	15.36	0.00011	0.83	8.78
869.66	15.33	0.000108	0.82	8.75
928.59	15.3	0.000105	0.82	8.72
947.43	15.26	0.000103	0.81	8.7
964.94	15.23	0.000101	0.81	8.69
982.55	15.21	0.000099	0.8	8.67
994.09	15.18	0.000095	0.8	8.66
991.29	15.15	0.00009	0.79	8.66
1095.13	15.13	0.000089	0.78	8.65
1198.74	15.1	0.000088	0.78	8.63
1318.4	15.07	0.000089	0.77	8.62
1376.91	15.05	0.00009	0.77	8.6
1494.37	15.02	0.000091	0.77	8.58
1482.95	15	0.000094	0.76	8.54
1580.63	14.97	0.000094	0.76	8.5
1669.9	14.94	0.000094	0.75	8.46
1744.68	14.92	0.000092	0.75	8.42
1813.8	14.89	0.000091	0.74	8.38
1877.64	14.87	0.00009	0.74	8.34
1937.33	14.84	0.000088	0.73	8.31
1991.7	14.82	0.000088	0.73	8.29
1840.97	14.79	0.000088	0.73	8.26
1986.95	14.77	0.000087	0.73	8.24
2031.87	14.74	0.000086	0.72	8.22
2071.19	14.72	0.000086	0.72	8.2
2103.71	14.69	0.000086	0.72	8.18
1977.56	14.67	0.000082	0.71	8.17
1858.49	14.65	0.000079	0.7	8.15

1746.97	14.62	0.000076	0.69	8.13
1639.69	14.6	0.000073	0.68	8.11
1538.55	14.58	0.000071	0.68	8.09
1442.7	14.56	0.000068	0.67	8.06
1350.68	14.54	0.000066	0.66	8.04
1263.92	14.52	0.000064	0.65	8
1181.9	14.51	0.000062	0.64	7.97
1103.54	14.49	0.00006	0.64	7.93
1080.85	14.47	0.000058	0.63	7.89
1007.97	14.46	0.000056	0.62	7.85
939.03	14.44	0.000055	0.62	7.8
874.16	14.42	0.000054	0.61	7.75
811.96	14.41	0.000052	0.6	7.7
752.96	14.39	0.000051	0.6	7.65
697.1	14.38	0.00005	0.59	7.59
643.01	14.37	0.000049	0.59	7.52
592.15	14.35	0.000048	0.58	7.46
542.85	14.34	0.000047	0.58	7.4
559.31	14.33	0.000046	0.57	7.35
529.23	14.31	0.000045	0.56	7.31
526.09	14.3	0.000044	0.56	7.27
519.9	14.29	0.000043	0.55	7.23
481.87	14.27	0.000043	0.55	7.2
481.07	14.26	0.000044	0.55	7.16
649.46	14.25	0.000046	0.56	7.12
826.08	14.23	0.000049	0.57	7.07
1010.49	14.22	0.000052	0.58	7.02
1200.67	14.2	0.000056	0.6	6.97
1394.49	14.19	0.000061	0.62	6.93

Table 5.5: Hydraulic properties at different section for the year 2019

XS ID	MAX LOB discharge	max WSE	max slope	max velocity	min WSE
13.00	8202	20.94	0.00	0.52	13.69
12.98	7566	20.94	0.00	0.50	13.69

12.95	7012	20.93	0.00	0.49	13.69
12.93	6527	20.93	0.00	0.48	13.69
12.91	6099	20.93	0.00	0.47	13.69
12.88	5722	20.93	0.00	0.45	13.69
12.86	5386	20.92	0.00	0.44	13.69
12.83	5088	20.92	0.00	0.44	13.69
12.81	4821	20.92	0.00	0.43	13.69
12.79	4582	20.92	0.00	0.42	13.69
12.76	4367	20.91	0.00	0.41	13.69
12.74	4174	20.91	0.00	0.41	13.69
12.72	4000	20.91	0.00	0.40	13.69
12.69	3843	20.91	0.00	0.40	13.69
12.67	3701	20.91	0.00	0.40	13.69
12.65	3573	20.91	0.00	0.39	13.69
12.62	3457	20.90	0.00	0.39	13.69
12.60	3353	20.90	0.00	0.39	13.69
12.57	3259	20.90	0.00	0.39	13.69
12.55	3175	20.90	0.00	0.39	13.69
12.53	3100	20.90	0.00	0.39	13.69
12.50	3033	20.90	0.00	0.39	13.69
12.48	2974	20.90	0.00	0.39	13.69
12.455*	2922	20.89	0.00	0.39	13.69
12.432*	2878	20.89	0.00	0.39	13.69
12.408*	2841	20.89	0.00	0.39	13.69
12.384*	2810	20.89	0.00	0.39	13.69
12.361*	2786	20.89	0.00	0.40	13.69
12.337*	2769	20.89	0.00	0.40	13.69
12.313*	2758	20.88	0.00	0.40	13.69
12.289*	2755	20.88	0.00	0.41	13.69
12.266*	2758	20.88	0.00	0.41	13.69
12.242*	2768	20.88	0.00	0.42	13.69
12.218*	2785	20.88	0.00	0.43	13.69
12.195*	2811	20.87	0.00	0.43	13.69
12.171*	2845	20.87	0.00	0.44	13.69
12.147*	2888	20.87	0.00	0.45	13.69
12.124*	3169	20.87	0.00	0.46	13.69
12.10	3465	20.86	0.00	0.48	13.69
12.096*	3777	20.86	0.00	0.49	13.69
12.092*	4107	20.85	0.00	0.51	13.69

12.088*	4455	20.85	0.00	0.52	13.69
12.085*	4823	20.84	0.00	0.54	13.68
12.081*	5212	20.84	0.00	0.56	13.68
12.077*	5623	20.83	0.00	0.58	13.68
12.073*	6057	20.82	0.00	0.60	13.68
12.069*	6517	20.81	0.00	0.62	13.68
12.062*	7002	20.80	0.00	0.64	13.68
12.058*	7513	20.79	0.00	0.67	13.67
12.054*	8056	20.77	0.00	0.69	13.67
12.050*	8634	20.76	0.00	0.72	13.66
12.046*	9243	20.74	0.00	0.74	13.66
12.042*	9888	20.72	0.00	0.77	13.65
12.038*	10541	20.67	0.00	0.80	13.64
12.035*	11279	20.66	0.00	0.83	13.63
12.031*	12044	20.63	0.00	0.87	13.62
12.027*	12852	20.60	0.00	0.90	13.61
12.02	13207	20.57	0.00	0.89	13.60
12.02	13531	20.50	0.00	0.90	13.59
12.015*	13917	20.46	0.00	0.89	13.58
12.012*	14341	20.44	0.00	0.89	13.57
12.008*	14786	20.42	0.00	0.89	13.56
12.004*	15258	20.39	0.00	0.88	13.55
12.00	15758	20.37	0.00	0.88	13.54
11.965*	16289	20.35	0.00	0.88	13.53
11.931*	16846	20.33	0.00	0.88	13.52
11.896*	17443	20.31	0.00	0.88	13.51
11.862*	18078	20.29	0.00	0.88	13.50
11.827*	18753	20.28	0.00	0.89	13.49
11.792*	18971	20.26	0.00	0.88	13.48
11.758*	19196	20.24	0.00	0.88	13.48
11.723*	19432	20.23	0.00	0.87	13.48
11.688*	19681	20.22	0.00	0.87	13.47
11.654*	19943	20.20	0.00	0.87	13.47
11.619*	20222	20.19	0.00	0.87	13.47
11.585*	20519	20.18	0.00	0.87	13.47
11.550*	20836	20.17	0.00	0.88	13.47

11.515*	21175	20.16	0.00	0.88	13.47
11.481*	21538	20.14	0.00	0.89	13.47
11.446*	21924	20.13	0.00	0.90	13.47
11.412*	22339	20.12	0.00	0.91	13.47
11.377*	21343	20.11	0.00	0.89	13.47
11.342*	20411	20.10	0.00	0.87	13.46
11.308*	19540	20.08	0.00	0.85	13.46
11.273*	18723	20.07	0.00	0.84	13.46
11.238*	17956	20.06	0.00	0.83	13.46
11.204*	17234	20.04	0.00	0.82	13.46
11.169*	16551	20.03	0.00	0.81	13.46
11.135*	15901	20.02	0.00	0.81	13.46
11.10	15276	20.00	0.00	0.80	13.45
11.096*	14675	19.98	0.00	0.80	13.45
11.093*	14092	19.95	0.00	0.80	13.45
11.089*	13950	19.93	0.00	0.80	13.44
11.085*	13811	19.91	0.00	0.80	13.44
11.081*	13666	19.89	0.00	0.80	13.44
11.078*	13527	19.87	0.00	0.80	13.43
11.074*	13389	19.84	0.00	0.80	13.43
11.070*	13248	19.82	0.00	0.80	13.43
11.067*	13108	19.80	0.00	0.80	13.42
11.063*	12967	19.78	0.00	0.80	13.42
11.059*	12832	19.76	0.00	0.80	13.42
11.056*	12696	19.73	0.00	0.80	13.41
11.052*	12559	19.71	0.00	0.80	13.41
11.048*	12425	19.69	0.00	0.80	13.41
11.044*	12290	19.67	0.00	0.80	13.40
11.041*	12157	19.65	0.00	0.80	13.40
11.037*	12025	19.62	0.00	0.80	13.40
11.033*	11893	19.60	0.00	0.80	13.39
11.030*	11761	19.58	0.00	0.80	13.39
11.026*	11630	19.56	0.00	0.80	13.39
11.022*	11584	19.54	0.00	0.80	13.38
11.019*	11538	19.52	0.00	0.81	13.38
11.015*	11493	19.50	0.00	0.81	13.38

11.011*	11448	19.47	0.00	0.81	13.37
11.007*	11403	19.45	0.00	0.81	13.37
11.004*	11357	19.43	0.00	0.81	13.36
11.00	11314	19.41	0.00	0.81	13.36
10.980*	11269	19.38	0.00	0.81	13.36
10.961*	11225	19.36	0.00	0.81	13.35
10.941*	11180	19.34	0.00	0.81	13.35
10.922*	11136	19.31	0.00	0.81	13.34
10.902*	11092	19.29	0.00	0.81	13.33
10.883*	11047	19.27	0.00	0.81	13.33
10.863*	11002	19.24	0.00	0.81	13.32
10.843*	10957	19.22	0.00	0.82	13.32
10.824*	10913	19.19	0.00	0.82	13.31
10.804*	10865	19.17	0.00	0.82	13.30
10.785*	10820	19.14	0.00	0.82	13.29
10.765*	10773	19.11	0.00	0.82	13.28
10.746*	10727	19.09	0.00	0.83	13.28
10.726*	10681	19.06	0.00	0.83	13.27
10.707*	10634	19.03	0.00	0.83	13.26
10.687*	10587	19.00	0.00	0.83	13.25
10.667*	10537	18.97	0.00	0.84	13.23
10.648*	10489	18.94	0.00	0.84	13.22
10.628*	10440	18.91	0.00	0.84	13.21
10.609*	9967	18.88	0.00	0.84	13.20
10.589*	9526	18.86	0.00	0.84	13.18
10.570*	9113	18.83	0.00	0.83	13.17
10.550*	8724	18.80	0.00	0.83	13.16
10.530*	8358	18.77	0.00	0.83	13.14
10.511*	8015	18.75	0.00	0.83	13.13
10.491*	7690	18.72	0.00	0.83	13.11
10.472*	7384	18.69	0.00	0.83	13.10
10.452*	7093	18.67	0.00	0.83	13.08
10.433*	6817	18.64	0.00	0.83	13.07
10.413*	6554	18.61	0.00	0.83	13.05
10.393*	6303	18.58	0.00	0.84	13.03
10.374*	6064	18.55	0.00	0.84	13.01

10.354*	5833	18.52	0.00	0.85	12.99
10.335*	5613	18.49	0.00	0.85	12.97
10.315*	5398	18.45	0.00	0.86	12.95
10.296*	5193	18.42	0.00	0.87	12.92
10.276*	4993	18.38	0.00	0.88	12.90
10.257*	4903	18.35	0.00	0.88	12.87
10.237*	4812	18.31	0.00	0.88	12.85
10.217*	4722	18.27	0.00	0.89	12.82
10.198*	4632	18.24	0.00	0.89	12.80
10.178*	4542	18.20	0.00	0.89	12.77
10.159*	4452	18.16	0.00	0.90	12.75
10.139*	4369	18.13	0.00	0.90	12.73
10.120*	4286	18.09	0.00	0.91	12.70
10.10	4202	18.06	0.00	0.91	12.68
10.095*	4118	18.02	0.00	0.92	12.66
10.091*	4036	17.99	0.00	0.92	12.64
10.086*	3952	17.95	0.00	0.93	12.62
10.082*	4215	17.92	0.00	0.93	12.60
10.077*	4490	17.88	0.00	0.94	12.58
10.073*	4776	17.85	0.00	0.94	12.56
10.068*	5073	17.81	0.00	0.95	12.53
10.064*	5381	17.77	0.00	0.96	12.50
10.059*	5701	17.73	0.00	0.97	12.47
10.055*	6035	17.70	0.00	0.97	12.43
10.050*	6379	17.66	0.00	0.98	12.40
10.045*	6736	17.61	0.00	0.99	12.37
10.041*	7106	17.57	0.00	1.00	12.34
10.036*	7492	17.53	0.00	1.01	12.31
10.032*	7887	17.48	0.00	1.02	12.29
10.027*	7731	17.43	0.00	1.02	12.27
10.023*	7573	17.39	0.00	1.01	12.25
10.018*	7409	17.34	0.00	1.01	12.23
10.014*	7245	17.29	0.00	1.01	12.20
10.009*	7073	17.24	0.00	1.00	12.18
10.005*	6900	17.19	0.00	1.00	12.16
10.00	6721	17.14	0.00	1.00	12.14

9.9438*	6539	17.08	0.00	1.00	12.11
9.8875*	6311	17.00	0.00	1.01	12.09
9.8313*	6050	16.89	0.00	1.03	12.07
9.7750*	5758	16.76	0.00	1.05	12.05
9.7188*	5569	16.65	0.00	1.05	12.03
9.6625*	5441	16.57	0.00	1.05	12.00
9.6063*	5363	16.51	0.00	1.05	11.98
9.5500*	5302	16.45	0.00	1.05	11.95
9.4938*	5263	16.39	0.00	1.05	11.91
9.4375*	5243	16.34	0.00	1.04	11.86
9.3813*	5241	16.29	0.00	1.04	11.82
9.3250*	5255	16.24	0.00	1.05	11.76
9.2688*	5284	16.19	0.00	1.05	11.69
9.2125*	5328	16.14	0.00	1.05	11.62
9.1563*	5387	16.09	0.00	1.06	11.54
9.10	5463	16.04	0.00	1.07	11.45
9.0941*	5554	15.99	0.00	1.08	11.36
9.0882*	5660	15.94	0.00	1.09	11.27
9.0824*	5785	15.88	0.00	1.11	11.17
9.0765*	5929	15.82	0.00	1.13	11.07
9.0706*	6076	15.76	0.00	1.15	10.96
9.0647*	6109	15.69	0.00	1.19	10.85
9.0588*	6098	15.63	0.00	1.22	10.72
9.0529*	5395	15.58	0.00	1.11	10.60
9.0471*	4610	15.54	0.00	1.04	10.50
9.0412*	4032	15.50	0.00	0.97	10.42
9.0353*	3598	15.48	0.00	0.93	10.35
9.0294*	3260	15.45	0.00	0.89	10.29
9.0235*	2988	15.43	0.00	0.86	10.23
9.0176*	2768	15.41	0.00	0.84	10.18
9.0118*	2582	15.39	0.00	0.83	10.13
9.0059*	2422	15.36	0.00	0.82	10.08
9.00	2278	15.34	0.00	0.82	10.04
8.9500*	2143	15.31	0.00	0.82	10.00
8.9000*	2010	15.28	0.00	0.83	9.94
8.8500*	1868	15.24	0.00	0.83	9.83

8.8000*	1840	15.21	0.00	0.83	9.70
8.7500*	1806	15.17	0.00	0.83	9.56
8.7000*	1765	15.14	0.00	0.82	9.43
8.65	1719	15.10	0.00	0.82	9.29
8.6000*	1669	15.07	0.00	0.82	9.16
8.55	1613	15.04	0.00	0.81	9.03
8.5000*	1554	15.01	0.00	0.81	8.89
8.45	1490	14.98	0.00	0.81	8.75
8.4000*	1424	14.95	0.00	0.80	8.60
8.3500*	1354	14.93	0.00	0.80	8.46
8.3000*	1281	14.90	0.00	0.80	8.32
8.2500*	1207	14.87	0.00	0.80	8.17
8.2000*	1131	14.84	0.00	0.79	8.02
8.1500*	1053	14.81	0.00	0.79	7.87
8.10	975	14.79	0.00	0.79	7.70
8.0960*	896	14.76	0.00	0.79	7.53
8.0920*	817	14.73	0.00	0.79	7.34
8.0880*	779	14.71	0.00	0.79	7.12
8.0840*	754	14.68	0.00	0.78	6.85
8.0800*	952	14.66	0.00	0.79	6.59
8.0760*	1172	14.63	0.00	0.80	6.37
8.0720*	1415	14.60	0.00	0.80	6.20
8.0680*	1680	14.57	0.00	0.81	6.07
8.0640*	1970	14.54	0.00	0.82	5.98
8.0600*	2284	14.51	0.00	0.82	5.91
8.0560*	2623	14.47	0.00	0.83	5.86
8.0520*	2987	14.44	0.00	0.84	5.83
8.0480*	3380	14.40	0.00	0.84	5.81
8.0440*	3800	14.37	0.00	0.85	5.79
8.0400*	4192	14.33	0.00	0.86	5.78
8.0360*	1056	14.88	0.00	0.62	8.06
8.0320*	1058	14.86	0.00	0.61	8.03
8.0280*	1058	14.85	0.00	0.60	7.99
8.0240*	1058	14.84	0.00	0.59	7.95
8.0200*	1058	14.83	0.00	0.57	7.91
8.0160*	1058	14.82	0.00	0.56	7.88
8.0120*	1057	14.81	0.00	0.55	7.84

8.0080*	1055	14.80	0.00	0.54	7.82
8.0040*	1053	14.79	0.00	0.53	7.79
8.00	1005	14.78	0.00	0.52	7.77
7.9250*	1003	14.77	0.00	0.51	7.76
7.8500*	998	14.76	0.00	0.50	7.74
7.7750*	927	14.75	0.00	0.51	7.73
7.7000*	857	14.75	0.00	0.52	7.70
7.6250*	953	14.74	0.00	0.53	7.66
7.5500*	883	14.73	0.00	0.54	7.61
	816	14.71	0.00	0.55	7.54

Table 5.6: Hydraulic properties at different section for the year 2020

XS ID	max LOB discharge	max WSE	max slope	max velocity	min WSE
13.00	10298.56	19.65	0.000031	0.64	13.9
12.98	9453.8	19.64	0.000028	0.63	13.9
12.95	8687.94	19.64	0.000025	0.62	13.9
12.93	7991.25	19.63	0.000023	0.61	13.9
12.91	7353.6	19.63	0.000021	0.6	13.9
12.88	6768.65	19.62	0.000019	0.59	13.9
12.86	6229.36	19.62	0.000018	0.58	13.89
12.83	5730.55	19.62	0.000016	0.57	13.89
12.81	5267.26	19.61	0.000015	0.57	13.89
12.79	4755.14	19.61	0.000014	0.56	13.89
12.76	4316.15	19.61	0.000013	0.55	13.89
12.74	3937.89	19.6	0.000013	0.54	13.89
12.72	3609.8	19.6	0.000012	0.54	13.89
12.69	3324	19.6	0.000012	0.53	13.89
12.67	3073.89	19.59	0.000012	0.53	13.89
12.65	2854.59	19.59	0.000012	0.53	13.89
12.62	2661.45	19.58	0.000012	0.53	13.89
12.60	2491.03	19.58	0.000012	0.54	13.89
12.57	2340.71	19.58	0.000013	0.55	13.89
12.55	2207.85	19.57	0.000013	0.55	13.89
12.53	2091.13	19.57	0.000014	0.56	13.89
12.50	1988.55	19.56	0.000015	0.58	13.89
12.48	1899.31	19.56	0.000017	0.59	13.89
12.455*	1822.52	19.55	0.000019	0.61	13.89

12.432*	1757.81	19.54	0.000022	0.64	13.89
12.408*	1705.12	19.53	0.000026	0.67	13.88
12.384*	1664.57	19.52	0.000031	0.7	13.88
12.361*	1637.36	19.51	0.000038	0.74	13.88
12.337*	1624.95	19.49	0.000048	0.8	13.87
12.313*	2440.13	19.48	0.000046	0.79	13.86
12.289*	3230.02	19.47	0.000044	0.77	13.86
12.266*	3999.43	19.46	0.000041	0.76	13.85
12.242*	4752.89	19.45	0.00004	0.75	13.85
12.218*	5495.56	19.44	0.000038	0.75	13.84
12.195*	6231.46	19.43	0.000037	0.74	13.84
12.171*	6964.94	19.42	0.000035	0.74	13.83
12.147*	7700.24	19.41	0.000034	0.73	13.83
12.124*	8441.16	19.4	0.000033	0.73	13.83
12.10	9192.76	19.39	0.000033	0.73	13.82
12.096*	9960.1	19.38	0.000032	0.73	13.82
12.092*	10746.17	19.37	0.000031	0.73	13.82
12.088*	11557.09	19.36	0.000031	0.73	13.82
12.085*	12398.27	19.35	0.000031	0.74	13.81
12.081*	13274.16	19.34	0.000031	0.74	13.81
12.077*	14191.61	19.33	0.000031	0.75	13.81
12.073*	15154.52	19.32	0.000031	0.76	13.81
12.069*	15128.25	19.31	0.000031	0.76	13.81
12.062*	15100.5	19.3	0.000032	0.77	13.8
12.058*	15072.35	19.29	0.000032	0.77	13.8
12.054*	15043.67	19.28	0.000033	0.77	13.8
12.050*	15012.91	19.27	0.000033	0.77	13.8
12.046*	14982.45	19.25	0.000034	0.77	13.79
12.042*	14950.75	19.24	0.000034	0.78	13.79
12.038*	14917.89	19.23	0.000034	0.78	13.79
12.035*	14883.7	19.22	0.000035	0.78	13.79
12.031*	14849.11	19.21	0.000035	0.78	13.78
12.027*	14812.99	19.2	0.000036	0.78	13.78
12.02	14774.9	19.19	0.000036	0.79	13.78
12.02	14736.04	19.18	0.000037	0.79	13.77
12.015*	14696.38	19.17	0.000037	0.79	13.77

12.012*	14654.33	19.16	0.000038	0.79	13.77
12.008*	14611.08	19.15	0.000038	0.8	13.76
12.004*	14566.48	19.14	0.000039	0.8	13.76
12.00	14520.64	19.12	0.000039	0.8	13.76
11.965*	14473.16	19.11	0.00004	0.8	13.75
11.931*	14423.78	19.1	0.000041	0.81	13.75
11.896*	14373.51	19.09	0.000041	0.81	13.74
11.862*	14321.54	19.07	0.000042	0.81	13.74
11.827*	14267.36	19.06	0.000042	0.82	13.73
11.792*	14212.42	19.05	0.000043	0.82	13.73
11.758*	14154.57	19.04	0.000044	0.82	13.73
11.723*	14095.52	19.02	0.000045	0.82	13.72
11.688*	14034.38	19.01	0.000045	0.83	13.72
11.654*	13972.81	19	0.000046	0.83	13.71
11.619*	13907.45	18.98	0.000047	0.83	13.71
11.585*	13840.95	18.97	0.000048	0.84	13.7
11.550*	13772.7	18.95	0.000048	0.84	13.69
11.515*	13702.36	18.94	0.000049	0.85	13.69
11.481*	13629.45	18.92	0.00005	0.85	13.68
11.446*	13554.76	18.91	0.000051	0.85	13.68
11.412*	13478.4	18.89	0.000052	0.86	13.67
11.377*	13398.3	18.88	0.000053	0.86	13.67
11.342*	13316.87	18.86	0.000054	0.86	13.66
11.308*	13232.11	18.84	0.000055	0.87	13.66
11.273*	13145.37	18.83	0.000056	0.87	13.65
11.238*	13056	18.81	0.000057	0.88	13.64
11.204*	12964.22	18.79	0.000058	0.88	13.64
11.169*	12631.59	18.78	0.000057	0.88	13.63
11.135*	12314.2	18.76	0.000057	0.87	13.63
11.10	12009.62	18.74	0.000056	0.87	13.62
11.096*	11717.82	18.73	0.000056	0.87	13.62
11.093*	11437.03	18.71	0.000055	0.86	13.61
11.089*	11168.49	18.69	0.000055	0.86	13.61
11.085*	10909.91	18.68	0.000054	0.86	13.6
11.081*	10661.54	18.66	0.000054	0.85	13.59
11.078*	10422.26	18.65	0.000054	0.85	13.59

11.074*	10192.58	18.63	0.000054	0.85	13.58
11.070*	9969.94	18.62	0.000054	0.84	13.58
11.067*	9756.63	18.6	0.000053	0.84	13.57
11.063*	9551.05	18.58	0.000053	0.84	13.57
11.059*	9351.78	18.57	0.000053	0.84	13.56
11.056*	9160.16	18.55	0.000054	0.84	13.55
11.052*	8974.42	18.54	0.000054	0.83	13.55
11.048*	8796.22	18.52	0.000054	0.83	13.54
11.044*	8622.07	18.51	0.000054	0.83	13.53
11.041*	8454.04	18.49	0.000054	0.83	13.53
11.037*	8291.55	18.47	0.000055	0.83	13.52
11.033*	8134.23	18.46	0.000055	0.83	13.51
11.030*	7981.9	18.44	0.000056	0.83	13.51
11.026*	7833.29	18.42	0.000056	0.83	13.5
11.022*	7689.42	18.41	0.000057	0.83	13.49
11.019*	7548.29	18.39	0.000057	0.83	13.48
11.015*	7412.83	18.37	0.000058	0.83	13.47
11.011*	7280.09	18.36	0.000059	0.83	13.46
11.007*	7150.74	18.34	0.00006	0.84	13.45
11.004*	7024.97	18.32	0.000061	0.84	13.44
11.00	6901.58	18.3	0.000062	0.84	13.43
10.980*	6781.49	18.28	0.000063	0.84	13.42
10.961*	6664.01	18.26	0.000065	0.84	13.41
10.941*	6549.44	18.25	0.000066	0.85	13.4
10.922*	6436.41	18.23	0.000067	0.85	13.39
10.902*	6326.19	18.21	0.000069	0.85	13.38
10.883*	6217.31	18.18	0.000071	0.86	13.37
10.863*	6110.55	18.16	0.000073	0.86	13.35
10.843*	6005.66	18.14	0.000075	0.87	13.34
10.824*	5902.09	18.12	0.000077	0.87	13.32
10.804*	5799.64	18.09	0.00008	0.88	13.31
10.785*	5698.06	18.07	0.000083	0.89	13.29
10.765*	5597.64	18.04	0.000086	0.89	13.27
10.746*	5497.43	18.02	0.000089	0.9	13.24
10.726*	5441.79	17.99	0.00009	0.9	13.22
10.707*	5385.46	17.96	0.000091	0.91	13.2

10.687*	5329.69	17.94	0.000092	0.91	13.17
10.667*	5273.96	17.91	0.000093	0.91	13.15
10.648*	5217.07	17.88	0.000095	0.91	13.12
10.628*	5161.04	17.85	0.000096	0.92	13.09
10.609*	5104.98	17.82	0.000097	0.92	13.07
10.589*	5048.17	17.8	0.000099	0.93	13.04
10.570*	4991.83	17.77	0.0001	0.93	13.01
10.550*	4933.57	17.74	0.000102	0.93	12.99
10.530*	4876.25	17.7	0.000104	0.94	12.96
10.511*	4817.95	17.67	0.000106	0.94	12.93
10.491*	4759.52	17.64	0.000108	0.95	12.91
10.472*	4700.75	17.61	0.00011	0.96	12.88
10.452*	4640.64	17.57	0.000113	0.96	12.85
10.433*	4580.04	17.54	0.000115	0.97	12.83
10.413*	4498.12	17.51	0.000117	0.97	12.8
10.393*	4435.91	17.47	0.00012	0.98	12.78
10.374*	4372.79	17.43	0.000123	0.99	12.75
10.354*	4333.33	17.4	0.000125	0.99	12.72
10.335*	4291.92	17.36	0.000128	1	12.7
10.315*	4248.21	17.33	0.00013	1	12.67
10.296*	4201.98	17.29	0.000133	1.01	12.64
10.276*	4153.36	17.25	0.000136	1.01	12.61
10.257*	4102.54	17.21	0.000139	1.02	12.58
10.237*	4048.6	17.17	0.000142	1.02	12.55
10.217*	3992.59	17.13	0.000145	1.03	12.52
10.198*	3933.34	17.09	0.000148	1.03	12.49
10.178*	3871.97	17.05	0.000152	1.04	12.46
10.159*	3808.18	17	0.000155	1.05	12.43
10.139*	3742.29	16.96	0.000159	1.05	12.4
10.120*	3622.73	16.92	0.000157	1.05	12.37
10.10	3510.97	16.87	0.000154	1.04	12.34
10.095*	3405.94	16.83	0.000152	1.03	12.31
10.091*	3307.76	16.78	0.00015	1.03	12.28
10.086*	3216.56	16.74	0.000149	1.02	12.24
10.082*	3130.19	16.7	0.000148	1.02	12.2
10.077*	3048.66	16.66	0.000147	1.02	12.15

10.073*	2971.47	16.61	0.000147	1.02	12.11
10.068*	2898.1	16.57	0.000147	1.01	12.05
10.064*	2828.74	16.53	0.000148	1.01	11.99
10.059*	2761.64	16.49	0.000149	1.02	11.93
10.055*	2697.61	16.44	0.00015	1.02	11.87
10.050*	2635.31	16.4	0.000152	1.02	11.8
10.045*	2574.95	16.36	0.000154	1.03	11.72
10.041*	2516.09	16.31	0.000156	1.03	11.65
10.036*	2458.74	16.27	0.00016	1.04	11.57
10.032*	2402.49	16.22	0.000163	1.04	11.49
10.027*	2346.49	16.17	0.000168	1.05	11.41
10.023*	2290.93	16.12	0.000173	1.06	11.32
10.018*	2235.44	16.07	0.000179	1.07	11.23
10.014*	2180.59	16.02	0.000186	1.09	11.14
10.009*	2091.53	15.96	0.000188	1.1	11.03
10.005*	2005.61	15.91	0.000191	1.12	10.92
10.00	1948.61	15.86	0.000162	1.04	10.81
9.9438*	1872.54	15.83	0.000133	0.98	10.71
9.8875*	1830.55	15.8	0.000114	0.94	10.63
9.8313*	1815.89	15.77	0.000099	0.9	10.55
9.7750*	1824.3	15.75	0.000089	0.87	10.49
9.7188*	1852.2	15.73	0.000082	0.84	10.42
9.6625*	1898.79	15.71	0.000077	0.83	10.36
9.6063*	1963.99	15.69	0.000074	0.81	10.3
9.5500*	2049.06	15.67	0.000073	0.8	10.24
9.4938*	2154.6	15.65	0.000073	0.8	10.19
9.4375*	2283.8	15.62	0.000075	0.8	10.14
9.3813*	2439.24	15.6	0.000079	0.8	10.08
9.3250*	2626.79	15.58	0.000084	0.81	10.01
9.2688*	2851.41	15.55	0.000092	0.82	9.88
9.2125*	2806.78	15.53	0.000092	0.82	9.7
9.1563*	2762.02	15.5	0.000091	0.82	9.49
9.10	2717.58	15.47	0.000091	0.82	9.27
9.0941*	2673.51	15.45	0.000091	0.82	9.04
9.0882*	2629.71	15.42	0.000091	0.82	8.82
9.0824*	2586.29	15.39	0.000091	0.82	8.62

9.0765*	2542.86	15.37	0.000091	0.82	8.42
9.0706*	2499.73	15.34	0.000091	0.82	8.22
9.0647*	2457.11	15.31	0.00009	0.82	8.02
9.0588*	2414.69	15.29	0.00009	0.82	7.83
9.0529*	2372.61	15.26	0.00009	0.82	7.65
9.0471*	2330.72	15.23	0.00009	0.82	7.48
9.0412*	2289.4	15.21	0.000089	0.82	7.32
9.0353*	2248.19	15.18	0.000089	0.82	7.17
9.0294*	2207.5	15.16	0.000089	0.82	7.04
9.0235*	2167.05	15.13	0.000088	0.82	6.93
9.0176*	2127.41	15.11	0.000088	0.82	6.83
9.0118*	2087.6	15.08	0.000088	0.82	6.75
9.0059*	2048.35	15.05	0.000087	0.82	6.67
9.00	2009.63	15.03	0.000087	0.82	6.61
8.9500*	1971.11	15	0.000086	0.81	6.56
8.9000*	1933.44	14.98	0.000086	0.81	6.52
8.8500*	1895.9	14.95	0.000085	0.81	6.48
8.8000*	1858.75	14.93	0.000085	0.81	6.45
8.7500*	1822.23	14.91	0.000084	0.81	6.43
8.7000*	1786.03	14.88	0.000084	0.81	6.41
8.65	1750.45	14.86	0.000083	0.81	6.39
8.6000*	1715.15	14.83	0.000083	0.81	6.37
8.55	1680.38	14.81	0.000082	0.81	6.36
8.5000*	1648.01	14.78	0.000081	0.8	6.35
8.45	1597.03	14.76	0.000086	0.82	6.34
8.4000*	1550.99	14.73	0.000091	0.84	6.32
8.3500*	1518.41	14.71	0.000096	0.85	6.31
8.3000*	1551.57	14.68	0.000101	0.87	6.29
8.2500*	1526.69	14.65	0.000106	0.89	6.27
8.2000*	1490.88	14.61	0.00011	0.91	6.25
8.1500*	1449.49	14.58	0.000115	0.93	6.23
8.10	1393.07	14.54	0.000119	0.95	6.21
8.0960*	1340.5	14.51	0.000124	0.97	6.19
8.0920*	1279.52	14.47	0.000129	0.99	6.16
8.0880*	1179.22	14.43	0.000129	1.02	6.13
8.0840*	1106.77	14.39	0.000132	1.04	6.1
8.0800*	994.11	14.35	0.000119	1	6.07

8.0760*	1931.58	16.13	0.000076	0.85	8.12
8.0720*	1923.97	16.11	0.000072	0.84	8.1
8.0680*	1916.81	16.09	0.000069	0.82	8.08
8.0640*	1909.27	16.07	0.000066	0.81	8.06
8.0600*	1900.6	16.05	0.000064	0.8	8.04
8.0560*	1892.41	16.04	0.000061	0.78	8.02
8.0520*	1884.03	16.02	0.000058	0.77	7.99
8.0480*	1874.21	16	0.000056	0.76	7.97
8.0440*	1863.35	15.99	0.000053	0.75	7.93
8.0400*	1852.88	15.97	0.000051	0.73	7.9
8.0360*	1763.8	15.96	0.000049	0.72	7.86
8.0320*	1752.02	15.95	0.000046	0.71	7.83
8.0280*	1739.27	15.93	0.000044	0.7	7.79
8.0240*	1727.22	15.92	0.000042	0.69	7.75
8.0200*	1713.97	15.91	0.00004	0.67	7.71
8.0160*	1701.36	15.9	0.000039	0.66	7.68
8.0120*	1688.56	15.89	0.000037	0.65	7.65
8.0080*	1676.02	15.88	0.000035	0.64	7.62
8.0040*	1663.53	15.87	0.000034	0.63	7.59
8.00	1649.03	15.86	0.000032	0.62	7.57
7.9250*	1635.43	15.85	0.000031	0.61	7.55
7.8500*	1618.68	15.84	0.000029	0.6	7.54
7.7750*	1522.5	15.83	0.000031	0.61	7.52
7.7000*	1428.02	15.82	0.000032	0.62	7.49
7.6250*	1335.11	15.81	0.000034	0.63	7.44
7.5500*	1243.95	15.8	0.000036	0.64	7.38
	1155.12	15.79	0.000038	0.66	7.3

Multi-variate Regression model

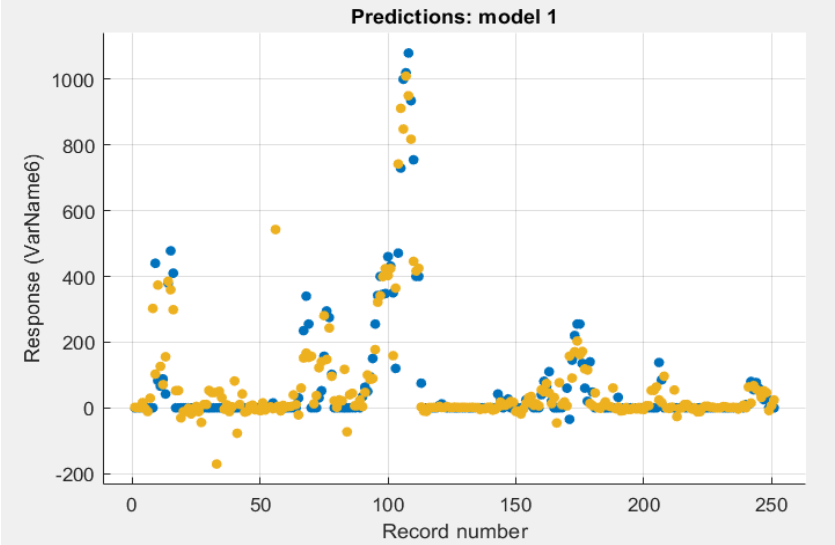

Figure 5.41: Calibration graph for the year 2019

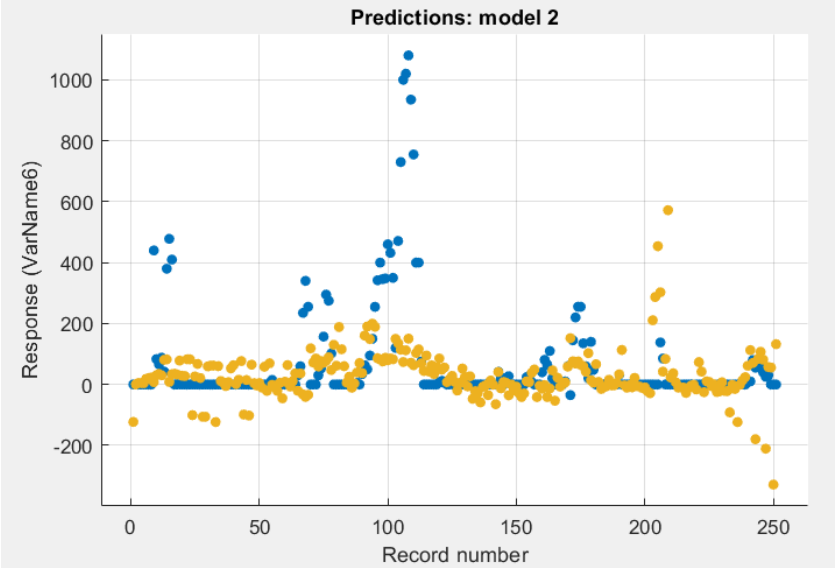

Figure 5.42: Calibration graph of the SVM regression model for the year 2019

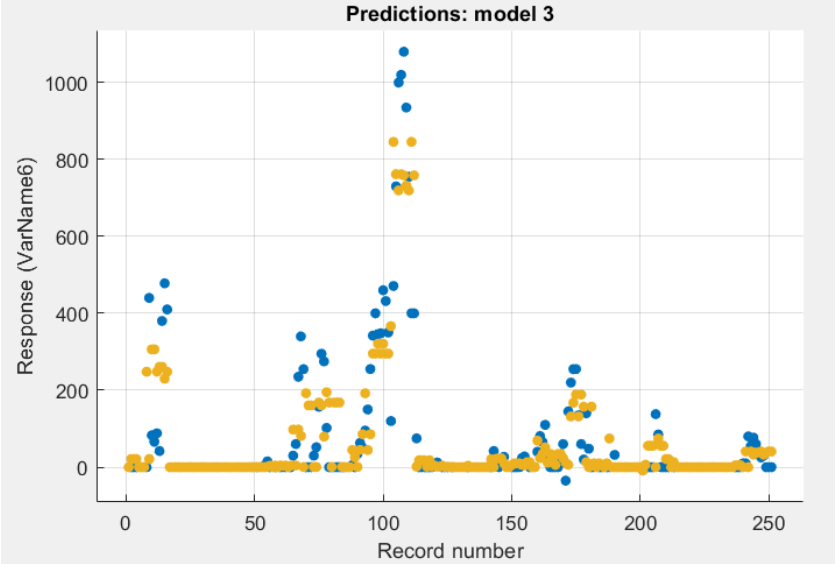

Figure 5.43: Calibration graph of the fine tree regression model for year 2019

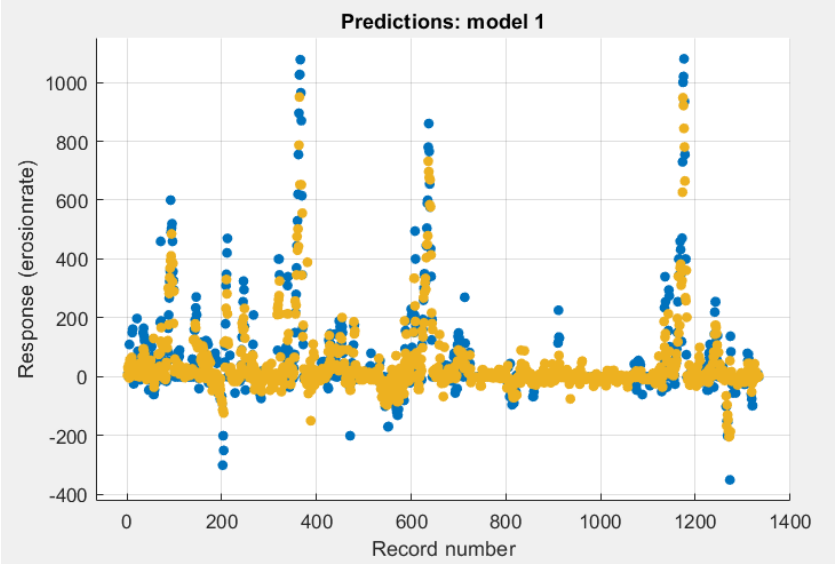

Figure 5.44: Calibration of the boosted regression model(with only WL) for the year 2015-2019

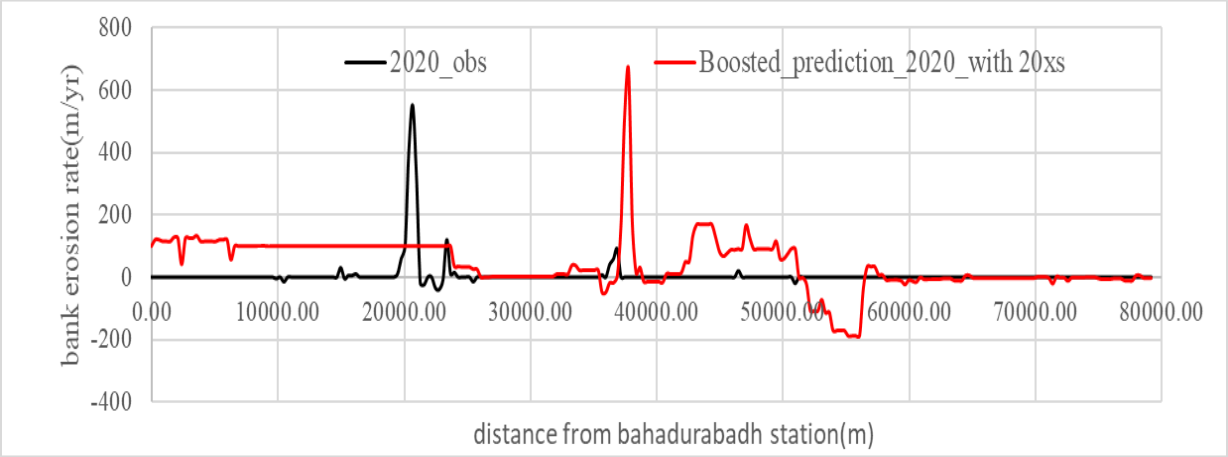

Figure 5.45: Prediction of the 5 yrs calibrated model

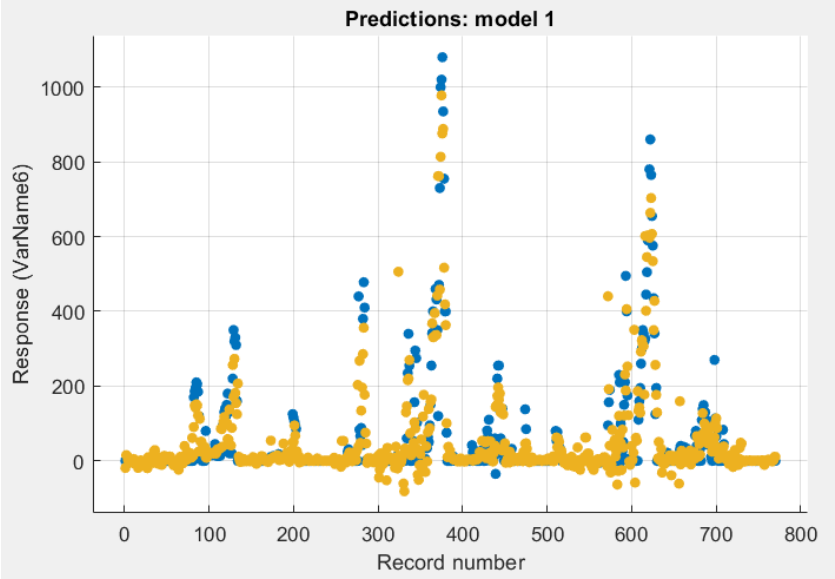

Figure 5.46: Calibration of the model(all variables) for the year 2017-2019

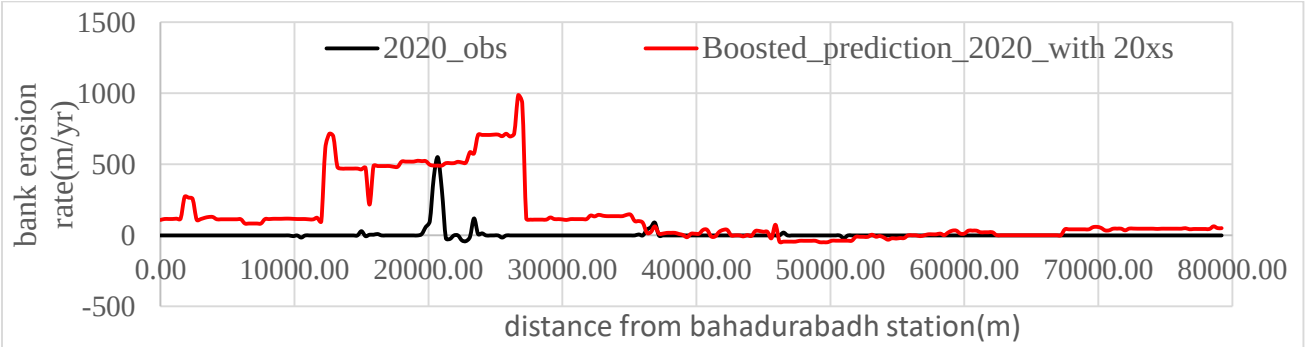

Figure 5.47: Prediction for the year 2020 of calibrated model(2017-2019)

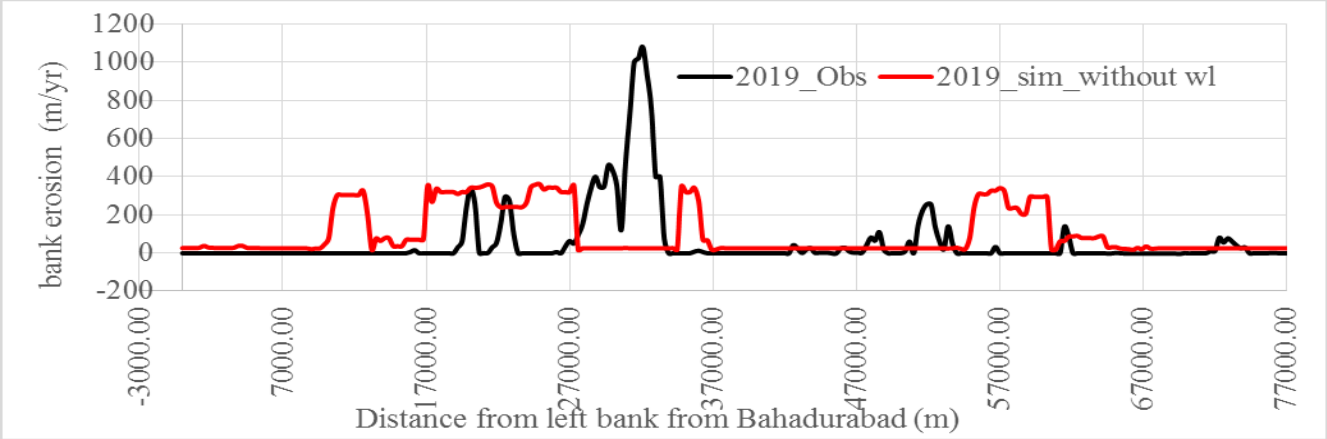

Figure 5.48 : Prediction of bankline shifting for the year 2019 without WL

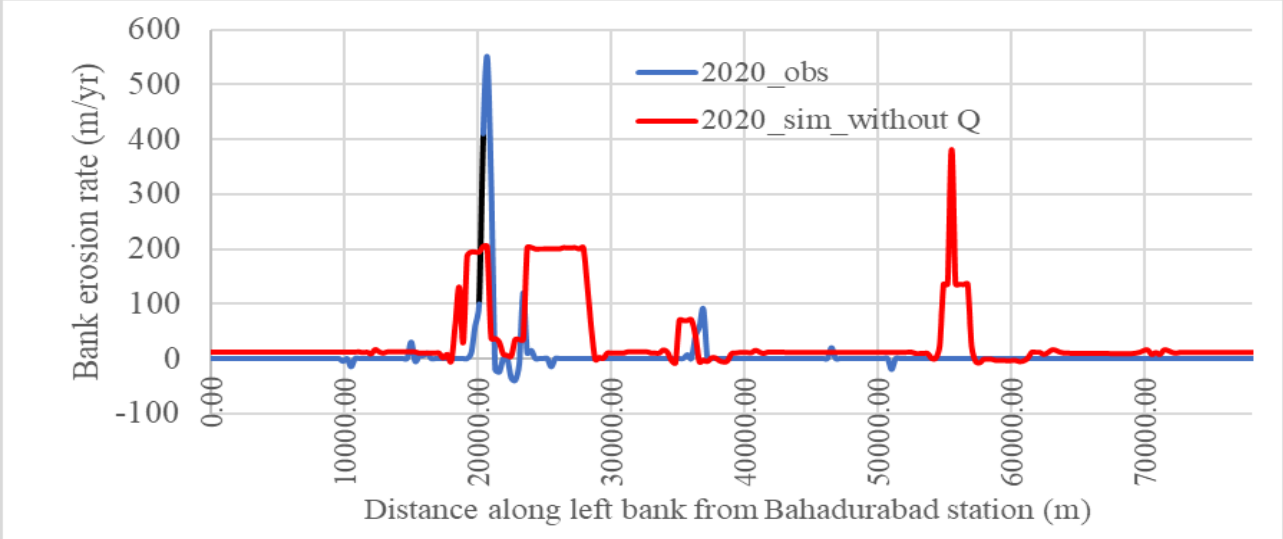

Figure 5.49 : Prediction of bankline shifting for the year 2020 without discharge (Q)

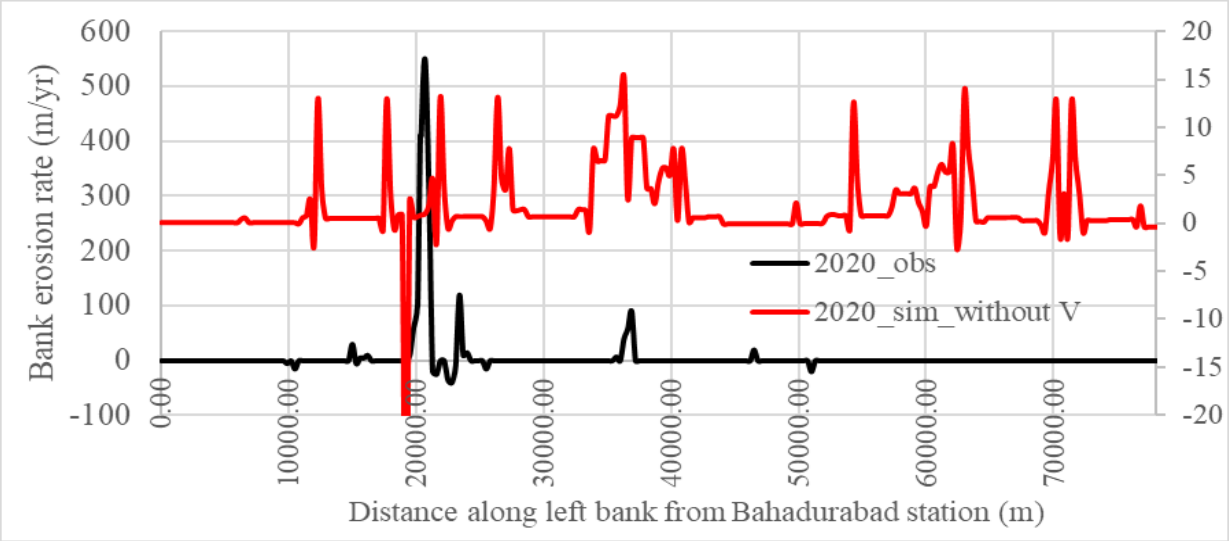

Figure 5.50 : Prediction of bankline shifting for the year 2020 without velocity (V)

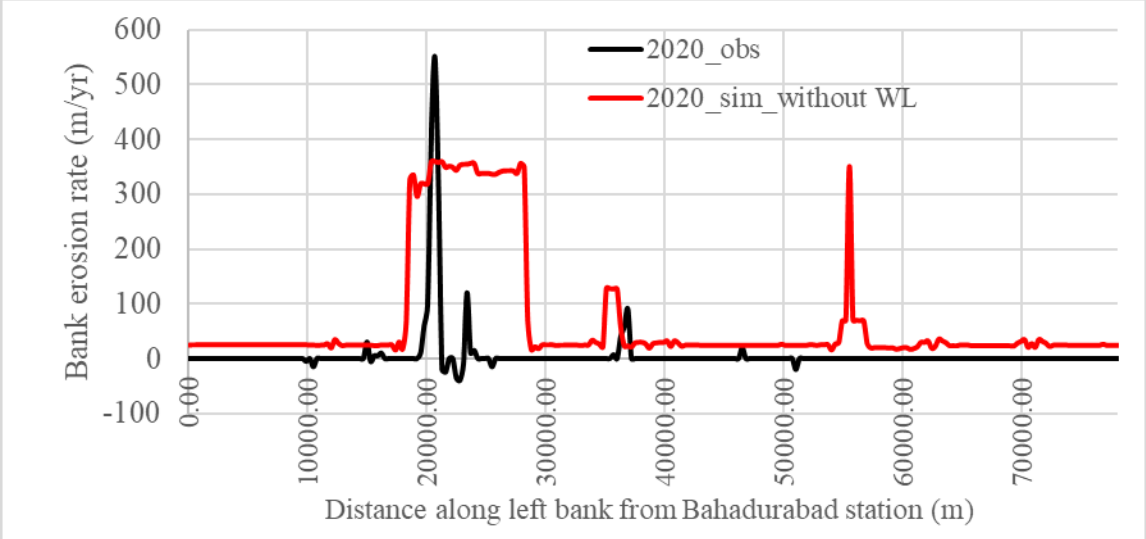

Figure 5.51: Prediction of bankline shifting for the year 2020 without WL

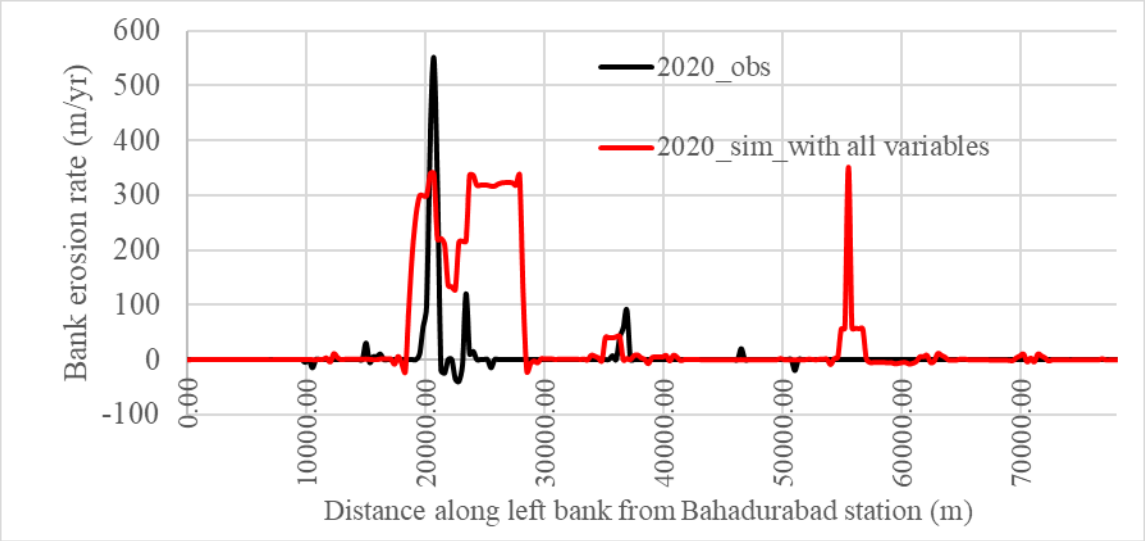

Figure 5.52 : Prediction of bankline shifting for the year 2020 with all variables

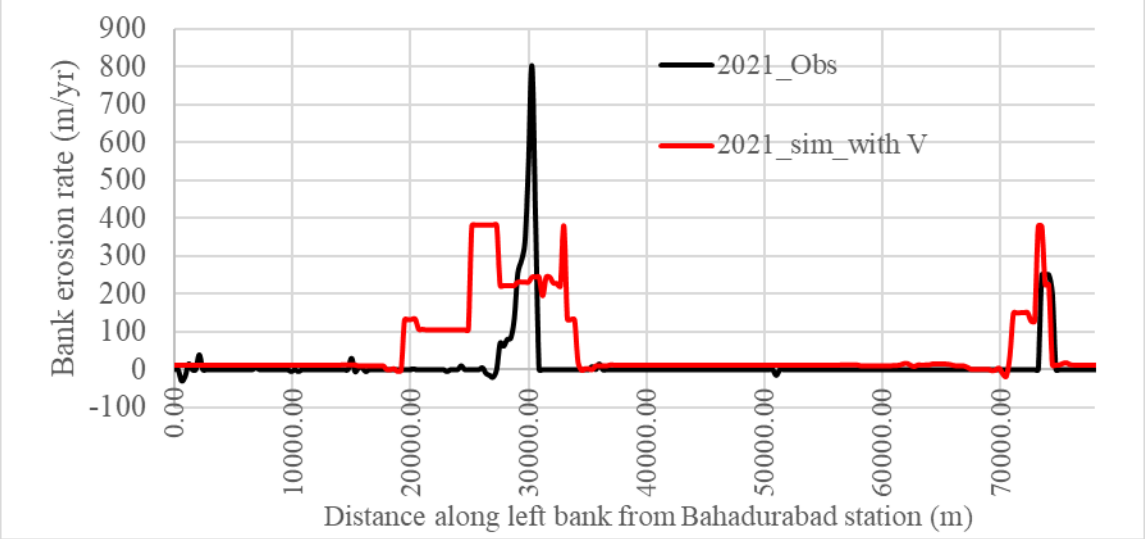

Figure 5.53 : Prediction of bankline shifting for the year 2021 only with velocity (V)

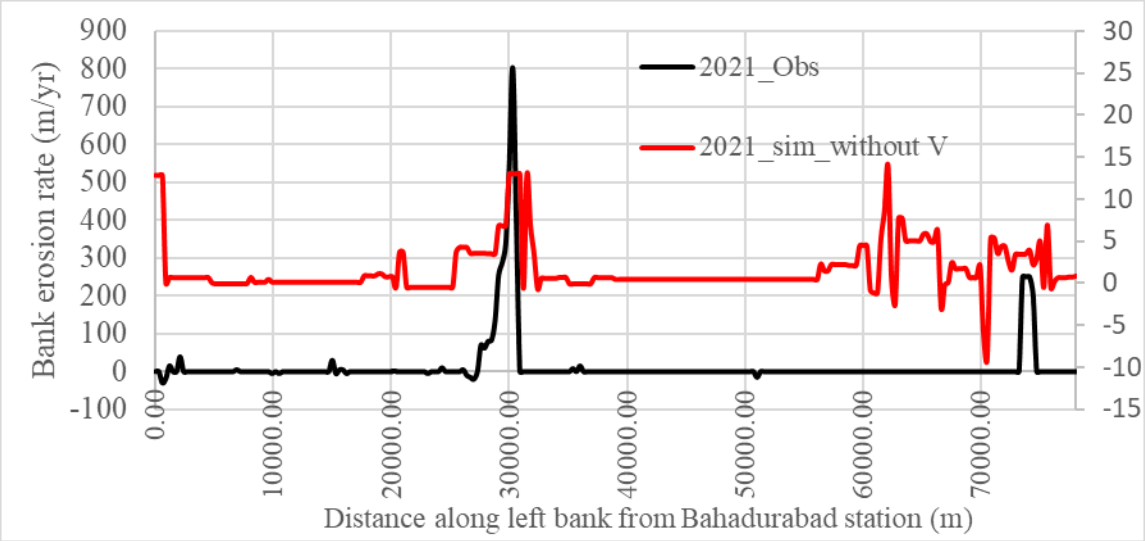

Figure 5.54 : Prediction of bankline shifting for the year 2021 without velocity (V)

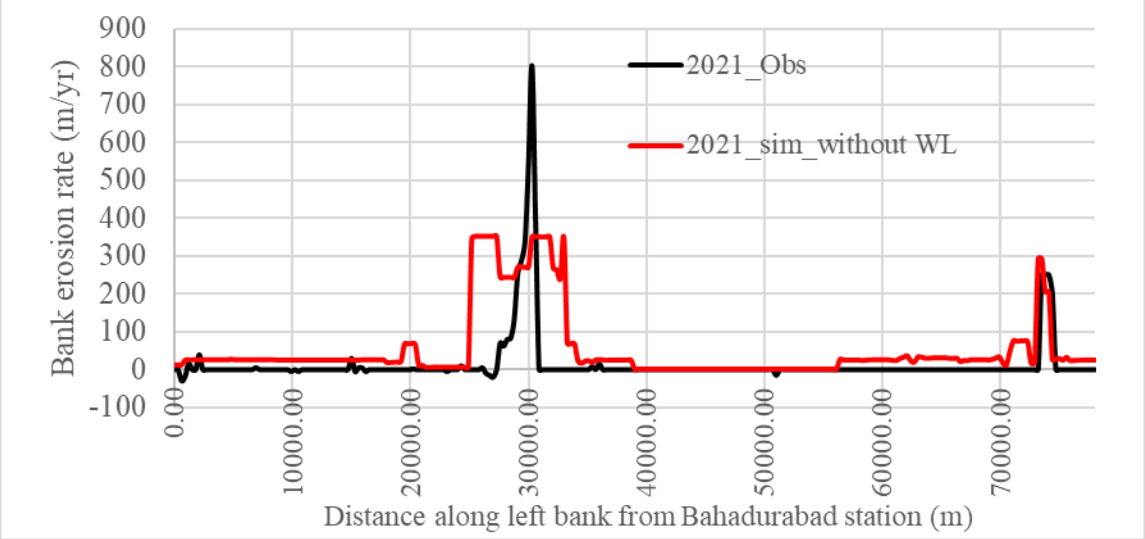

Figure 5.55 : Prediction of bankline shifting for the year 2021 without WL

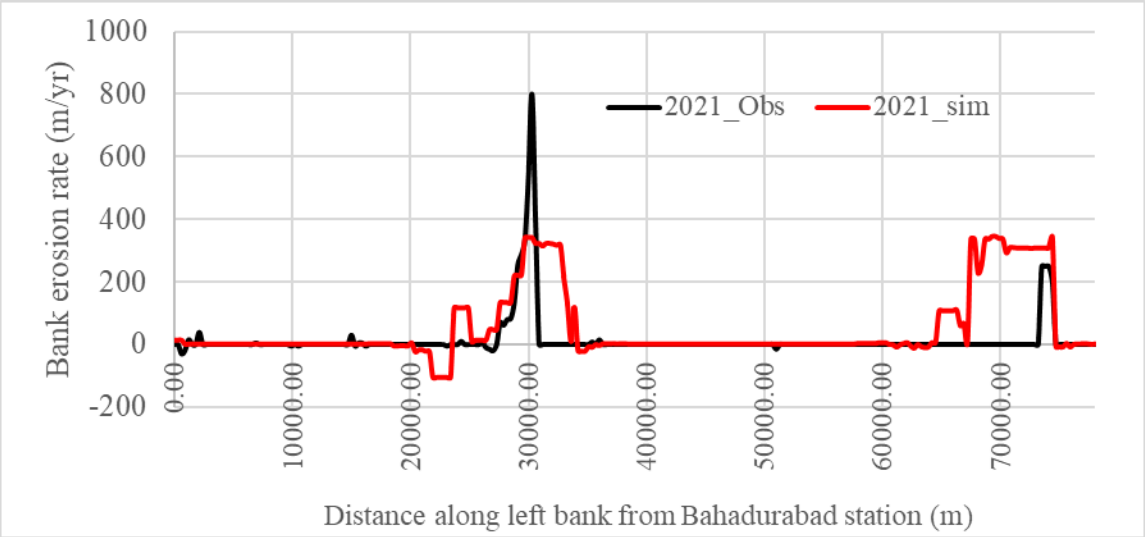

Figure 5.56 : Prediction of bankline shifting for the year 2021 with all variables